



**Michigan
Technological
University**

Michigan Technological University
Digital Commons @ Michigan Tech

Dissertations, Master's Theses and Master's Reports

2022

PROPERTIES AND ENVIRONMENTAL IMPACTS OF SUSTAINABLE ELECTRICALLY CONDUCTIVE COMPOSITES OF CARBONIZED PULP FIBERS AND RECYCLED POLYAMIDE 12

Chinmoyee Das
Michigan Technological University, cdas2@mtu.edu

Copyright 2022 Chinmoyee Das

Recommended Citation

Das, Chinmoyee, "PROPERTIES AND ENVIRONMENTAL IMPACTS OF SUSTAINABLE ELECTRICALLY CONDUCTIVE COMPOSITES OF CARBONIZED PULP FIBERS AND RECYCLED POLYAMIDE 12", Open Access Dissertation, Michigan Technological University, 2022.
<https://doi.org/10.37099/mtu.dc.etr/1412>

Follow this and additional works at: <https://digitalcommons.mtu.edu/etr>



Part of the [Wood Science and Pulp, Paper Technology Commons](#)

PROPERTIES AND ENVIRONMENTAL IMPACTS OF SUSTAINABLE
ELECTRICALLY CONDUCTIVE COMPOSITES OF CARBONIZED PULP
FIBERS AND RECYCLED POLYAMIDE 12

By

Chinmoyee Das

A DISSERTATION

Submitted in partial fulfillment of the requirements for the degree of

DOCTOR OF PHILOSOPHY

In Forest Science

MICHIGAN TECHNOLOGICAL UNIVERSITY

2022

© 2022 Chinmoyee Das

This dissertation has been approved in partial fulfillment of the requirements for the Degree of DOCTOR OF PHILOSOPHY in Forest Science.

College of Forest Resources and Environmental Science

Dissertation Advisor: *Dr. Xinfeng Xie*

Committee Member: *Dr. Mark Rudnicki*

Committee Member: *Dr. David Shonnard*

Committee Member: *Dr. Alper Kiziltas*

College Dean: *Dr. David Flaspohler*

Table of Contents

<i>List of Figures</i>	<i>vi</i>
<i>List of Tables</i>	<i>x</i>
<i>Preface</i>	<i>xi</i>
<i>Acknowledgements</i>	<i>xiii</i>
<i>Abstract</i>	<i>xv</i>
1. Chapter 1. Introduction and Literature Review	1
1.1. Abstract	1
1.2. Introduction	2
1.2.1. Biocarbon	2
1.3. Structure of Biocarbon	5
1.4. Composite Formation	7
1.5. Composite Properties	12
1.5.1. Mechanical Properties	12
1.5.2. Thermal Properties	37
1.5.3. Electrical Conductivity in Composites	48
1.5.4. Morphological Properties	54
1.6. Gaps and Improvements	61
1.7. Conclusion	63
1.8. Goals and research questions	64
2. Chapter 2- Newly Developed Biocarbon to Increase Electrical Conductivity in Sustainable Polyamide 12 Composites	66
2.1. Abstract	66
2.2. Introduction	68
2.3. Material and Methods	73
2.3.1. Biocarbon and polyamide	73
2.3.2. Characterization of biocarbon	74
2.3.2.1. <i>Elemental Analysis of Biocarbon</i>	74
2.3.2.2. <i>Ash Content Analysis</i>	75
2.3.2.3. <i>XRD Analysis of Biocarbon</i>	75
2.3.3. Composite formation.....	76
2.3.4. Electrical conductivity measurement.....	79
2.3.5. Dynamic Mechanical Analysis	81
2.3.6. Thermal Properties	81
2.3.7. Scanning Electron Microscopy Analysis	82
2.4. Results and Discussion	82
2.4.1. Elemental and Ash content Analysis.....	82
2.4.2. XRD Analysis.....	83
2.4.3. Electrical property of composites	84
2.4.4. Dynamic Mechanical Analysis	87

2.4.5.	Thermal properties.....	89
2.4.6.	SEM Analysis.....	92
2.5.	Conclusion	93
3.	Chapter 3- Development of Theoretical Modelling Framework for Biocarbon fiber filled Composites	95
3.1.	Abstract	95
3.2.	Introduction:.....	96
3.3.	Percolation theory	96
3.3.1.	Thermodynamic Models.....	100
3.3.2.	Geometric models of Percolation.....	105
3.3.3.	Structure oriented model.....	107
3.4.	Material and Methods	109
3.4.1.	Biocarbon and polyamide	109
3.4.2.	Composite formation.....	110
3.4.3.	Electrical conductivity measurement.....	111
3.5.	Results.....	113
3.5.1.	Electrical conductivity	113
3.6.	Modelling electrical conductivity of the composites..	116
3.6.1.	Volume Fraction and conductivity of biocarbon filled composites.	116
3.6.2.	Modelling of biocarbon filled composites using combination of original and updated Mamunya model.....	117
3.6.3.	Updated modelling framework	121
3.6.4.	Updated A, B and n	121
3.6.5.	Iterations for surface energy	124
3.6.6.	Iterations for F.....	125
3.6.7.	The modelling curve with updated inputs.....	127
3.7.	Conclusion	130
4.	Chapter 4 - A comparative study on the effect of morphology of fillers on the properties of biocarbon filled polyamide 12 composites. 131	
4.1.	Abstract	131
4.2.	Introduction.....	133
4.3.	Materials and methods	137
4.3.1.	Biocarbon, Carbon fiber and recycled Polyamide 12	137
4.3.2.	Composite Fabrication.....	140
4.3.3.	Elemental analysis and morphology of filler.....	142
4.3.4.	Electrical conductivity measurement of composites.....	143
4.3.5.	Thermal Properties of composites	146
4.3.6.	Mechanical Properties	146
4.4.	Results and discussion.....	147
4.4.1.	Morphology of biocarbon fillers and carbon content	147

4.4.2.	Electrical Properties	151
4.4.3.	Thermal Properties	153
4.4.4.	Mechanical Properties	158
4.5.	Scaling up of composites	163
4.5.1.	Results.....	164
4.5.1.1.	<i>Electrical Conductivity</i>	164
4.5.1.2.	<i>Mechanical properties</i>	166
4.5.	Conclusion	169
5.	Chapter 5 - Cradle to grave life cycle analysis of biocarbon fiber filled composites used to manufacture an automotive component.....	171
5.1.	Abstract	171
5.2.	Introduction.....	172
5.3.	Goal and Scope.....	174
5.4.	Objectives.....	175
5.5.	Functional Unit.....	175
5.6.	Lifecycle System Boundaries	176
5.6.1.	Manufacturing biocarbon filler.....	177
5.6.2.	Transport	179
5.6.3.	Recycled polyamide (PA) 12.....	179
5.6.4.	Electrically conductive composite manufacturing	180
5.6.5.	Use phase.....	181
5.6.6.	End of life scenario of the composites	182
5.6.7.	Life cycle analysis and impact assessment	183
5.7.	Results.....	183
5.7.1.	Greenhouse gas emissions and cumulative energy demand.....	183
5.7.2.	Impact Assessment	186
5.8.	Conclusion	189
	List of Refences.....	190
6.1.	Appendix.....	210
6.1.1.	Supplementary information for Chapter 5	210

List of Figures

Figure 1. SEM images showing biocarbon produced from different lignocellulosic feedstocks. This image is taken from (27) from Applied Sciences Open Access journal MDPI publications.7

Figure 2. The mechanical properties of biocarbon filled polypropylene composites a) Tensile strength, b) Tensile modulus and c) Percentage elongation (56). Figure is taken from refence (56) with permissions to reuse from Elsevier Publications 201617

Figure 3. The tensile properties of biocarbon filled composites, a) neat polymer, b) & c) LtBioC filled composites and d) & e) HtBioC filled composites. The tensile properties of composites filled with HtBioC was shown to be better than neat polymer and composites filled with LtBioC(37). Figure is taken from (37) with permissions to reuse from Elsevier publications 2017.23

Figure 4. The TGA and DTG curves of biocarbon filled polypropylene composites, a) TGA (mass loss) curve b) DTG curve. A significant shift in the degradation temperature of the composite in comparison to neat polymer can be observed (5). Figure modified from refence (5) with permission from Elsevier publication 2016 to use and modify the Figure.38

Figure 5. DSC thermogram of biocarbon filled polypropylene composites, no change in melting temperature was observed but a rise in crystallization temperature was observed due to the nucleation effect of biocarbon(5). Figure modified from refence(5) with permission from Elsevier publication 2016 to use and modify the Figure.43

Figure 6. Electrical conductivity of biocarbon filled PVA composites filled with 2, 6 and 10 wt.% biocarbon filler respectively. An increase in conductivity is observed with increase in loading rate of biocarbon (25). Figure taken from refence (25) with permission to use from SagePub Publications 2016.50

Figure 7. The SEM images of fractured surfaces of biocarbon filled polypropylene composites, the images show mechanical interlocking between the filler and the matrix polymer even at 1% concentration of compatibilizer attributing o its excellent mechanical properties. Figure taken from refence (41) with permission to use from Elsevier Publications 2016.56

Figure 8. SEM images showing biocarbon fibers before and after dispersion in PA 12 matrix using coffee grinder.78

Figure 9. Composite fabrication process for development of biocarbon filled PA 12 composites.	79
Figure 10. The setup used to characterize the composites for electrical conductivity.	80
Figure 11. XRD pattern of pulp fiber vs biocarbon.	84
Figure 12. The electrical conductivity trend of biocarbon filled PA 12 composites.	87
Figure 13. The dynamic mechanical analysis curves of biocarbon fiber filled composites (a) tan delta curves, (b) storage modulus curve.	88
Figure 14. The thermogravimetric analysis curves of biocarbon fiber filled composites (a) mass loss curves (b) DTG curves.	91
Figure 15. SEM images of biocarbon fibers and biocarbon-polyamide 12 composites, (a) 7.5% biocarbon filled composites, (b) 9% Biocarbon filled composites, (c) 15% Biocarbon filled composites, (d) 25% biocarbon filled composites (e) 35% biocarbon filled composites. The biocarbon fibers are indicated by the arrows on the images.	93
Figure 16. S shaped curve depicting the percolation behaviour in polymer/conducting filler (Carbon fiber) composites (148).	97
Figure 17. Composite fabrication process for development of biocarbon filled PA 12 composites.	111
Figure 18. The equipment set up used to measure the electrical conductivity of PA 12-Biocarbon composites. The composite sample is placed between two electrodes while the measurements are done.	112
Figure 19. Electrical conductivity trend of PA 12-biocarbon filled composites.	114
Figure 20. SEM images of biocarbon carbonized at 1000°C and fractured composite surface, (a) shows the fibrous morphology of the Douglas fir fibers maintained even after carbonization, (b) the arrows indicated the localized biocarbon fibers that are still in fiber form even after composite processing.	115
Figure 21. The curves representing experimental and theoretical conductivity values for biocarbon filled composites.	120
Figure 22. Presenting the iterations for the constant A, from the iterations it can be seen the curve representing A + 50 is the closest to experimental values curve.	122
Figure 23. The curves presenting the iterations for constant B and the curve plotted with B+0.045 is the closest to experimental values curve.	123
Figure 24. The curves presenting iterations for constant n, the curve with n value 1 is the closest to the experimental values curve.	124

Figure 25. The curves presenting the iterations for surface energy values for composite components, the curve developed using SE-24 is the closest to experimental values.....	125
Figure 26. The curves representing iterations for F, the curve developed with F+0.3 is the closest to the experimental curve.	126
Figure 27. The curves representing the iterations for F. No clear distinction can be seen in the modelling curve and the iterated curves.....	127
Figure 28. The curves presenting all updated values with iterations for F, it can be observed the value for F-0.01 is closest to the experimental curve.	128
Figure 29. The curves presenting the experimental values and the updated modelling values.	130
Figure 30. Milled wood used as feedstock for biocarbon production.....	138
Figure 31. Deagglomerated Douglas fir pulp used as feedstock for biocarbon production.	139
Figure 32. Recycled PA 12 powder used as matrix in biocarbon filled composites.....	140
Figure 33. Process flow for the fabrication of PA 12-biocarbon composites. ..	142
Figure 34. The equipment used to measure the electrical resistivity of PA 12-Biocarbon composites.	145
Figure 35. The particle size distribution of biocarbon powder shows 3.3 μm had the maximum volume.....	148
Figure 36. The frequency distribution of aspect ratio of 200 biocarbon fibers.	149
Figure 37. Biocarbon particles observed under optical microscope set to 40X magnification.	149
Figure 38. (a) Biocarbon fiber after carbonization as seen using SEM at 100X magnification; (b)Biocarbon fibers dispersed in PA 12 matrix, as seen under an optical microscope set to 40X magnification.	150
Figure 39. Electrical conductivity trends of biocarbon fiber filled composites and biocarbon powder filled composites.	153
Figure 40. TGA weight loss curves of biocarbon filler filled PA 12 composites (a) weight loss curves of biocarbon fiber filled PA 12 composites, (b) weight loss curves of Biocarbon powder filled PA 12 composites.....	156
Figure 41. Derivative thermogravimetry (DTG) curves of (a) biocarbon fiber filled PA 12 composites, (b) Biocarbon powder filled PA 12 composites.	157
Figure 42. Storage modulus curves of (a) biocarbon fiber filled PA 12 composites, (b) Biocarbon powder filled PA 12 composites.	160

Figure 43. Tan delta curves of (a) PA 12-biocarbon fiber composites (b) PA 12-biocarbon powder filled composites.	162
Figure 44. Tensile properties of pure PA 12 and 15 wt.% biocarbon fiber filled composites.....	167
Figure 45. Flexural properties of pure PA 12 and 15 wt.% biocarbon fiber filled PA 12 composites.....	168
Figure 46. Life Cycle Analysis Framework (based on ISO 14040, 1997) modified from Rebitzer et al. 2004 (182).....	174
Figure 47. The system boundaries of PA 12-biocarbon fiber composites.....	177
Figure 48. Cumulative energy demand for recycled PA 12-biocarbon manufacturing and use phase.	185
Figure 49. Cumulative energy demand for recycled PA 12-biocarbon composites lifecycle	186
Figure 50. Environmental impact assessment of recycled PA 12-biocarbon composites (manufacturing and use phase).....	187
Figure 51. Comparative impact assessment of PA 12-carbon fiber filled composite production and PA 12-biocarbon composite production including end of life scenario.	188

List of Tables

Table I. Fabrication methods and composition of biocarbon filled polymer composites.....	9
Table II. Mechanical properties of biocarbon filled polymer composites.	35
Table III. Electrical conductivity values reported for biocarbon filled polymer composites.....	53
Table IV. Application of ECPCs based on their resistivity range (140).....	70
Table V: Composite composition with different filler loading rates.	110
Table VI: Electrical conductivity of biocarbon filled composites.....	117
Table VII. Inputs and calculated electrical conductivity values for modelling of biocarbon filled composites.....	120
Table VIII. The updated input and calculated values for modelling of biocarbon filled composites.	129
Table IX. Electrical conductivities of pure PA 12, biocarbon fiber filled composites and carbon fiber filled composites.....	165
Table X. Lifecycle inventory data for manufacturing recycled PA 12-biocarbon fiber composites. (*energy consumption is calculated based on power consumption and time taken to complete the process).....	181
Table XI. Emissions produced in the different phases in the lifecycle of biocarbon filled recycled PA 12 composites.....	184

Preface

This dissertation is submitted for the partial fulfillment for the Doctoral Degree in Forest Science at Michigan Technological University. In this dissertation two major aspects have been investigated 1) Incorporation of biocarbon fiber as an electrically conductive filler in recycled polyamide 12 matrix; and 2) cradle to grave comparative life cycle analysis of biocarbon fiber filled composite and carbon fiber filled composite used to manufacture an automotive component. The research work for the dissertation conducted within the period from 2019 to 2022, under the supervision of Dr. Xinfeng Xie (advisor), Dr. Mark Rudnicki, Dr. David Shonnard and Dr. Alper Kiziltas.

The work to my best knowledge is original except for sections where references and acknowledgements are made to previous works. Part of this work contains materials that have been published and submitted for peer review; “**Chapter 1 – Incorporation of biocarbon to improve mechanical, thermal and electrical properties of polymer composites**” has been published in the special issue “Wood [polymer composites: modification processing and characterization” of journal Polymers (MDPI); “**Chapter 2 - Newly Developed Biocarbon to Increase Conductivity in Sustainable Polyamide 12 Composites**”, is accepted for publication in the special issue “Advances in Automotive Composites” of journal Polymer Composites. It also contains work that will be submitted for review in peer reviewed journals; Chapter 3 – “**Development of a**

theoretical modelling framework for biocarbon filled recycled polyamide 12 composites” in the journal Biochar; “***Chapter 4 – A comparative study on the effect of morphology of fillers on the properties of biochar filled polyamide 12 composites***” will be submitted for peer review in the journal Composites part B and Chapter – 5 “***Cradle to grave life cycle analysis of biocarbon fiber filled composites***”, will be submitted for peer review in the Journal of Industrial Ecology. Data collection and analyses were completed by Chinmoyee Das, the lab space was provided by Dr. Xinfeng Xie. Dr. Mark Rudnicki and Dr. Alper Kiziltas provided their comments and feedback for the publications. Dr. David Shonnard and Dr. Robert Handler of the Sustainable Futures Institute, Department of Chemical Engineering guided me through the life cycle analysis process using Sima pro included in Chapter 5 Dr. Sandeep Tamrakar from Ford Motor Company provided a lot of help with the SEM imaging, melt compounding and injection molding of composites and mechanical property analysis of composites.

Acknowledgements

There are so many people who have contributed in so many ways to the fruition of my Ph.D. First of all, I am immensely grateful to my advisor Dr. Xinfeng Xie, for believing in me. It was an honor to have worked with you. I would like to thank my committee members Dr. Mark Rudnicki, Dr. David Shonnard and Dr. Alper Kiziltas for their expert advice, feedback, and words of encouragement till the very end. I am extremely grateful to Dr. Daniel Seguin for all his help with my experiments. I cannot thank Dr. Robert Handler enough for all his help with the LCA, even at short notice. I am extremely thankful to Dr. Sandeep Tamrakar for his help with the mechanical properties analysis and SEM along with his feedback on my work.

I am very grateful to everyone at the College of Forest Resources and Environmental Sciences for being a part of my journey so far. I would like to especially thank Mr. Joe Plowe for always being ready to help me whenever I was need. Marjorie and Phyllis were my second mothers here at MTU who were there for me when I needed them, I am forever grateful to you both. I cannot thank Dr. Tara Bal enough for being so kind to me in these three years and providing me with a shoulder to cry and an ear to listen when needed.

I would like to thank my lab mates Dr. Munkaila Musah and Peng Quan for being so helpful throughout the course of my Ph.D. My friends at CFRES and MTU you

folks are the best! Lastly, I would like to thank my Ma and Baba for their constant support and unconditional love and trust.

Thank you very much. I owe my Ph.D and my success to all of you.

Abstract

Electrically conductive composites are polymer composites filled with electrically conductive filler. Electrically conductive composites can be implemented in development of light weight electrically conductive components for the automotive industry. Traditional electrically conductive composites incorporate synthetic carbon-based fillers that have good properties but are very expensive and highly energy intensive, creating the need for a sustainable and cost-effective replacement. This study explores the effectiveness of biocarbon fibers developed from Douglas fir pulp fibers as a potential electrically conductive filler in recycled polyamide (PA) 12 composites.

Biocarbon fibers were developed from pulp by carbonization of the feedstock at 1000° C in an inert nitrogen environment. These biocarbon fibers were incorporated in a recycled polyamide 12 matrix in varying concentrations and characterized for electrical, thermal, and mechanical properties. The results indicate that incorporation of biocarbon fibers can improve the electrical properties drastically, as the electrical properties of composites filled with 35 wt.% biocarbon was – 0.33 S/cm, that is several orders higher compared to pure polymer conductivity of -14 S.cm. The thermal properties of composites also showed an improvement with increase in maximum thermal degradation temperature from 407.26 °C to 442.74 °C at 35 wt.% filler concentration indicating improved thermal properties. The storage modulus values of the composites also increased for 1500 MPa to 3500 MPa on incorporation of 35

wt.% biocarbon fibers. The modelling study of the biocarbon fiber filled composites was built upon updating a previous carbon fiber filled composites modelling study and improved the fit between the experimental and theoretical electrical conductivity curves yet leaving room for improvement. Upon comparing biocarbon fiber fillers with biocarbon powder fillers, it was observed that the former has better electrical properties as biocarbon fiber filled composites reported an electrical conductivity value of -0.33 S/cm while biocarbon powder filled composites reported electrical conductivity values -2.541 S/cm . This shows that biocarbon fibers with higher aspect ratio have better electrical properties in composites.

Finally, the lifecycle analysis of the recycled PA 12-biocarbon composites was carried out to determine the environmental impacts of the composites throughout their lifecycle. The emissions and environmental impacts were estimated using IPCC GWP 100 and TRACI USA 2008 method. The cumulative energy demand was estimated for the composites as well. The total emissions generated in the lifecycle of the composites was estimated to be 124 kg CO_2 equivalents with the highest contributor being the use phase of the composites.

1. Chapter 1. Introduction and Literature Review

1.1. Abstract

The increased demand for utilization of green fillers in polymer composite has increased focus on the application of natural biomass-based fillers. Biocarbon has garnered a lot of attention as a filler material and has the potential to replace conventionally used inorganic mineral fillers. Biocarbon is a carbon-rich product obtained from thermochemical conversion of biomass in a nitrogen filled environment. In this review, current studies dealing with incorporation of biocarbon in polymer matrices as a reinforcement and conductive filler have been addressed. Each study mentioned here is nuanced, while addressing the same goal of utilization of biocarbon as a filler. In this review paper, an in-depth analysis of biocarbon and its structure is presented. The paper explores the various method employed in fabrication of the biocomposites. A thorough review on the effect of addition of biocarbon on the overall composite properties showed that biocarbon has shown immense promise as a good composite filler in improving the overall composite properties. An analysis of the possible knowledge gaps was also conducted, and improvements have been suggested. Through this study we have tried to present the status of application of biocarbon as a filler material and its potential future applications.

Keywords: biocarbon; carbonization; polymer composites; sustainability; composite properties

1.2. Introduction

1.2.1. Biocarbon

Biocarbon is the carbon-rich solid material that is left after the thermochemical conversion of biomass in an oxygen limited environment(1). Features like low density and ecological sustainability make it an attractive replacement for inorganic fillers (2). Biocarbon can be obtained from biomass by various thermal decomposition methods like pyrolysis, combustion, gasification and liquefaction (3). More precisely biocarbon is produced by a method called carbonization. Carbonization and pyrolysis share the same fundamental principle where the raw material undergoes thermal decomposition in an inert atmosphere. However, the process of carbonization is undertaken in a much lower pace and heating rate in order to enhance carbon yield of the process. Several factors, such as feedstock type, carbonization process, pyrolysis temperature, heating rate, and residence time can influence the physiochemical properties of biocarbon (3). Biocarbon produced using various lignocellulosic resources that can be incorporated into composites as fillers to enhance various properties of composites. Pyrolysis is the process of thermal decomposition of raw material in an oxygen free environment to obtain a carbon rich product. Behazin et al. 2018 (4) used miscanthus grass as the raw material for biocarbon. Waste

materials generated from processing can be used as a raw material. Waste materials like pine wood, date palm, oil palm empty fruit bunch and rice husk, cashew nut shell have been used to produce biocarbon, used as reinforcing filler in polymer matrices(5–8) Utilization of processing waste materials as biocarbon feedstock closes the loops of production making it a circular and sustainable process(9). Zhang et al. 2018 used bamboo to produce biocarbon, as filler in the composites. Bartoli et al. 2020 used olive tree pruning as raw material for production of biocarbon used in manufacture of biocarbon filled epoxy composites. Idrees, Jeelani, and Rangari 2018 produced biocarbon out of packaging waste consisting primarily of starch-based packing peanuts. Other organic materials like sewage sludge and bird litter has been reportedly implemented for manufacturing biocarbon(13,14). The feedstock of biocarbon is fairly versatile, and the properties can be tailored by fine tuning the carbonization process.

The morphological structure and properties of biocarbon have made its implementation possible in diverse arenas. The excellent adsorption capabilities of biocarbon makes it a great soil conditioning agent and is used to contribute to soil health by restoring trace elements(15). Biocarbon can be used as an adsorbent in wastewater treatment systems and has been used in several water filtration systems as well. The hygroscopicity of biocarbon can be altered by controlling the temperature of carbonization and the resultant biocarbon can be used as a soil additive to improve moisture holding capacity of the soil. A major sector that is looking into the application of biocarbon is the plastic composite

industry. Polymer composites are multiphase materials reinforced with a filler, resulting in improved mechanical properties due to the synergistic effect of the two (16). Automobiles are a major contributor to greenhouse gas emissions. As per Environmental Protection Agency(EPA) on an average 8,887 grams of CO₂ is emitted from 1 gallon of gasoline and 10,180 grams of CO₂ is emitted from 1 gallon of diesel(17). Annually 4.6 metric tons of CO₂ is released from a typical passenger vehicle(17). These emissions have a highly detrimental effect on the global climate scenario. Increased fuel efficiency of vehicles can lead to lower fossil fuel consumption, in turn lower greenhouse gas emissions. To achieve this, the automobile manufacturers have resorted to lightweighting of the vehicles. As per the EPA 2020 Automotive trends report, the heaviest vehicles produced in model year 2020 generate half the amount of CO₂ compared to what was generated in model year 1978(18). The CO₂ generated for lighter vehicles in 2020 is two thirds of what was generated in 1978, all owing to the massive design changes and advancements undertaken by the automakers(18). Lightweighting can be done by making smaller cars or by material substitution without compromising on the capacity and size(19). Traditional materials are being replaced by light weight metals and largely by polymer composites. These composites are generally filled with fillers like talc, glass fibers, calcium carbonate (CaCO₃) etc. These polymer composites are lighter than the conventional metals, but the inorganic fillers have a high density making the end products bulky. Biocomposites come into play here, biocomposites, are a category of polymer composites that are biocompatible and/or eco-friendly(20–

22). The fillers in biocomposites are biomass derived from plants or animals, however, natural fillers are generally polar leading to interfacial adhesion issues with the fairly non-polar polymer matrices. Biocarbon is relatively inert compared to unprocessed natural fillers and can serve as filler in polymer composites fortifying the composites and with further calibration additional properties like electrical conductivity can also be introduced in the composites, as per requirement.

In this review paper we have presented a comprehensive description of the current research on the utilization of biocarbon as a filler in polymer composites. A description of the different methods and parameters used in these studies is summarized along with a critical analysis of their results and findings. An overall representation of the research including the bottle necks and possible solutions to it has been included in the end of this review. Adhering to the objective of the review paper the state of art research in this field is summarized in this review to have an overview of the different approaches and results developed based on these approaches.

1.3. Structure of Biocarbon

The inherent properties of biocarbon are greatly dependent on the structure. Properties like electrical conductivity can be manipulated greatly by the structure of biocarbon. Carbon has several allotropes that are crystalline and amorphous. Graphite is a crystalline carbon allotrope with great electrical properties owing to

its structure known as graphitic structure. Graphitic structure of material can be characterized by the presence of highly ordered well stacked graphene sheets (23). Carbons derived from biomass have the tendency to form a very highly arranged structure at a very high ($>2000^{\circ}\text{C}$) treatment temperature(23). The biocarbon structure is thought to be composed of turbo statically arranged crystalline regions and disordered amorphous regions (24), that could be obtained from the intrinsic structure of biomass, predominantly composed of cellulose, depending on the heating rate of the carbonization process. The presence of these turbo static regions contribute to the electrical conductivity of biocarbon(25). This isotropic structure results in spaces forming a porous structure (23) from atomic to nanometer level. At a larger scale the honeycomb like pores as seen in Figure 1 on the surface of biocarbon may provide mechanical interlocking of polymer with the biocarbon making it a very good reinforcing agent (26).

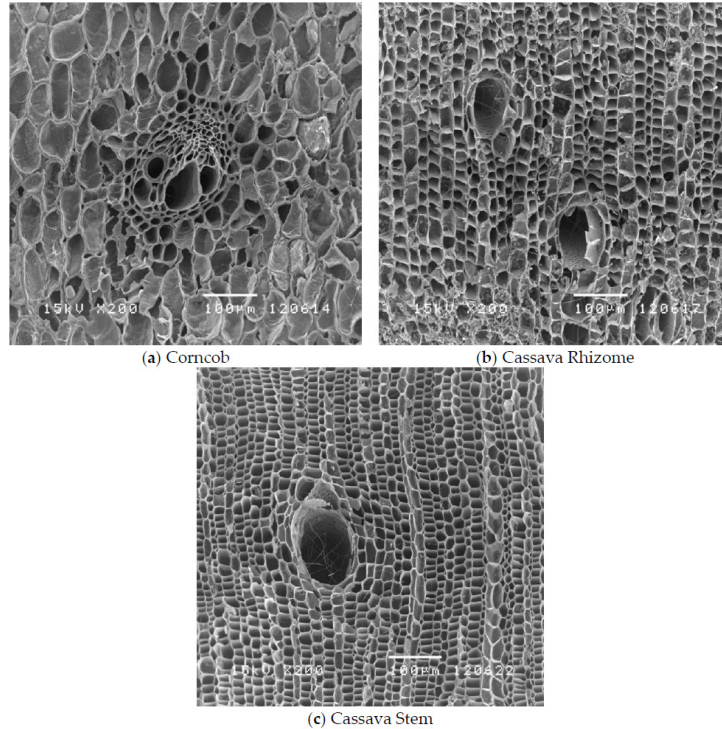


Figure 1. SEM images showing biocarbon produced from different lignocellulosic feedstocks. This image is taken from (27) from Applied Sciences Open Access journal MDPI publications.

1.4. Composite Formation

Polymers like polypropylene, polyethylene, nylon, epoxy etc., are used in the form of composites filled with inorganic fillers such as CaCO_3 , talc, glass fiber (28). Carbon based fillers like carbon fibers, carbon nanotubes and carbon black have been used to improve the mechanical properties, along with making the non-conductive matrix electrically conductive(28–30). These conventional fillers can be substituted with biocarbon to develop light sustainable composites that

are cost effective and improve the carbon footprint of the products throughout their lifecycle. The fabrication of biocarbon filled composites is carried out using common composite fabrication methods like melt extrusion and injection molding. Some of the studies addressed here have used less common methods like solvent casting, resin curing etc., (31,32). The melt processing of polymer takes place in three steps involving melting, shaping and solidification of polymer in the desired shape (33). Melt extrusion of polymers can be done using a single screw extruder or a twin-screw extruder. Application of heat and pressure results in dispersion of external filler, coloring agents etc., in the polymer matrix. Melt processing of plastics depends on several polymer characteristics like melting point, melt viscosity, etc. The process can be optimized by controlling the barrel temperature of the extruder and the rotation speed of the screw. In injection molding, which is largely used on an industrial scale, the molten polymer is injected into a mold and casted into the shape of the mold. Solution casting of polymers is based on Stokes law and is done by dissolution of the polymer and the additives in a solvent or different solvents and then mixing them together, the mixture is then dried to evaporate the solvent and render the composite(34). The various fabrication methods and compositions used in the studies done on biocarbon filled polymer composites is summarized in Table I.

Table I. Fabrication methods and composition of biocarbon filled polymer composites.

Matrix	Filler	Filler Loading Rate (w.%t)	Carbonization Temperature (°C)	Fabrication method	
Ultrahigh Molecular weight Polyethylene (UHMWPE)	Nano Bamboo charcoal	1, 3 and 9	1000	Compression	
				Molding (35)	
Polypropylene	Maleic Anhydride grafted Polypropylene (MAPP)	0 and 4	900	Melt extrusion and injection molding (26)	
		Biocarbon (1000µm and 50 µm)			24
		Wood			0 and 30
Polypropylene	Compatibilizer	0,2.5,5, 7.5.	~630	Injection molding(36)	
	Biocarbon (<20µm, 106-125 µm)	Not reported			
Polypropylene	Poly Octene Ethylene copolymer (POE)	30	500 (LtBioC)	Melt compounding and injection molding (37)	
		10 and 20	900 (HtBioC)		
	Biocarbon				
Polyamide 6,10	Biocarbon (<63, 213-250, 426-500 µm)	20	500	Melt compounding and injection molding (38)	
Nylon 6	Biocarbon	20	500 – 900	Melt compounding	

				and injection molding
Polypropylene	Bamboo particles	5, 10, 15, 20, 25 and 30	Not reported	Melt compounding and injection molding(10)
	Ultrafine bamboo char (UFBC)			
Polyethylene	Biocarbon	1 and 5	480	Solvent casting and Melt Mixing(39)
Polypropylene	Biocarbon	15, 25,30 and 35	900	Melt compounding and Injection molding(5)
Polypropylene	Biocarbon	24	900	Melt extrusion and injection molding(40)
	Wood	Concentration not reported		
	MAPP	0 to 3		
Polypropylene	Biocarbon	6,12,18,24,30.	400 and 450	Melt extrusion and Hot compression(41)
	Wood	30		
	MAPP	4		
Poly Lactic Acid (PLA)	Biocarbon	2, 6 and 10	Not Reported	Solvent casting(31)
Epoxy	Biocarbon	2, 4 and 20	950 (BCHT)	Resin curing(30)
	Multiwalled Carbon Nanotubes (MWCNT)			
Epoxy	Biocarbon	5,10,15 and 20	400,600,800 and 1000	Resin curing(32)

UHMWPE	Biocarbon	60,70 and 80	1100	Melt extrusion and hot compression(42)
PLA	Biocarbon	1, 2.5, 5 and 7.5	700	Melt mixing and Solvent casting(43)
High Density Polyethylene (HDPE)	Biocarbon	30,40,50,60, 70	500	Melt mixing and extrusion(44)

A few studies have reported very interesting and novel methods undertaken in their particular studies, Li et al. 2016 (35) induced a negative charge on their polymer using a high shear mixing technology to obtain segregated biocarbon network in the composites (45). This method has been deemed successful in the study. Utilization of intrinsic properties of the polymer to customize biocomposite properties has not been reported anywhere else so far. Ferreira et al. 2019(39) Used commercially available sugarcane bagasse biocarbon in their study. They chemically treated their filler with a base (NaOH) and acid (HCL) in a leaching process followed by Isopropanol vapor thermal annealing to remove polar groups from the biocarbon surface for better interfacial adhesion in composites. The method developed by them is quite unique and has been successful in improving interfacial properties of the composites. It can be observed that injection molding and melt compounding methods have been largely used for composite fabrication. These methods have been largely used since melt extrusion and injection molding are practical and more efficient on a commercial

scale. They are equipped to process large amount of material with ease making the overall process efficient. Solvent casting and resin curing methods work on a smaller scale however, they are not preferred commercially as scaling up of these methods to a commercial level will not be as efficient as injection molding and/or melt compounding. Another factor to look into in the fabrication process is addition of external additives as compatibilizers. Maleic anhydride grafted polypropylene (MAPP) is the most commonly used additive reported in most of the studies using a polypropylene matrix.

1.5. Composite Properties

1.5.1. Mechanical Properties

The mechanical properties of the composites are determined by testing the composites for tensile strength, tensile modulus, flexural strength and modulus, impact strength, elongation on break. There are several factors like filler loading rate, interfacial adhesion, presence of compatibilizer, distribution of filler, particle size, carbonization temperature etc., that play an important role in determining the mechanical properties of biocarbon filled polymer composites.

The amount of filler in a composite is an important factor determining the properties of the composites. The quality of a composite depends a lot on the amount of filler incorporated in it. Das, Bhattacharyya, et al. 2016 (5) characterized their composites for tensile strength and flexural strength. The tensile strength results show that the composites with 15% biocarbon exhibited

higher stress yield compared to higher loading rates (5) The composites with higher quantities of biocarbon (25, 30 and 35%) showed fractured earlier showing semi-brittle behavior under tensile stress (46). The tensile strength of the composites however did not undergo a drastic change and the values were close to the tensile strength value of polypropylene. The tensile modulus values however showed a positive trend with increase in the amount of filler. The modulus value for the composite with 35% biocarbon was recorded to be 3.82 GPa (5). This property is attributed to the high surface area of biocarbon developed as a result of carbonization at 900°C, enabling better stress transfer between polypropylene and biocarbon (5). Stiffness of polypropylene increased steadily on addition of biocarbon. The increased stiffness resulted in lower percentage elongation for composites with higher biocarbon values. The composites with 15% biocarbon reported the best elongation. Both flexural strength and modulus of the composites showed an improvement with the addition of biocarbon. The factors affecting flexural strength of a composite are particle dispersion, wetting and infiltration of polymer in filler particles (5). High surface area of biocarbon resulted in physical/mechanical interlocking between polypropylene and biocarbon, as molten polypropylene entered the pores present on biocarbon surface. This interlocking caused a reinforcing effect in neat polypropylene and facilitated stress transfer (5). Khan et al. 2017 (30) observed transition of a brittle epoxy into a ductile matrix on addition of any carbon filler in small amounts. The addition of carbon fillers irrespective of the amount enhanced the mechanical properties of the composites (30). However,

an increase in filler content was associated with the decline in tensile strength and elongation of the composite, this property has been consistent in most of the studies addressed here. Improved mechanical properties is attributed to the stress transfer mechanism between the filler and matrix obstructing failure. It is stated that addition of biocarbon also improved the cross linking of epoxy matrix blocking the molecular motion of the polymer adding to the strength of the matrix (47,48). Enhanced thermal conductivity of the composite due to the higher thermal conductivity of filler leads to lower concentration or faster diffusion of heat generated due to plastic deformation at a given section improving the ability to tolerate higher strain before reaching the glass transition temperature (T_g) (49). The Ultimate Tensile Strength (UTS) of the composites improved at lower filler loading and showed drastic decline with increasing filler loading rate, this trend was also consistent with the load bearing capacity of the composite. The deterioration in the load bearing capacity of the composite was due to the transition of behavior of matrix from plastic to semi-brittle (46). With higher filler concentration the stacking and cross linking of polymer increases leading to a brittle behavior (50).

Interfacial adhesion is a phenomenon that is observed when two or more components are mixed with each other (51). Good interfacial adhesion usually means better dispersion of filler in the matrix, leading to improved composite properties. Good interfacial adhesion is achieved when there is no or negligible polarity differences between the components of a composite. In case of polarity differences additives like compatibilizers can be included in the composition to

improve the compatibility between the matrix and the polymer by serving as an adhesive between the two. Composites can also be developed using additional fillers that can be biomass based or inorganic, such composites are known as hybrid composites. These composites are developed with an intention to study the effect of filler individually and collectively on composite properties. A very commonly used compatibilizer is Maleic anhydride grafted polypropylene (MAPP), that is usually used in composites developed using polypropylene matrix. The presence of MAPP reinforces the interfacial adhesion in the composites by forming a bond between the hydroxyl groups of the compatibilizer and polypropylene matrix(26). Das, Bhattacharyya, & Sarmah, 2016 (40) developed hybrid composites filled with wood and 24% biocarbon along with compatibilizer MAPP(0-3%) in a polypropylene matrix. They reported improved tensile strength in composites with increasing compatibilizer content. The highest value for tensile strength was obtained for composite samples with 3% MAPP and the lowest for composites with no compatibilizer (40). Even at 1% compatibilizer loading rate, a significant improvement in composite properties was observed, indicating synergistic effect of MAPP on composite mechanical properties. The tensile strength of composites mainly depends on the quality of bonding that includes chemical, physical, adsorption, electrostatic forces etc., between the polymeric matrix, the filler and the additives in the composite (52). The tensile modulus values for the composites were much higher when compared to neat polypropylene. The statistical analysis of the tensile modulus values for the composites with and without MAPP did not show much difference

indicating the occurrence of higher values irrespective of the compatibilizer being present or absent (40). The percentage elongation values for the composites were low due to the increased brittleness introduced upon adding biocarbon (53). The flexural strength and modulus values for the composite were reported to be significantly higher compared to neat polypropylene; this improvement is attributed to addition of wood and biocarbon that improved the flexural properties. The flexural strength of a composite depends on factors like particle dispersion, wetting and infiltration of molten polymer in the filler particles (40). The interlocking between the polymer matrix and filler particles resulted in the improved flexural strength of the composites. Impact analysis of a composite gives an idea of the interfacial adhesion between the polymer and the filler. Wambua, Ivens, & Verpoest, 2003 (54) stated that composites with poor interfacial adhesion show fiber pull out and expend more energy while composites with good interfacial adhesion show fiber fracture and dissipate less energy (54). Therefore a composite with good interfacial adhesion will have lower values for impact strength (40). The impact strength results for the composites indicate good interfacial adhesion between the polymer and filler; this phenomenon is not affected by the presence and amount of MAPP. The micro-hardness of the biocomposites were analyzed using Vickers hardness test. The test results showed the positive impact of addition of biocarbon with better hardness in the composites in comparison to neat polypropylene. The composites without MAPP had lower hardness value in comparison to the composites with MAPP, as the presence of MAPP resulted in better adhesion

between wood and polypropylene specifically, as the lack of functional groups on the surface of biocarbon resulted in no bonding between the biocarbon filler and MAPP (40). As a result, the effect of MAPP was more pronounced in regions of the composite with a higher wood filler concentration respectively. The Figure 2 below indicates that the mechanical properties did not express a drastic change with the presence of MAPP. This indicates compatibilization, even though its synergy doesn't necessarily have a significant impact on the composite properties in this study (40).

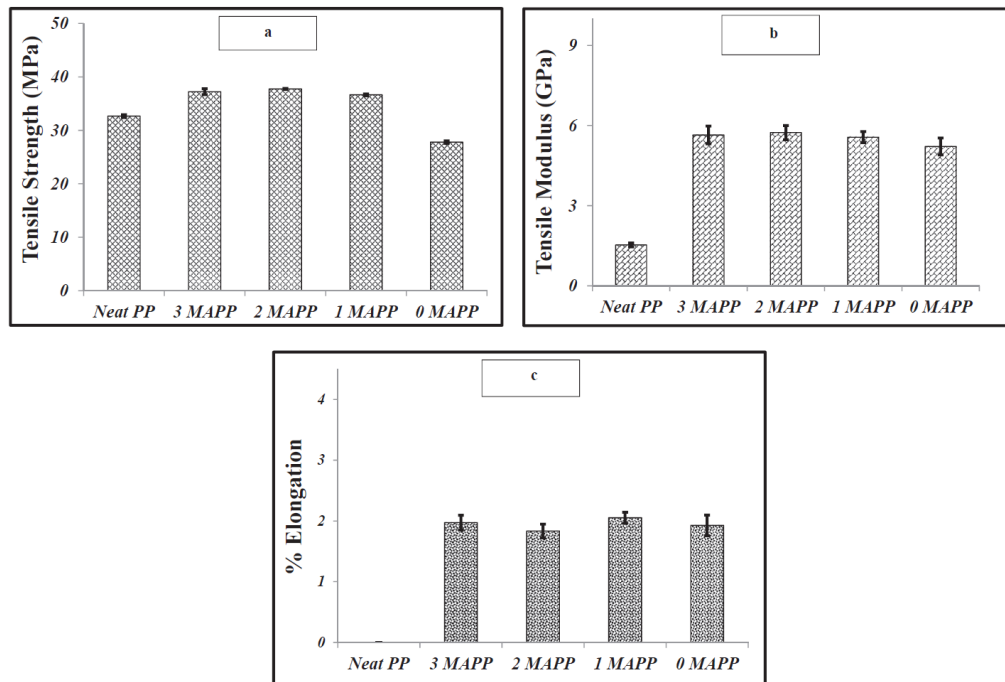


Figure 2. The mechanical properties of biocarbon filled polypropylene composites a) Tensile strength, b) Tensile modulus and c) Percentage elongation (55). Figure is taken from reference (55) with permissions to reuse from Elsevier Publications 2016 .

Ikram et al., 2016 reported the tensile strength of the composites having MAPP to be better than those not containing the compatibilizer. Another factor attributing to good tensile strength is the mechanical interlocking between the PP matrix and biocarbon filler facilitated by the high surface area of biocarbon, due to the absence of functional groups on its surface. Similar trend was observed for tensile modulus. In case of tensile modulus, the presence or absence of wood played a major role. Presence of wood improved the tensile modulus of the composite as distance between the particles was reduced improving the rigidity and stiffness of the composite (56). The samples containing higher amount of wood and biocarbon had improved modulus values (26). Flexural strength of the composites followed similar pattern as tensile properties due to the presence of coupling agent MAPP. An important physical process contributing to this trend is the infiltration of polypropylene matrix in the pores present on biocarbon surface. Like tensile properties presence of wood enhanced the flexural properties of the composites. Das, Sarmah, & Bhattacharyya, 2016(57) developed biocomposites having a polypropylene matrix filled with biocarbon at different loadings (6, 12, 18, 24 and 30 wt%), wood and coupling agents. The modulus and hardness assessment of each component indicated that neat propylene had the highest load vs displacement curves exhibiting a plastic behavior compared to wood and biocarbon(57). The behavior of biocarbon was found to be more elastic compared to the behavior of wood due to the presence of C-C covalent bonds (57). The results for hardness

and modulus value for neat PP was reported to be 1.5 GPa and those for wood and biocarbon were reported to be 5.6 GPa and 5 GPa (57). The slightly lower modulus value of biocarbon when compared to wood can be attributed to the increased stiffness caused by degradation of biopolymers like cellulose in the process of carbonization (58). The indentation of the composites with varying filler loading indicated the influence of individual mechanical properties of wood and biocarbon on the mechanical properties of the composite at areas near the interface. Incorporation of wood and biocarbon into the matrix reinforced the hardness of the matrix improving the modulus of the composites. Enhanced reinforcement is a result of mechanical interlocking of polymer with biocarbon owing to enhanced matrix wettability due to high surface area of biocarbon (59). The bulk properties of the composites were predicted using various models like rule of mixtures, Halpin-Tsai-Nielsen and Verbeek models. To overcome the possible shortcomings of nanoindentation, the composite samples were characterized for Vickers hardness test. The hardness of the composites improved with the increase in biocarbon content, which was an expected phenomenon. The bulk hardness of the composites was predicted using the rule of mixtures and it was observed that a good correlation was found between the predicted values and the values obtained using Vickers hardness test (57). Similarly, Das, Sarmah, & Bhattacharyya, 2016 (57) stated that a strong positive correlation was found between the predictive models (rule of mixtures, Halpin-Tsai-Nielsen and Verbeek models) and experimental values for flexural moduli of the composites, a moderate correlation was found between the predictive

models and the bulk experimental tensile moduli values. This study was a novel approach taken by the researchers to study the individual components as well as the composites. It was concluded that, prediction of overall composite properties requires determination of other factors like aspect ratio and filler orientation which cannot be assessed with nanoindentation, hence the indentation study worked better for individual components rather than the whole composite. Behazin, Misra, & Mohanty, 2017a (36), designed an experimental study to investigate the effect of biocarbon particle size, type of compatibilizer and concentration of compatibilizer on polypropylene/biocarbon composite properties. The results for mechanical properties were reported for matrix alone and for biocomposites as well. The matrix which was composed of polypropylene hardened by POE showed higher stiffness and lower impact toughness when MAPP was used as compatibilizer instead of MAPE(36). Similar trends are also observed for tensile properties. On an average the addition of compatibilizer without a filler was observed to be detrimental to the properties of the composites. In biocomposites, filler particle size, compatibilizer type and concentration had impact on the composite stiffness and impact properties. It was observed that there was a steep increase in the Young's Modulus of the composites at a concentration of 5 wt% of MAPP (36). The impact of factor "compatibilizer type" was the most pronounced compared to the other two. Improvement in mechanical properties was seen for larger particle size in the presence of MAPP. H. Zhang et al., 2018 (7) reported the results for mechanical properties of polypropylene (PP)/bamboo particles (BP)/ultrafine bamboo

biocarbon (UFBC). With the increase in content of UFBC from 15% to 30% there was a considerable improvement in the tensile strength and elongation at break values of the composite. This enhancement is assumed to be contributed by the intrinsically strong biocarbon that is adding to the tensile strength of the composites by synergistic interaction between the three components. The elongation at break also experienced similar trend. The composites were prepared with two different particle sizes of biocarbon P1 and P2. The composites filled with P2 showed better properties compared to composites filled with P1. The flexural strength of the composites showed an improvement at a loading of 20% for biocarbon particle size P1 and no difference was observed for filler loading lower or higher than 20%. For composites filled with biocarbon particles P2 showed a steep increase in flexural properties with increase in biocarbon loading. The moisture resistance of the composites was also evaluated. The moisture resistance of the composites seemed to be increasing at 5% biocarbon loading but then with increasing biocarbon loading a decline in the moisture resistance was observed.

The properties of biocarbon filled composites can be altered by the carbonization temperature of the filler. The carbonization temperature of filler can alter the surface area and the functionality of biocarbon greatly. Several studies have been designed around this particular factor. Behazin, Misra, & Mohanty, 2017 studied the mechanical properties of biocomposites having miscanthus biocarbon as filler. The tensile strength of the composites was reported to be lower than toughened polypropylene matrix. The tensile modulus values on the

other hand were higher for the composites having High Temperature Biocarbon (HtBioC) in comparison to the toughened matrix and composites having Low Temperature Biocarbon (LtBioC). The biocarbon used in the composites have higher modulus (60) compared to the polypropylene used in the matrix resulting in composites to have higher modulus. The highest value for tensile modulus was seen for biocomposite having 20% HtBioC filler. This property however was observed only in composites with 20% filler content, which is due to the encapsulation of hard filler particles with softer phase of the hardening agent Polyolefin elastomer (POE) hindering stress transfer to the filler (61). In case of composites having 20% biocarbon in composition as biocarbon has higher ratio the effect of the modulus of filler was more visible. Elongation at break and impact strength of the composite showed a declining trend and had significantly lower values when compared to the hardened matrix. This is the result of the incompatibility of the matrix and filler, predominantly in the case of LtBioC due to the presence of functional groups on its surface. Composites having HtBioC showed higher values in comparison to LtBioC composites. The effect of carbonization temperature is quite prominent as indicated in Figure .3.

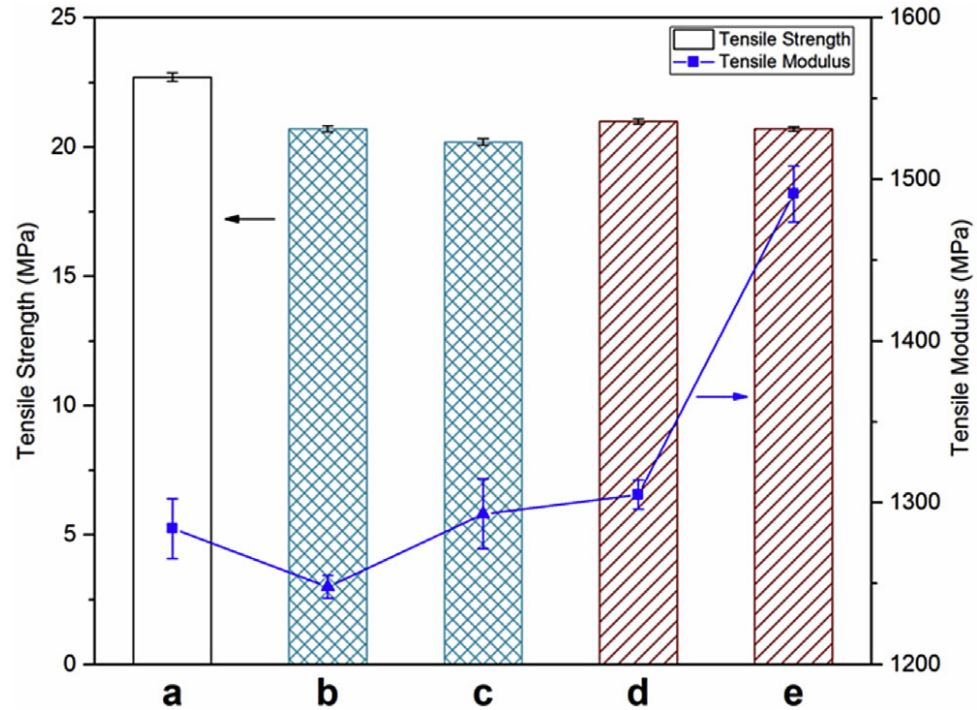


Figure 3. The tensile properties of biocarbon filled composites, a) neat polymer, b) & c) LtBioC filled composites and d) & e) HtBioC filled composites. The tensile properties of composites filled with HtBioC was shown to be better than neat polymer and composites filled with LtBioC(37). Figure is taken from (37) with permissions to reuse from Elsevier publications 2017.

Ogunsona, Misra, and Mohanty 2017a (62) developed a similar study exploring the effect of biocarbon carbonization temperature in biocarbon filled nylon 6 composites to study the impact of interfacial adhesion on the composite properties. A 20% increase in the tensile properties of composites filled with B1 was observed, the increase is attributed to good interfacial adhesion between

the polymer and filler facilitated by enhanced wetting of filler. The enhanced interfacial adhesion resulted in efficient stress transfer between the polymer and filler improving the mechanical properties (62). In composites filled with B2 the increase was of 12.6% and a significant difference was not observed between the value obtained for the composite and neat nylon 6, however a huge standard deviation value was recorded. This was reported to be a result of improper wetting of the filler by the polymer matrix causing irregular stress transfer, hence the result. A hybrid composite was developed combining B1 and B2 filler in nylon 6 matrix and was characterized. The value of tensile strength of the hybrid composite was a value falling in between the values recorded for B1 and B2. It is stated that the strength value of the hybrid composite was more dependent on B1 as it comprised 50% of the filler content (62). On incorporation of B1 and B2 an increase of 30% and 26% in the flexural strengths of composites was observed. The flexural strength values follow the similar trend as observed in tensile strength values as the enhancement of value is higher in B1 filled composites compared to B2 filled composites, this variation is again attributed to the interaction between the filler and matrix facilitating transfer of stress and relaxation owing to better flexural properties (62). As observed before, in this case as well better interaction between nylon matrix and B1 has resulted in improved flexural properties in the composite. The tensile modulus of the composites also observed an increase in value compared to neat polymer, however the improvement was not reflective of the huge difference in modulus values recorded for the biocarbons B1 and B2 (62). In the case of tensile

modulus the difference in wetting of filler by molten polymer has been reported to have insignificant effect on the difference of values (56). Similar results were obtained for flexural modulus values as well. The impact strength values however showed an interesting trend, as composites filled with B2 showed a drastic decrease in impact properties. The decrease was recorded to be almost 32%, while for composites filled with B2 a huge difference was not observed when compared to neat polymer(62). In the hybrid composite a pattern like B1 filled composites was observed. The lower values of impact strength of B1 filled composites is actually attributed to good interfacial adhesion between polymer and filler as a good adhesion results in transfer of crack energy through the composite and due to absence of voids or deformities the crack energy cannot be dissipated resulting in inferior impact properties (62). In case of composites filled with B2 the poor interfacial adhesion between matrix and filler forms many voids in the interface resulting in energy dissipation also lowering of glass transition temperature T_g in these composites enhances the matrix ability to plastically deform improving the impact properties of the composite. The elongation at break values reduced on addition of biocarbon filler. However, the values for B2 filled composites were higher compared to B1 filled composites due to the poor interfacial adhesion, allowing easier flow of polymer chains. This is also supported by the lower T_g value of composite on addition of biocarbon (62). The difference in interfacial adhesion results in difference in mechanical properties of respective composites. This difference in property can be applied in defining different functions for the composites based on the mechanical

performance. Like B1 filled composites can be used in applications which require higher tensile strength and modulus, similar to applications implementing use of talc filled composites in automobile components (62). While B2 filled composites can be applied to use where composites having high impact resistance with moderate strength and modulus values are required (62). Giorcelli et al. 2019 (63) carried out a study to determine the applicability of biocarbon as a cheap and environmental friendly filler to improve properties of epoxy polymer. The mechanical analysis of the composites showed that incorporation of 1% of biocarbon filler did not affect the ductility of the polymer much, at loading rates of 2% and 4% wt of both biocarbon and biocarbon(HT) the brittle matrix became ductile improving the elongation of the composite (63). The tensile strength analysis showed that even at 1%wt biocarbon loading the load bearing capacity of the composite increased to 63%, compared to neat polymer. The improved properties are attributed to the transfer of stress from the matrix to the filler. A phenomenon of cavitation or debonding of polymer on application of stress have been observed (63). The phenomenon of cavitation and filler pull out is considered the reason for improved mechanical property of the composite (64,65). Another reason attributed to the enhancement of tensile strength is the crosslinking between the polymer and the filler which is believed to be effective in blocking the molecular motion of the polymer molecules and enhancing the strength of the matrix as well as the composite (47,48). The Young's modulus of the composite saw an improvement even at 1%wt biocarbon and biocarbon (HT) loading, the values were enhanced by 33% and 20% biocarbon addition

enhanced it by 41% only which is very close to the value achieved using 1% filler loading (63). Overall, an improvement in the stiffness of composite was observed on addition of biocarbon and biocarbon (HT) filler. Tensile toughness is another property of composite that was analysed in the study. Tensile toughness is defined as the capacity of the composite to withstand load before breakage or the energy per unit volume needed to break the composite (63). Addition of 1% of biocarbon filler did not show much difference, while at 2%wt filler loading the value for tensile toughness saw 11-fold increase. However, increase in the loading rate of filler did not further make any improvements rather it deteriorated. This is attributed to the fact that a semi brittle behavior is observed as large chunks of filler are unevenly dispersed through the matrix, usually at higher loading rates of filler (46,66).

Bartoli et al. 2020 designed a study to investigate the effect of treatment temperature and heating rate of biocarbon carbonization process. They produced biocarbon using different carbonization temperatures and heating rates. This biocarbon was incorporated at 2% loading rate into epoxy matrix to study the effect of the pyrolytic thermal history of biocarbon on composite properties (11). It was observed that composites incorporated with biocarbon produced at treatment temperature 400°C using lower heating rates like 5°C and 15°C per minute had a detrimental effect on the Young's modulus (YM), similar effect was observed for Ultimate Tensile Strength (UTS) (11). Higher heating rate of 50°C had a synergistic effect on the Young's modulus (YM) and Ultimate Tensile Strength (UTS), the elongation of composite dramatically

reduced on incorporation of biocarbon produced at a heating rate of 50°C. At 600°C treatment temperature better results were obtained for biocarbon produced using lower heating rates. A significant effect of different heating rates on the young's modulus and the Ultimate Tensile strength were not observed for composites filled with biocarbon carbonized at 1000°C and 800°C respectively. The elongation of composites was observed to have improved on incorporation of biocarbon produced using higher treatment temperatures (11). This is attributed to the different morphologies of biocarbon which is obtained on using different carbonization temperatures (67). Q. Zhang, Xu, et al. 2020 (69), developed high density polyethylene composites filled with rice husk biocarbon. The biocarbon was carbonized at 200, 300, 400, 500, 600, 700, 800 and 900°C to study the effect of carbonization temperature on biocarbon morphology(69). A comparison between rice husk filled composites and rice husk biocarbon filled composites having filler and matrix at one-to-one ratio (50% filler loading) was done to compare the physical properties of the composites. The tensile properties of the biocarbon filled composites was observed to be better than both neat HDPE and Rice Husk (RH) filled composites. The reason for poor tensile properties of rice husk filled composites is the incompatibility between the matrix and the filler, due to the polar nature of rice husk (68). Upon carbonization the polarity of the filler goes down due to the removal of polar functional groups, this phenomenon improves as the temperature of carbonization increases. A mechanical interlocking is created between the molten polymer and the biocarbon as it enters the pores present on the surface of biocarbon improving

the mechanical properties of the composites (5). In this study a decline in tensile strength was observed for composites filled with biocarbon carbonized at temperatures 700, 800 and 900°C. This decline is attributed to deformation of pores on biocarbon surface impacting the mechanical interlocking therefore the tensile properties(69). The Young's modulus (YM) for the composites also followed similar trend, the highest YM value of 1.87GPa was recorded for biocomposites filled with biocarbon produced at 500°C treatment temperature, this is also attributed to the pore structure of biocarbon which improves the stiffness of composite by mechanical interlocking between the polymer and the filler (69). The viscoelastic behavior of the composites was studied using Dynamic Mechanical Analysis (DMA). It was observed that the storage modulus of the composites decreased on increase in temperature throughout the experiment. This was observed due to the increase of thermal movement of thermoplastic matrix molecules in the composite (69,70). It was reported that the storage modulus of all the composites was higher compared to neat HDPE, the highest modulus value was reported for composites filled with biocarbon carbonized at 600°C as a result of mechanical interlocking between the matrix and filler. The creep compliance of the composites was also determined in the study, the creep behavior curve also presents information on the elastic deformation, viscoelastic deformation and viscous deformation of the composites (44). Improved creep resistance was observed in the composites filled with rice husk and rice husk biocarbon when compared to HDPE, the creep resistance of biocarbon filled composites was better than rice husk filled

composite (69). The relaxation modulus values were observed to have improved for the biocarbon filled composites compared to rice husk filled composites and neat HDPE. The relaxation modulus provides information on the stress relaxation behavior of polymers and composites (71).

Filler particle size is another important factor that contributes to composite properties. The shape and size of filler can greatly alter composite properties. It is often observed the higher the aspect ratio of filler the better the properties of the composite. The effect of variable particle size of biocarbon on the mechanical properties of nylon composites was studied by Ogunsona, Misra, and Mohanty 2017 (38). The tensile modulus of the composites showed improvement when composites were filled with milled biocarbon having particle size $<500 \mu\text{m}$. The modulus however kept on deteriorating as the particle size kept reducing. The tensile modulus however was observed to be increasing in the composite filled with milled biocarbon compared to crushed biocarbon, which is believed because of greater interfacial adhesion between the matrix and the filler (72). However, as the particle size of milled biocarbon kept decreasing the modulus also kept decreasing. A reason that is stated in literature for the decline in tensile strength is aspect ratio of filler. A larger aspect ratio is believed to have a synergistic effect on the tensile modulus of the composite. Higher tensile modulus is observed in composites with filler having higher aspect ratio compared to composites with filler having sheet like or globular structures (73). Similar trends were observed for tensile strength of composites as well. On addition of crushed biocarbon, a decline in tensile strength was observed unlike

when milled biocarbon was added and an improvement in the tensile strength of the composite was recorded. A decline in tensile strength was observed as the particle size of biocarbon kept reducing. Addition of crushed biocarbon results in mechanical failure of composite samples due to the presence of micropores on the surface of biocarbon that created weak points throughout the composite (38). Reduced aspect ratio of particles on reduction of particle size results in increased failure due to elastic deformation in the direction of force (56). Flexural properties of the composite also showed similar results. However, the overall flexural properties of the composites were better than neat PA 6, 10. The composites filled with milled biocarbon having a particle size $<500\mu\text{m}$ showed the best properties, a further decline was observed as the particle size kept decreasing. The impact properties on the other hand showed a different trend and it was observed that on addition of milled biocarbon the impact properties improved, and it kept improving as the particle size reduced progressively. A reason attributed to this is the reduction in ductility of the composite and hampers plastic deformation in the composite (38), reduction in particle size promotes shape homogeneity and reduction in defects also improving the impact properties of the composite. The incorporation of more globular particles results in higher energy dissipation and higher impact strength owing to the shape of the filler (74). Behazin, Misra, & Mohanty, 2017a (36), designed an experimental study to investigate the effect of biocarbon particle size, type of compatibilizer and concentration of compatibilizer on polypropylene/biocarbon composite properties. The results for mechanical properties were reported for matrix alone

and for biocomposites as well. The matrix which was composed of polypropylene hardened by POE showed higher stiffness and lower impact toughness when MAPP was used as compatibilizer instead of Maleic Anhydride grafted Polyethylene (MAPE) (36). Similar trends are also observed for tensile properties. On an average the addition of compatibilizer without a filler was observed to be detrimental to the properties of the composites. In biocomposites, filler particle size, compatibilizer type and concentration had impact on the composite stiffness and impact properties. It was observed that there was a steep increase in the Young's Modulus of the composites at a concentration of 5 wt% of MAPP. The impact of factor "compatibilizer type" was the most pronounced compared to the other two. Improvement in mechanical properties was seen for larger particle size in the presence of MAPP. The particle size of filler was the next most influencing factor after compatibilizer type in this study. It was observed the particle size between 106-125 μ m gave the best results for mechanical properties of the composites (36). Ferreira et al. 2019 (39) characterized the three different composites filled with carbon black, bagasse biocarbon milled for 72 h (SBB-72h) and milled and treated biocarbon(rSBB-ABL-72h) at 1% and 5%wt loading rates. The study reported close values for young's modulus for all the composites, however, the values for composites filled with only milled biocarbon was lowest among the three. A better adhesion between the rSBB-ABL-72 h biocarbon and the matrix is attributed to the lack of oxygenated carbon groups (39). The authors stated that factors like polarity difference between matrix and filler, particle size and morphology of additives

have a predominant effect on the mechanical properties of the composites (62,75,76). It was observed that the mechanical properties of composites filled with rSBB-ABL-72h biocarbon were relatively more similar to the values obtained for carbon black filled polyethylene composites, compared to SBB-72h biocarbon filled composites (39).

Li et al. 2016 (35) developed UHMWPE composites filled with biocarbon with segregated filler network where the filler network is confined in a certain space and is not dispersed throughout the composite volume. . An increase in the tensile modulus of the composites was observed with increase in filler loading rate, at the highest loading rate of 9%wt a Young's modulus value of 388.4MPa was recorded which is 18.9% higher than neat polymer (35). The tensile strength however showed improvement on addition of filler, at 3% filler loading, an increase of 10% was observed compared to neat UHMWPE, but it kept deteriorating with increasing loading rate. The improvement in tensile properties of the composite is due to the good interfacial adhesion between the charcoal filler and UHMWPE polymer matrix (35). The segregated networks of filler have added stiffness to the composite by restricting the movement of polymer chains in the composite (77,78). The occurrence of voids along the segregated pathways on increase of filler content was observed leading to the impairment of mechanical properties (35). A decrease in ductility was observed in composites, compared to neat polymer matrix. Behazin et al., 2018 (4) studied the mechanical properties of biocarbon filled composites heat aged for 1000 hours. The mechanical testing results were compared to the specified values set

by automobile manufacturers, the values were set precisely $\pm 15\%$ of the set values. The mechanical properties of the composites remained same through the periods of heat aging except for the control sample which showed about 85% failure at 500 hours of aging (4). Behazin et al., 2018 reported no loss in tensile properties of heat stabilized samples throughout the heat aging period and reported around 5% improvement in yield strength compared to the lab conditioned samples. This improvement is attributed to increase in the β crystals content. Compared to the laboratory conditioned samples the heat aged samples irrespective of the presence of stabilizers showed reduced impact properties. Arrigo, Bartoli, and Malucelli 2020 (43) reported enhancement of the tensile modulus for both the composites fabricated using melt mixing and solvent casting. The increase is attributed to the uniform dispersion of filler through out the matrix (43). A decline in tensile strength of the composites was reported, premature failing of the composites due to presence of voids was stated as the reason by the authors (43).

Overall improvement in composite mechanical properties was observed on incorporation of biocarbon into the composite system. Compatibilizer was shown to be helpful in improving properties due to the lack of functional groups in biocarbon, however, the porous structure of biocarbon also does a great job in reinforcement of matrix (26). Biocarbon produced at higher temperatures have showed better interfacial adhesion compared to biocarbon carbonized at lower temperatures due to the abundance of pores on biocarbon surface attributes to the better quality of biocarbon filled composites. A considerable reduction in the

ductility of the composite samples is observed as addition of biocarbon makes composites stiffer than the neat polymer. This property is further enhanced by addition of natural additives like wood fiber or flour. Particle size of biocarbon has not been selected as a crucial property but has been reported to have an impact on the final properties of the composites (26,79). The DMA also provided an overview of the thermomechanical properties of the composite. It provides an opportunity to look at the rheology and mechanical properties of the composite with respect to temperature. An improvement in viscoelastic properties was also observed on incorporation of biocarbon(69). The mechanical properties as reported in the studies addressed here is summarized in Table II.

Table II. Mechanical properties of biocarbon filled polymer composites.

Polymer	Effective Biocarbon loading rate (%)	Young's Modulus	Flexural Strength	Impact Strength	Contributing Factor	
Polypropylene	35	3.82 GPa	58.26 MPa	Not reported	Loading rate of biocarbon	(5)
Polypropylene	24	37.76 MPa	75.12	~ 3 KJ/m ²	Presence of MAPP and interlocking between polymer and filler	(40)

UHMWPE	9	388.4 MPa	Not reported	Not reported	Interfacial Adhesion between matrix and filler	(35)
Polypropylene	Not reported	~ 5 GPa	~ 70 MPa	Not Reported	Presence of MAPP and porous structure of biocarbon	(26)
Polypropylene	24	3.5 GPa	Not Reported	Not Reported	Porous structure of biocarbon facilitating mechanical interlocking	(57)
Polypropylene	20	~1500 MPa	Not Reported	50 J/m	Higher carbonization temperature	(37)
Polyamide 6,10	20	~ 2.5 GPa	~ 110 MPa	~ 60 J/m	Particle size of biocarbon	(38)
Nylon 6	20	3.3 GPa	140 MPa	50 J/m	Carbonization temperature of biocarbon	(62)
Polypropylene	10	460.59 MPa	Not reported	~18 KJ/m ²	Improved interfacial adhesion on biocarbon addition	(10)
Polyethylene	5	25 MPa	Not reported	Not reported	Lack of functional groups on biocarbon surface	(39)

1.5.2. Thermal Properties

Addition of biocarbon to polymers is expected to positively impact the thermal properties of polymer matrix. The thermal stability, melting point, crystalline properties and flammability the composites are analyzed using methods like Thermogravimetric Analysis (TGA), Differential Scanning Calorimetry (DSC), etc.

Thermal degradation studies done of the biocarbon filled composites in the different studies indicated increased thermal stability on addition of biocarbon, compared to thermal degradation of neat polymer. The TGA results reported by Das, Bhattacharyya, et al. 2016(5) indicated that the composites with biocarbon had higher thermal stability compared to neat polypropylene. The temperature of degradation increased with amount of biocarbon in the composite indicating improved thermal properties. The onset of thermal degradation for neat PP was observed at $\sim 390^{\circ}\text{C}$ however, with the addition of biocarbon the temperature for degradation increased to $\sim 412^{\circ}\text{C}$ just at 15% biocarbon content(5). The trend showed an increase with increase in biocarbon content along with increased char or residue. The TGA curves are presented in Figure 4.

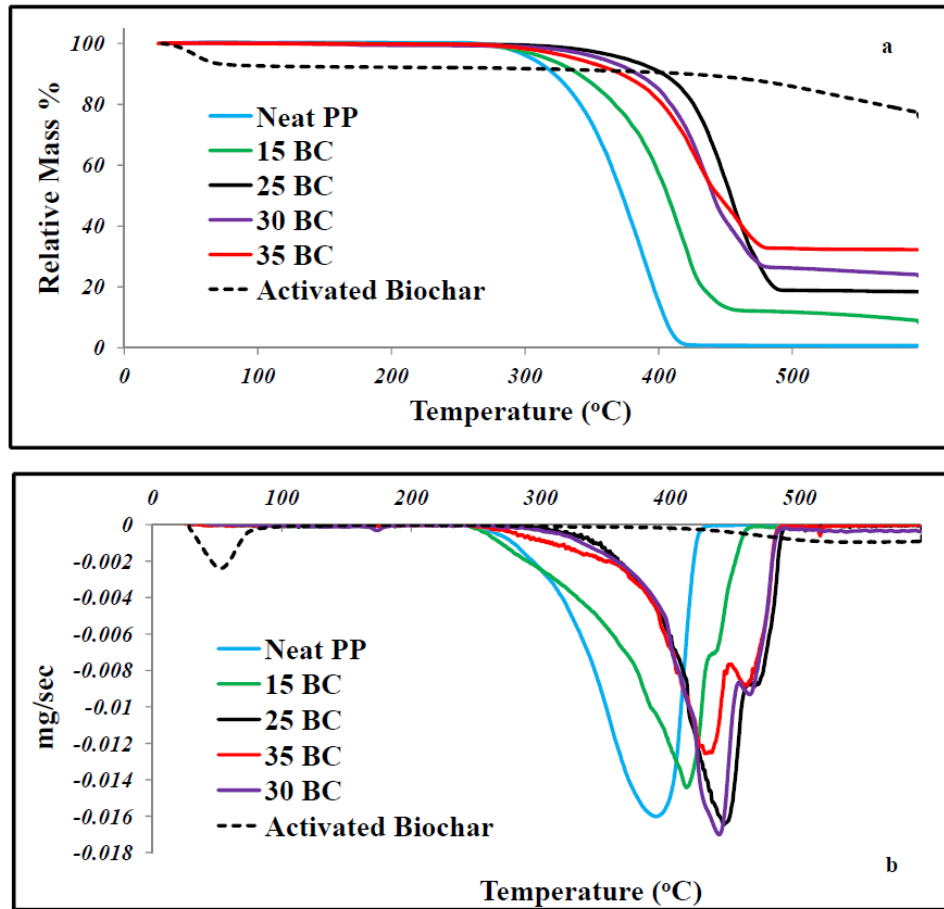


Figure 4. The TGA and DTG curves of biocarbon filled polypropylene composites, a) TGA (mass loss) curve b) DTG curve. A significant shift in the degradation temperature of the composite in comparison to neat polymer can be observed (5). Figure modified from reference (5) with permission from Elsevier publication 2016 to use and modify the Figure.

Das, Bhattacharyya, & Sarmah, 2016c (14), reported the thermal properties of composites composed of 24% biocarbon, wood and MAPP (0-3%). The TGA thermograms showed two peaks of weight loss due to degradation, one at ~370°C and one at ~450°C respectively. The peak at ~370°C is due to the degradation of cellulose in wood, while the peak at ~410 - ~450°C was due to

the degradation of PP(80). In this case the decomposition of composites was inversely related to the amount of MAPP present, that is the composite with 3% MAPP had the lowest degradation temperature. This happens due to the better interfacial adhesion between wood and PP due to the presence of MAPP, resulting in better heat dissipation, and higher the amount of MAPP better the interfacial bonding (40).

Das, Bhattacharyya, & Sarmah, 2016 (26) reported TGA analysis of neat PP and hybrid composites filled with wood and biocarbon. The TGA data showed onset of decomposition of neat PP before 300°C and it leaves no residue post decomposition (26). Due to the presence of thermally stable biocarbon, the composites left a higher amount of residue after decomposition. It was observed that the composites having no wood in them were relatively much more thermally stable when compared to composites having wood as a component. The derivative curves for the composites showed similar trends, the composites not having wood were more thermally stable. The composites having wood had two decomposition peaks, the first peak being for decomposition of cellulose in wood at a much lower temperature like 370°C (26). This peak was not observed for the composites that did not have wood as one of the composite components. However, the overall thermal stability of the composites was enhanced on addition of biocarbon. Li et al. 2016 (35) analyzed the nano bamboo charcoal filled UHMWPE composites with segregated networks for thermal stability using TGA. A shift in thermal degradation temperatures to a higher temperature was observed for the charcoal filled composites indicating improved thermal

properties. No residue was left post the thermal degradation of neat UHMWPE, but an increase in the residue retention was observed for the charcoal filled composites indicating improved thermal stability. Similar results were obtained for thermal properties in studies done by Meng et al. 2013 (81). In the study, the effect of bamboo charcoal powder on the curing characteristics, mechanical and thermal properties of styrene butadiene rubber was studied. The results indicated improved thermal stability of the composite with biocarbon (81). Similarly Abdul Khalil et al. 2010 (82) in the study carbon black derived from natural sources like bamboo, coconut shell and empty palm fruit bunch was incorporated into epoxy matrix to evaluate its effect on mechanical and thermal properties. They also reported improved thermal stability for all the composites filled with the different biocarbons (82). Q. Zhang, Zhang, Lu, et al. 2020 (83) developed rice husk biocarbon filled composites. The TGA analysis of neat HDPE was observed to have a thermal degradation temperature of 480°C (69,84). The DTG curve of the composites filled with biocarbon carbonized at 200°C, 300°C and 400°C showed peaks mainly due to pyrolysis and volatilization of cellulose and hemicellulose at 330°C and 380°C respectively suggesting the incomplete carbonization of feedstock with the respective temperatures (69). The advent of thermal degradation of composites took place at a higher temperature of 490°C, showing improvement in thermal properties of the composites compared to neat HDPE. A higher residue was also retained for biocarbon filled composites, filled with filler carbonized at temperatures 600, 700, 800 and 900°C respectively. This phenomenon indicates increase in the thermal

stability of polymer on addition of filler (69,85). Arrigo, Bartoli, and Malucelli 2020 (43), reported the TGA of biocarbon filled polylactic acid (PLA) composites, the TGA was performed by heating the samples to 600°C in nitrogen atmosphere. A weight loss step was observed for solvent cast composites which is believed to be the loss of residual solvents from the films (86). A decrease in degradation temperature was observed for both the composites at a higher filler loading rate. This detrimental effect of addition of biocarbon on the thermal properties of PLA has also been reported in the studies Ho et al. 2015 (75) and Moustafa et al. 2017 (87) and the cause is believed to be potassium present in biocarbon which affects the thermal decomposition of polymer matrix (75,87). An increasing phosphorous content can further deteriorate the thermal stability of PLA polymer (43). It is also stated by the authors that the residual hydroxyl groups on biocarbon can lead to hydrolytic and back biting reactions mechanisms in PLA (88,89). Ferreira et al. 2019 (39) studied the effect of the three different fillers carbon black, SBB-72h biocarbon and rSBB-ALB-72h biocarbon on the thermal stability of polyethylene. An improvement in the thermal stability was observed for the composites when compared to neat polyethylene. It is stated that the improvement in thermal properties of biocarbon filled composites is 15% higher than the values reported for commercial carbon black filled composites (39). Similar effect of addition of carbon black nano particles was observed on polypropylene and the enhancement in thermal stability was attributed to changes on the degradation mechanism and kinetics of the polymer on addition of filler (90,91).

The effect of incorporation of biocarbon filler on the melt characteristics and crystallinity of the polymer are analyzed using Differential Scanning Calorimetry (DSC). The results of different studies are summarized here, Das, Bhattacharyya, et al. 2016 (5) reported that the DSC thermograms show no change in the melting temperature of polypropylene but, there was an increase in the energy required to melt the biocarbon filled biocomposites. On the other hand, there was an increase in the crystallization temperature, this is believed to be the effect of the biocarbon particles acting as nucleating agents and resulting in crystal growth. Another phenomenon observed in the biocarbon filled biocomposites was, that the intensity of crystallization peak reduced with the increase in filler quantity. This resulted in less energy required for crystallization. The DSC Thermogram of the polypropylene composites is presented in Figure 5.

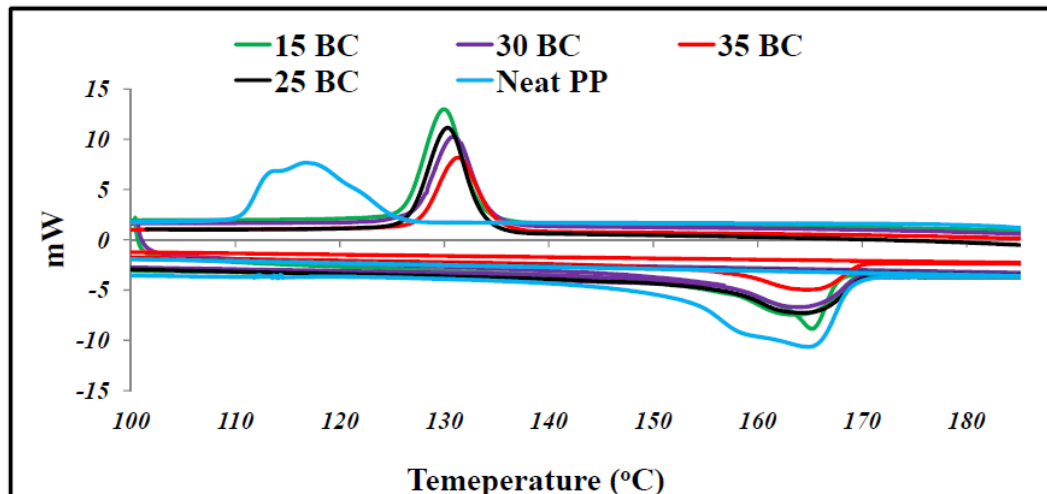


Figure 5. DSC thermogram of biocarbon filled polypropylene composites, no change in melting temperature was observed but a rise in crystallization temperature was observed due to the nucleation effect of biocarbon(5). Figure modified from reference(5) with permission from Elsevier publication 2016 to use and modify the Figure.

The DSC thermograms of the pine biocarbon filled polypropylene composites reported by Ikram et al., 2016 (26) showed no change in the melting temperature in comparison to neat polypropylene. The energy needed for melting however increased on inclusion of thermally stable biocarbon in the composites. A change in crystallization temperature was observed as it moved to a higher temperature due to the nucleation effect of biocarbon resulting in crystal growth. H. Zhang et al., 2018 (7) evaluated the thermal properties of polypropylene/bamboo particles/ultrafine bamboo biocarbon. On addition of biocarbon specifically biocarbon P2 there was an increase in crystallization temperature. This is attributed to the nucleating effect of biocarbon. An improvement in melting

temperature was also reported indicating enhanced thermal stability. The crystallinity of the composites also improved. Nylon composites filled with clay filler also showed similar results when analyzed using FTIR and XRD analysis (92). It was observed that addition of clay filler enhanced formation of γ phase crystals which is a relatively less ordered crystal structure causing reduction in crystallinity of the polymer (62,92). The reason behind the favored phase formation is still not understood, however, probable reasons behind this phenomenon are suggested that conformational changes in the structure are caused by fillers by forcing the amide groups of nylon onto out of plane formation resulting in reduction of hydrogen bonded sheets in the polymer (93,94). Behazin et al., 2018 (4) reported the crystalline phase alterations in control and heat stabilized heat aged composite samples. The DSC thermograms show an increase in the crystallinity of control samples that flattened after 500 hours of aging. The increase in the crystallinity of the control samples is attributed to thermo-oxidative chain scission and annealing. Ferreira et al. 2019 (39) studied the effect of the three different fillers carbon black, SBB-72h biocarbon and rSBB-ALB-72h biocarbon on the thermal stability of polyethylene. An improvement in the thermal stability was observed for the composites when compared to neat polyethylene. It is stated that the improvement in thermal properties of biocarbon filled composites is 15% higher than the values reported for commercial carbon black filled composites (39). Similar effect of addition of carbon black nano particles was observed on polypropylene and the enhancement in thermal stability was attributed to changes on the degradation

mechanism and kinetics of the polymer on addition of filler (90,91). The DSC analysis of the composites reported no major impact of fillers on the transition temperatures of the polymer. The enthalpy values for fusion and crystallization however, were observed to have decreased (39). This change in the polymer is due to the heterogenous nucleation effect onset by the addition of fillers to the polymer (95–97). Even in this scenario the composites filled with treated biocarbon rSBB-ABL-72h produced results similar to the results obtained for composites filled with commercial carbon black, indicating its ability as a potential carbon black replacement (39). Q. Zhang, Zhang, Lu, et al. 2020, developed high density polyethylene (HDPE) composites filled with rice husk and rice husk biocarbon. Neat HDPE shows endothermic melting and exothermic crystallization characteristics (98), on addition of the fillers rice husk and rice husk biocarbon to the matrix, a shift in the melting and crystallization behavior of the polymer was observed. It was observed that on introduction of filler the melting temperature experienced a decline, while the crystallization temperature was observed to have increased (69). The shift in the crystallization temperature is explained by the nucleation effect of filler on the polymer promoting crystal growth and facilitating early crystallization of HDPE (99). Arrigo, Bartoli, and Malucelli 2020 (43) DSC results stated that in the melt mixing composites a decrease in the glass transition temperature (T_g) and cold crystallization temperature (T_{cc}) was observed, owing to the increased mobility of PLA molecules as a result of degradation during processing (43). The percentage crystallinity of the composite remains unchanged and presents an

amorphous structure (43). The solvent casting composites showed lower T_g , T_c and melting temperature T_m indicating enhanced crystallinity, which was presented in composites with filler loading of 1% and 2.5% (43). At higher filler loadings such a dramatic of crystallinity was not observed as a higher concentration of filler interferes with the process of crystallization (43).

The flammability of composites was studied by Das, Bhattacharyya, et al. 2016 (5), to see if biocarbon acts as a flame retardant and has the potential to replace conventional chemical flame retardants used with polypropylene. The composites were tested for flammability and data for time to ignition (TTI), peak heat release rate (PHRR) and total heat release rate (THR) was obtained. It was observed that the PHRR was significantly reduced on addition of biocarbon. The TTI also reduced with increased biocarbon content. The THR values did not show much change. The CO and CO₂ production was significantly reduced. Addition of biocarbon and wood reduced the PHRR value in composites, this was not in conjunction with the amount of MAPP in the sample. It is believed that the C-C covalent bonds present in biocarbon (100) result in the thermal stability preventing transfer of heat to the polypropylene matrix. This phenomenon is the evidence for the use of biocarbon as a fire retardant additive and can replace conventional fire retardants which compromise the mechanical properties of the composite (40). Das, Bhattacharyya, & Sarmah, 2016 reported significantly lower production of CO₂ and CO, which is attributed to the presence of thermally stable biocarbon in the composites. On addition of wood and biocarbon the PHRR value of neat PP is reduced by almost 50% due to the formation of a layer

of char on the surface of the polymer hindering heat transfer (26). The composites not containing wood had slightly higher values for PHRR and THR compared to those containing wood, as presence of lignin in wood facilitates char formation which along with thermally stable biocarbon does a great job in hindering heat transfer enhancing thermal stability. Compared to neat PP the TTI of composites containing wood reduced due to earlier onset of thermal decomposition of wood compared to polypropylene and biocarbon (26).

The effect of biocarbon on the viscoelastic properties of the polymer and the composites can be studied using Dynamic Mechanical Analysis (DMA). These properties essentially indicate the effect of filler addition on the viscosity along with the elastic (properties inherent to the polymer matrix) properties of the composite. The viscoelastic properties of polypropylene composites filled with biocarbon were analysed by Behazin et al., 2017 (37) using Dynamic Mechanical Analysis (DMA). Two glass transition peaks were observed for polypropylene and POE indicating the two polymers being thermodynamically immiscible(37). Addition of biocarbon led to shifting of the peak towards lower temperature, this was more proficient in composites having LtBioC, this was not observed for polypropylene. This is believed to be due to the free movement of POE chains around LtBioC, due to weaker interaction between the two. The Dynamic mechanical analysis (DMA) of the composites showed a shift in glass transition temperature T_g of the polymer to a higher temperature on incorporation of biocarbon. The T_g value kept increasing with the decrease in biocarbon particle size. The Heat Deflection Temperature HDT was seen to increase on addition of

biocarbon filler in the matrix and it kept increasing as the particle size of biocarbon was reduced. This phenomenon is explained to occur due to the reduction of interparticle distance limiting the radius of gyration of polymer, hence making it hard to displace (38).

A shift in the thermal degradation temperature of composites when compared to neat polymer was observed in most of the studies through the TGA analysis. Through DSC it was observed that biocarbon acts as a nucleating agent in the matrix leading to heterogenous crystallization of the matrix and an increase in the crystallization temperature of the polymer. The flammability of the polymer was reduced on incorporation of the biocarbon which will pave a way for enhanced applicability of the polymer.

1.5.3. Electrical Conductivity in Composites

Electrically conductive polymer composites(ECPC) are developed by incorporation of conductive filler material into a non-conductive matrix (101–103). Electrically conductive polymer composites are manufactured using carbon-based fillers like carbon nanotubes, carbon fibers, carbon black etc. Manufacture of these synthetic fillers is quite time and energy intensive. Biocarbon when carbonized at high treatment temperatures above 500°C shows electrical conductivity. Gabhi, Kirk, and Jia 2017 (104), R. Gabhi et al. 2020 (105) in their studies observed that carbonization of wood blocks at higher temperatures of 1000°C leads to a subsequent increase in carbon content in the

char. This temperature of pyrolysis and carbon content plays an important role in electrical conductivity of biocarbon. The study reported that biocarbon monoliths carbonized at 1000°C had electrical conductivity between the range of 2300 – 3300 S/m (105).

Nan et al. 2016 (31) reported electrical conductivity in biocarbon filled composites fabricated using solution casting method. As per their study at a filler concentration of 6 wt. % transition from non-conductive to electrically conductive was observed and at 10 wt. % filler concentration a conductivity of 1.833×10^3 S/cm (31). The electrical conductivity value for composites filled with 10% biocarbon were comparable to electrical conductivity values obtained for composites filled with 1% single walled carbon nanotubes and 6 wt.% graphene. Figure 6 shows the electrical conductivity trend for their composites.

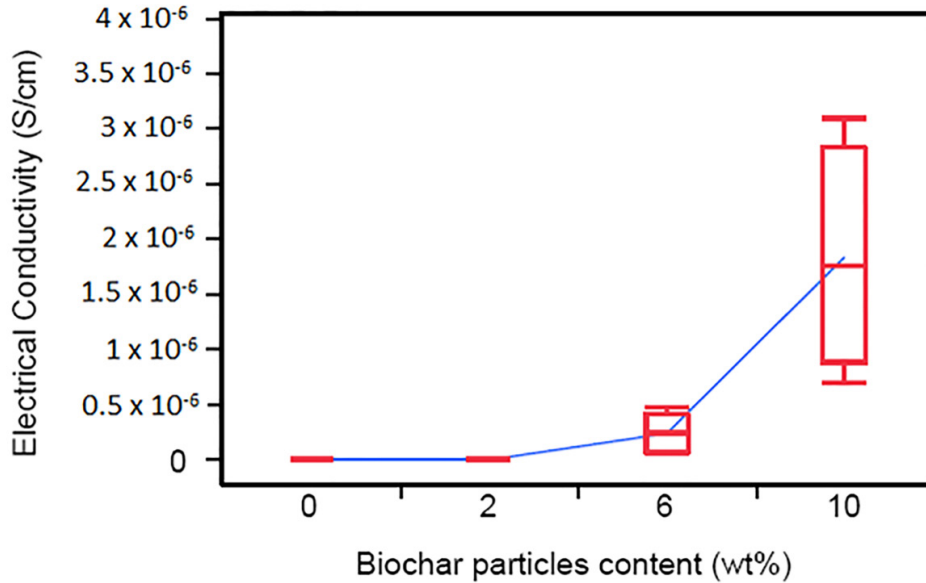


Figure 6. Electrical conductivity of biocarbon filled PVA composites filled with 2, 6 and 10 wt.% biocarbon filler respectively. An increase in conductivity is observed with increase in loading rate of biocarbon (25). Figure taken from reference (25) with permission to use from SagePub Publications 2016.

Li et al. 2016 (35) have reported a typical percolation behavior for their composites by drastic increase in conductivity at a filler concentration of 0.8 and 2.3 vol%. The percolation threshold is the quantity of filler that is needed to make a non-conductive matrix conductive by formation of conducting networks in the composite system (106). The percolation threshold for conductivity was determined to be 2.0 vol% corresponding to 2.6 wt.% of filler, the value was reported to be higher than percolation threshold values reported for Carbon nanotube, Graphene nanosheets and carbon black filled composites developed using the same matrix and composite preparation method (107,108). The high

percolation value is believed to be due to lower inherent conductivity, high particle size and low aspect ratio of filler (35). Electrical conductivity value of 1.1×10^{-2} S/cm was recorded at 7 wt.% charcoal loading composite. Gao et al. 2008 (109) reported a conductivity value of 2.0×10^{-2} S/cm at a percolation threshold of 0.88 vol% for CNT filled UHMWPE composites fabricated using an alcohol assisted dispersion method combined with hot compression method. Yan et al. 2014 (110) were able to a conductivity value of

3.4×10^{-2} S/cm at a filler concentration of 0.66 vol% in reduce graphene filled UHMWPE composites. A higher concentration of filler is required to achieve such high electrical conductivity values in case of charcoal/biocarbon fillers when compared to the studies using synthetic carbon-based fillers. The authors have suggested that even if the loading rate of filler is high in the study the developed composite has a lot of advantages like being sustainable, cheap, less time consuming and has a potential for commercial application (35).

Khan et al. 2017 (30) reported an increase in the real part of dielectric constant and electric conductivity on increasing filler concentration. A higher loading rate of 10 wt.% was needed to observe an enhancement in conductivity of composites, while for MWCNTS the change could be observed even at low concentrations of the filler (111–115). The high aspect ratio of MWCNTs also attribute to the high electrical conductivity compared to the three dimensional structure of biocarbon (30). It was observed that the removal of several functional groups from the surface of biocarbon also contribute to the lower permittivity and

conductivity of biocarbon. Biocarbon 20 wt.% and MWCNTs 4%wt were showed to have similar values for the microwave properties, but, with a very high difference in loading rate (30). The more graphitic structure of MWCNTs compared to the structure of biocarbon could be one of the reasons behind this difference in property as per the authors (30).

Li et al. 2018 (35) developed biocarbon filled polyethylene composites, using biocarbon carbonized at 1100°C. The composites were developed with of 60, 70 and 80 wt.% biocarbon loading rates. The study reported excelled conductivity value of 107.6 S/m at 80 wt.% biocarbon loading rate. This is by far the highest conductivity value obtained for biocarbon filled polymer composites (42).

Giorcelli and Bartoli 2019 (32) developed biocarbon from coffee waste by carbonizing the biomass at 400, 600, 800 and 1000° C temperatures. The biocarbon was incorporated in epoxy matrix to form composites at different loading rates of 5, 10, 15 and 20 wt.%. At 20 wt.% loading rate the electrical conductivity values for composites filled with biocarbon carbonized at 1000°C was reported to be 2.02 S/m which was 4 orders more than the electrical conductivity value reported for 20 wt.% carbon black loading (32). The electrical conductivity values are summarized in Table III.

Table III. Electrical conductivity values reported for biocarbon filled polymer composites.

Polymer	Highest Biocarbon loading rate (wt.%)	Carbonization Temperature (°C)	Fabrication method	Conductivity (S/cm)	
Polyvinyl Alcohol (PVA)	10	Not reported	Solution casting	1.8×10^{-3}	(31)
Ultra-High Molecular Weight Polyethylene (UHMWPE)	80	1100	Melt extrusion and hot compression	107.6	(42)
Epoxy	20	1000	Resin curing	2.02	(32)
Epoxy	20	950	Resin curing	~0.75	(30)

It was observed that biocarbon produced at high carbonization temperatures have a significant impact on conductivity of composites and have done a great job in making non-conductive polymer electrically conductive as indicated in the studies. It is observed that the conductivity follows a positive trend and shows increase on increase of loading rate of filler. Enhanced mechanical properties were reported in all the three studies on incorporation of biocarbon in the polymer matrix. The review for applications of biocarbon as an electrically conductive filler indicated that the research is still in its very initial stages. The number of articles reporting the application of biocarbon as a fortifying filler are much more

compared to papers reporting the use of biocarbon as a electrically conductive filler. This indicates there is so much more to explore with the application of biocarbon as electrically conductive filler.

1.5.4. Morphological Properties

Study of morphology of the composites gives us information on how well the interfacial interaction between the filler and the matrix is. The morphological properties are mainly studied using Scanning Electron Microscopy(SEM). The fractured surface is subjected to viewing under the microscope which gives us information about the filler distribution and interaction with the matrix.

Lignocellulosic Biomass on carbonization results in formation of a honeycomb like structures with pores. When this biocarbon is incorporated into a polymer matrix the molten polymer enters these pores establishing a mechanical interlocking that improves the mechanical properties of the composites (5),(40,69,116).

As described in earlier sections compatibilizers like MAPP have shown synergistic effects on the mechanical properties of composites. The effect of MAPP on the composite mechanical properties can be presented better on a morphological level. The studies discussed in this section explain how presence of MAPP affected the final properties of their respective composites. Das, Bhattacharyya, et al., 2016 reported uniform distribution of biocarbon filler in the PP matrix in 15% biocarbon filled samples, this is attributed to the physical

missing of samples prior to extrusion. Infiltration of biocarbon pores with molten PP was observed in the SEM images, resulting in interlocking between the polymer matrix and the filler (5). This is believed to be the reason behind improved mechanical properties on addition of biocarbon filler to polypropylene matrix. The SEM analysis results for PP, biocarbon, wood and MAPP composites showed mechanical interlocking between biocarbon and polypropylene as the molten polymer has infiltrated the pores present on the biocarbon surface. Due to the absence of functional groups on the surface of biocarbon MAPP assisted chemical bonding of biocarbon and PP could not be formed. In the presence of 3% and 2% MAPP there is a good interfacial adhesion between polypropylene and wood, while in the case of 1% MAPP interfacial bonding between PP and wood was poor. It is suggested that addition of biocarbon can compensate for the poor interfacial adhesion (40). The SEM images of the composites developed by Ikram et al., 2016 showed that the composites having wood and compatibilizer MAPP showed good bonding between the wood and polypropylene matrix where as in the case of composites having wood and no MAPP showed debonding. Mechanical interlocking between the molten polymer and biocarbon due to the abundance of pores on the biocarbon surface resulted in enhanced mechanical properties (5). Behazin et al., 2017a (36) studied the correlation between morphology of the composites and its properties. The evaluation was carried out keeping the compatibilizer concentration constant at 7.5%. When no compatibilizer or MAPE was used as a compatibilizer voids were observed around the filler particles, this was not

observed when MAPP was used (36). In the absence of compatibilizer or in presence of MAPE the rubbery phase of the matrix POE encapsulated the filler particles resulting in the voids, which did not happen in the presence of MAPP. A closer look at the morphology of the composites showed that when MAPE is used, it changes the shape of POE from semi-spherical to elongated fibrillar shape. This change in morphology is considered a reason for improvement of impact properties on addition of MAPE.

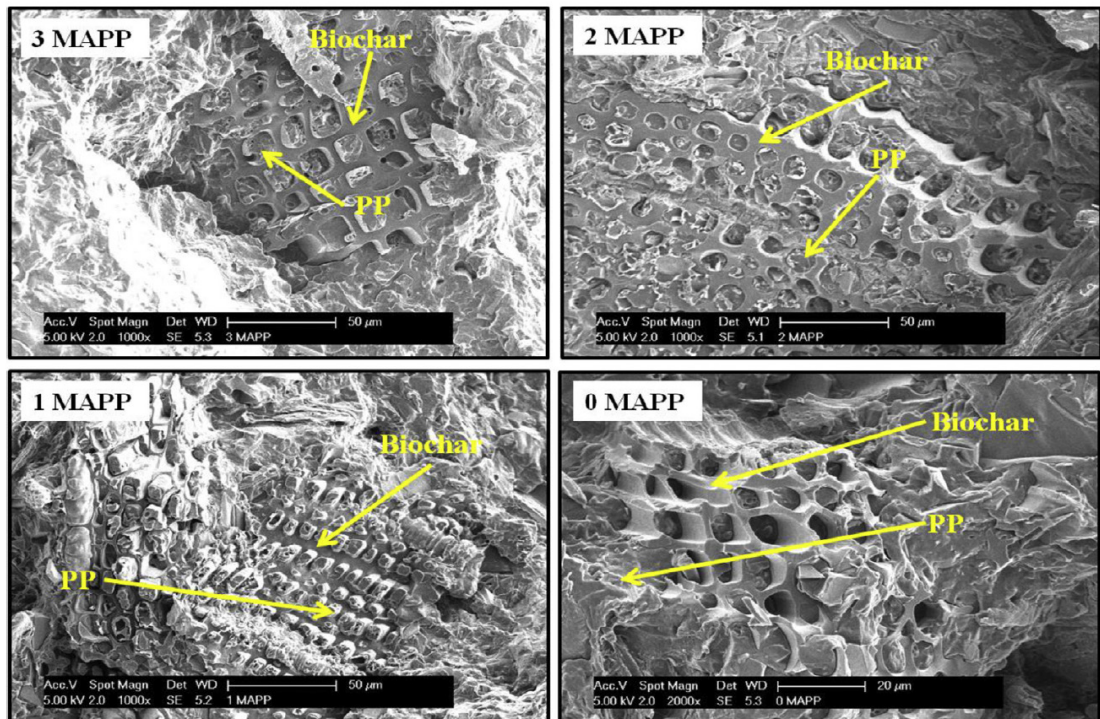


Figure 7. The SEM images of fractured surfaces of biocarbon filled polypropylene composites, the images show mechanical interlocking between the filler and the matrix polymer even at 1% concentration of compatibilizer attributing o its excellent mechanical properties. Figure taken from reference (40) with permission to use from Elsevier Publications 2016.

Temperature of carbonization of biomass is a very important factor impacting the structure of the final product. A higher temperature of carbonization results in a biocarbon with higher surface areas and a more prevalent pore structure that when incorporated into a composite has synergistic effects on the overall composite properties. Li et al. 2016 (35) reported the SEM images for nano bamboo charcoal. The average particle size for the filler was reported to be 606nm. The charcoal particles showed irregular shape with a porous structure including narrow micro pores with width less than 2nm and wide macropores with width higher than 50nm (117). The SEM images of fractured surface of the composites showed the dispersion of charcoal filler on the interface owing to the fabrication process that intended this particular segregated distribution pattern. It is concluded that segregated networks of filler can be obtained for natural filler using the fabrication method discussed in this study (35). Behazin et al., 2017 (37) reported the SEM analysis of fractured surface of the composites, the SEM images showed good distribution of filler in the matrix in case of 20% HtBioC filled composites. In case of LtBioC the images indicated poor compatibility between matrix and filler. Ogunsona, Misra, and Mohanty 2017a(62) developed biocarbon filled nylon 6 composites to study the impact of interfacial adhesion on the composite properties. The Atomic Force Microscopy (AFM) analysis of the composites provided the DMT modulus for the biocarbon embedded in the matrix. It was observed that the modulus values of the biocarbon's were directly corresponding to the temperature of pyrolysis (100). The DMT modulus value for

B1 was reported to be in the range of approximately 4-5 GPa, the fluctuations of the modulus value is related to the turbostratic structure of biocarbon which is composed of both crystalline and amorphous regions. The peak intensity is increased when the probe comes across a highly ordered crystalline region in the biocarbon and vice-versa when a not very ordered amorphous region is encountered(62). Ogunsona, Misra, and Mohanty 2017a (62) reported a high fluctuation in the peaks of B1 due to the presence of numerous small crystalline phases distributed across the biocarbon system. The DMT modulus of B2 was reported to be approximately 13 to 19 GPa and in the analysis fewer and pristine peaks were observed due to the presence of larger and well developed crystalline phases in B2 owing to the higher temperature of pyrolysis (62),(118,119). The SEM analysis of biocarbon B1 and B2 filler showed the particle size was under 5 μ m even for agglomerates, particle size as low as nanometres was also observed. The presence of particles in nanometric level is attributed to the reinforcement ability of the biocarbons. Formation of agglomerates is also reported, this is attributed to presence of Van der Waals attractive forces causing agglomerate formation (120). The formation of agglomerates is higher in B1 as compared to B2 owing to its lower temperature of pyrolysis causing presence of residual functional groups on the surface of biocarbon. The reduction of biocarbon particle size to nanometric levels is attributed to the milling conditions that can lead to increase in pressure exerted on the particles along with increase in temperature exacerbating the breakdown of biocarbon particles while milling (121). The SEM analysis of fractured surfaces

of the composites show better wetting in case of B1 filled biocarbon composites as the polymer was seen to form a layer around the filler indicating good interfacial adhesion. In case of B2 filled composites, the SEM images showed presence of voids indicative of poor interfacial adhesion between polymer and filler. The presence of functional groups on the surface of B1 biocarbon is believed to have facilitated good interfacial adhesion by interacting with the functional groups present in nylon matrix (122). The surface properties of biocarbon which are a result of temperature of pyrolysis have played important role in determining the interfacial adhesion between the polymer matrix and filler affecting the properties of the composites. The SEM analysis of the biocarbon and biocarbon (HT) filler filled epoxy composites developed by Giorcelli et al. 2019 (63) showed uniform dispersion of filler in the matrix at lower loading rates. Agglomeration of filler can be observed in composites filled with higher loading rates of biocarbon filler. It was observed that the porous morphology of biocarbon was lost during the milling of biocarbon into a fine powder. It was observed that the filler particles were embedded very well in the matrix, this facilitated the improvement in mechanical properties of the composites. The microstructure of fractured surfaces of rice husk filled and rice husk biocarbon filled composites was observed under Scanning Electron Microscopy (SEM) using different magnifications to study the interfacial morphology and the filler-matrix interactions by Q. Zhang, Zhang, Lu, et al. 2020 (69) reported that biocarbons carbonized at lower temperatures of 200 and 300°C showed a similar morphology to that of rice husk filled composite. The microstructure of these

composites showed the filled wrapped in HDPE matrix (69,123,124). The SEM images of composites filled with biocarbon carbonized at 400°C showed presence of both rice husk and rice husk biocarbon, indicating incomplete carbonization of feedstock. The composites with biocarbon carbonized at 500 and 600°C showed mechanical interlocking between the matrix and the polymer, this is reflected in the mechanical properties discussed in earlier sections, as composites having biocarbon produced at 500 and 600°C showed the best tensile and viscoelastic properties (69). Composites filled with biocarbon produced at 700, 800 and 900°C showed the destruction of the micropore structure on the surface of biocarbon hampering the mechanical interlocking (69). This resulted in the decline in mechanical properties of the composites filled with biocarbon produced beyond 600°C. The microstructure of composites filled with of the biocarbon produced at higher temperatures like 800°C show a lot of cracks not supporting the formation of the physical interlocking of the molten polymer matrix and filler (69). Arrigo, Bartoli, and Malucelli 2020 (43) studied the micro structure of their composites using SEM. A homogenous distribution of filler was observed for both the processes, a reduction in filler size was observed in composites fabricated using melt mixing (43). The intense shear forces applied on the samples during melt mixing fabrication process resulted in the reduction of particle size of filler(65).

1.6. Gaps and Improvements

It was observed that biocarbon is an excellent filler that can be incorporated into polymer matrices to improve their overall properties. One major factor that has not been addressed in any study is the effect of feedstock source on the biocarbon properties. Even though the end chemical composition and microscopic morphology of the biocarbon is fairly same for biocarbon developed from any feedstock, it would be interesting to see if the nature of feedstock meaning the source, the type of source (grass, wood, fruit bunch etc.,) has any effect on the final product. As it can be seen a large emphasis has been given to the application of biocarbon in improving the mechanical and thermal properties of the filler. The application of biocarbon as an electrically conductive filler is still not quite explored. More parametric studies need to be developed to determine the impact of biocarbon on the mechanical and thermal properties of composites holistically. Rheological studies on the effect of biocarbon addition to the polymer was also not addressed in most of the studies discussed here. The study of rheology is important as it can have an impact on the processing and fabrication methods of the composite. Keeping in mind end use application of the composites, more focus on water absorption and dimensional stability is needed in the study. In the electrically conductive composite studies emphasis on the temperature of pyrolysis and loading rate has been observed. Other fundamental properties like particle size of filler and morphology of filler have not yet been fully explored. Based on modelling studies on electrically conductive

composites done by Clingerman et al. 2003 morphology of filler and particle size of filler have a significant effect on the electrical conductivity of the composite. There is a significant lack of modelling studies on the mechanical properties of the composites, development of such studies would help in further optimization of composite fabrication and properties. Another important factor ash content is not considered as relevant factor in majority of the studies. This gap of knowledge needs to be addressed, as ash content of biocarbon can greatly impact the properties of biocarbon and ultimately have an effect on the properties of the composites and its applications. Introduction of external coupling agents like compatibilizers has been done in studies and the effect of compatibilization has been observed on the mechanical properties of the composite. However, the effect of compatibilization of electrical conductivity of biocarbon filled composites is still yet to be explored. As most of these agents are polymeric in nature, it makes it interesting to see the effect of more polymeric material on the overall electrical conductivity of the composite. More studies can be based on development of biocarbon from waste based sources like the studies conducted by Das, Sarmah, and Bhattacharyya 2016a, Ketabchi et al. 2017 and Poulouse et al. 2018. The area of incorporation of biocarbon synergistically in polymer matrices to improve their properties is still being explored and there are several such gaps that can be addressed in future studies.

1.7. Conclusion

Biocarbon is an excellent additive to composites as most of the studies here have reported significant enhancement of composite properties with biocarbon addition. Biocarbon has properties like increased thermal stability, decay resistance etc. that can make it better than the natural fillers like wood powder. The light weight of biocarbon makes it an attractive choice over conventional mineral fillers while considering weight reduction in automobiles. The ease of production of biocarbon from basically any lignocellulosic source makes it easy to procure and makes the entire process cost effective. So far biocarbon has been successfully utilized in soil amendment and quality improvement. It has also shown its potential as a reinforcing filler in improvement of polymer mechanical and thermal properties opening up a plethora of application opportunities. Most of the studies addressed here have reported improvement in mechanical and thermal properties of polymer composites. With improved properties the applicability of the polymers is diversified. Composites can be developed using recycled polymers or biodegradable polymers to improve the sustainability of the entire lifecycle of the composites. There is a great promise in the application of biocarbon as an electrically conductive filler and needs more exploration. However, it has been observed that biocarbon definitely acts as a conductive filler and has the potential to become a filler in conductive polymer composites. The ease of manufacturing and the freedom of customizing the properties as per need makes it very useful. Biocarbon is an emerging filler

material in the field of material and polymer science. It has a lot of potential that needs harnessing, all is needed is focus on the right direction to make the most of it.

1.8. Goals and research questions

The goal of this dissertation was to introduce biocarbon as a potential filler material in polymer composites to improve mechanical, thermal and electrical properties. This study aims at showing effectiveness of biocarbon fiber produced from Douglas fir pulp as a potential sustainable and cost-effective replacement for traditionally used carbon-based synthetic fillers like carbon fiber for applications in automotive industry. The study was developed based on the following questions.

1. When carbonized at temperatures above 600° C, will biomass feedstock develop electrical conductivity?
2. Can morphological similarities between biochar and carbon fiber can help develop a theoretical modelling framework for biochar filled electrically conductive composites?
3. Is the morphology of filler an important property in composites? With higher aspect ratio of filler contributing to better electrical properties.

4. Can incorporation of biochar in composites make the composites sustainable? What are the associated environmental impacts?

2. Chapter 2- Newly Developed Biocarbon to Increase Electrical Conductivity in Sustainable Polyamide 12 Composites

2.1. Abstract

Sustainable manufacture caused shift in automotive manufacturing practices. Polymer-based composites make up almost 15% mass of the entire vehicle, most importantly the fuel system of the vehicle. Poor electrical conductivity of the polymer composites leads to electrostatic deposition which can lead to issues like charging of the surface, burn accidents, possible electric shocks etc., Carbon based synthetic fillers like carbon fiber and carbon nanotubes are attractive options to develop electrically conductive composites, owing to their excellent electrical and mechanical properties. However, the production process of these reinforcements is highly time and energy intensive making it quite expensive and not sustainable. Lignocellulosic feedstock can be carbonized at a high treatment temperature of $\geq 1000^{\circ}\text{C}$ to produce electrically conductive biocarbon filler. In this study biocarbon fibers developed using Douglas fir pulp, were incorporated into polyamide 12 matrix to develop composites. The composites were fabricated using hot compression mounting. At a filler loading of 7.5 wt. % the composites reported log electrical conductivity value of -6.67 S/cm and at 35 wt. % filler loading rate the composite conductivity was -0.31 S/cm. An electrical conductivity of -8.70 S/cm for polyamide 6 composites filled with 20 wt.% carbon

fiber and -1.03 S/cm were reported for 40 wt. % carbon fiber concentration in reviewed literature. The electrical conductivity values for both 20 wt.% and 40 wt.% carbon fibers is significantly lower compared to biocarbon fiber filled composites at 25 wt.% and 35 wt.% biocarbon filler loading. This indicates the effectiveness of biocarbon filler as a conductive filler, in developing electrically conductive, sustainable composites.

Keywords

Biocarbon, Sustainable composites, electrically conductive composites, recycled PA 12, compression mounting.

2.2. Introduction

Automobiles are a major contributor to greenhouse gas emissions. As per Environmental Protection Agency(EPA) on an average 8,887 grams of CO₂ is emitted from 1 gallon of gasoline and 10,180 grams of CO₂ is emitted from 1 gallon of diesel in tail pipe emissions (17). Annually 4.6 metric tons of CO₂ is released from a typical passenger vehicle (17). These emissions have a highly detrimental effect on the global climate scenario. Increased fuel efficiency of vehicles can lead to lower fossil fuel consumption, in turn lower greenhouse gas emissions. To achieve this feat, the automobile manufacturers have resorted to lightweighting of the vehicles. As per the EPA 2020 Automotive trends report, the heaviest vehicles produced in model year 2020 generate half the amount of CO₂ compared to model year 1978 (18) all owing to the massive design changes and advancements undertaken by the automakers (18). Traditional materials are being replaced by light weight metals and largely by polymer composites. These polymer composites are generally filled with fillers like talc, glass fibres, calcium carbonate (CaCO₃), clay nanoparticles etc., (127,128). Ideally fibrous fillers like glass fibre have been largely incorporated in polymer matrices to reinforce the composites by enhancing the mechanical and thermal properties (129–131). Thomason et.al, (129) discuss different methods of recycling and reutilization of glass fibres recovered from used composites. Polymer composites filled with

inorganic fillers are lighter than the conventional metals, but the fillers have a high density, making the finished products bulky. A potential solution to this issue can be incorporation of natural fibers derived from biomass like hemp, sisal, jute, kenaf and even wood. However, in order to facilitate improved mechanical properties in natural fiber filled composites, the fibers need to be treated chemically to reduce the polarity in order to facilitate good interfacial bonding between the polymer matrix and the fibers (132,133). Natural fibers show a great promise as sustainable, lightweight reinforcing fillers in polymer composites, but improvement of composite properties depends on addition of external additives and surface modifications of the fibers making the process tedious and impact the cost of production as well. Polymer composites are bringing down the weight of the vehicles but being poor conductors of electricity can lead to electrostatic accumulation causing further issues. A potential solution to this issue is incorporation of electrically conductive fillers in polymer composites. Electrically conductive polymer composites (ECPCs) are polymer composites developed by incorporation of conductive filler material into a non-conductive matrix (25,101–103,134). Carbon based fillers like carbon nanotubes, carbon fibers, carbon black etc., have been reported to be used as filler and the composites have shown good conductivity values (29,135,136). Among the synthetic carbon based fillers, carbon fiber has been widely incorporated in several studies as an electrically conductive filler with exceptional electrical, mechanical and thermal properties(137–139). Electrically conductive polymer composites (ECPCs) have a wide range of application in sensors, electromagnetic shielding, capacitors etc.

based on their electrical properties. Table IV shows different resistivity scales and application of ECPCs based on the resistivities. ECPCs are now being used in automobile industry to produce light weight electrically conductive parts to achieve fuel efficiency and cut down emissions. However, carbon fiber that has become quite popular in the last decade as an exceptional electrically conductive filler is quite expensive and not sustainable, therefore, a lot of research is being focused on recycling and reusing the carbon fibers as well. Piñero-Hernanz et al. 2008 and Oliveux et al. 2015 (131,137) in their studies have discussed several chemical and mechanical methods to successfully recycle and reuse carbon fiber from used polymer composites yet there are still a few shortcomings. A cost effective and sustainable solution to develop lightweight electrically conductive composites is utilization of biocarbon as conductive filler.

Table IV. Application of ECPCs based on their resistivity range (140).

Resistivity (Ω cm)	Electrical property	Applications and Products
$>10^{14} - 10^{11}$	Insulating	Insulators
$10^{10} - 10^6$	Electrostatic Dissipative	Anti-static Materials
10^5-10	Conductive	Sensors and EMI Shielding
$10^{-1}-10^{-6}$	Highly Conductive	Conductors

Biocarbon is the carbon rich solid material that is left after the thermochemical conversion of biomass in an oxygen deficit environment (1). Compared to

synthetic carbon-based fillers, biocarbon is relatively cost effective and sustainable as it uses biomass-based feedstock as raw materials that are less expensive, also waste materials like lignocellulosic waste can be a potential feedstock for biocarbon production reducing production costs and enhancing sustainability. Biocarbon has been largely implemented in soil amendment and soil quality enhancement. Biocarbon has been reported to be a great filler that is used for improvement of mechanical and thermal properties of polymer matrices. Das et al. 2016 (5) have reported improved tensile modulus and improved thermal stability in polypropylene filled with biocarbon developed from pine wood recovered from landfills. Similarly, Behazin, Mohanty, and Misra 2017 (36) incorporated ball milled switch grass (miscanthus) based biocarbon into a toughened polypropylene matrix and observed better mechanical properties in the composites. Nan et al. 2016 (31) developed electrically conductive Poly Vinyl Alcohol (PVA) composites by incorporating wood biocarbon developed from 3 different wood species, carbonized at different temperatures and reported electrical conductivity comparable to composites filled with carbon nanotubes in the polymer composites along with improved mechanical properties. On a similar note, Giorcelli and Bartoli 2019 (32) developed biocarbon from coffee grounds by carbonizing the biomass at different temperatures and incorporated this biocarbon into epoxy matrix and reported electrical conductivity in composites filled with biocarbon carbonized at 1000°C. Biocarbon has been successfully implemented as a filler in many different polymer matrices to improve mechanical and thermal properties, however, not many studies have reported the

incorporation of biocarbon as an electrically conductive filler to make non-conductive matrices electrically conductive creating a gap that needs to be addressed.

Polyamide is a semi-crystalline polymer and has widespread application in daily life and in industrial manufacturing processes. The exceptional properties of Polyamide 12 have attributed to its wide use in the plastic industry and the automotive industry. Vasileva Dencheva, Braz, and Denchev 2022 (141) developed PA 12 based neat, hybrid and co-polymeric micro-particulate based materials for additive manufacturing by combining different monomers for PA 12 and PA 6 respectively . They used different fillers namely Aluminum, Iron and Carbon Black at 2 wt.% to develop composites(141). Characterization of the composites fabricated from these micro-particulate materials showed promising mechanical properties, and a drop in melting point compared to commercial PA 12 showing potential of applicability in additive manufacturing. Similarly Dul, Fambri, and Pegoretti 2021(142) developed 3-D printed short carbon fiber filled polyamide composites. The composites showed a 34% increment in tensile strength and 147% increment in tensile modulus(142). A drop in electrical resistivity was also observed in the fabricated composites.

The objective of this study is to incorporate sustainable, cost-effective biocarbon fiber in a polymer (PA 12) matrix to develop electrically conductive composites. The effectiveness of biocarbon fiber filler in making the otherwise non-conductive matrix electrically conductive, along with its effects of thermal

and mechanical properties of PA 12 are analyzed using various analytical methods.

2.3. Material and Methods

2.3.1. Biocarbon and polyamide

The biocarbon used in this study was produced in the lab at Michigan Technological University. The Douglas fir pulp feedstock was procured from Domtar paper company. The pulp was received in the form of compressed sheets and was deagglomerated prior to carbonization. The pulp was dispersed in water to deagglomerate the fibers followed by washing with alcohol and then dried overnight at 90 °C. The dried fibers were deagglomerated in a coffee grinder prior to carbonization, the blades of the coffee grinder were masked using duct tape to minimize the effect of blade edges on the aspect ratio of fibers. The fibers were then carbonized in three heating zone tube furnace (Model 23-891, Lindberg, Watertown, WI, USA). The samples were loaded into a quartz tube and the ends were sealed. The fibers were heated to 1000 °C at a heating rate of 10 °C/min. A steady flow of nitrogen was maintained at 1000 cc/min throughout the process of carbonization. The samples were maintained at 1000°C for 60 minutes. The samples were weighed before and after carbonization to determine biocarbon retention. The biocarbon retention after carbonization at 1000 °C was about 14 – 16 wt. %. The same procedure is applied to carbonize biocarbon at 800°C and 600 °C.

Recycled polyamide 12 recovered from selective laser sintering (SLS) method was used as matrix. It was provided to us by Ford Motor company. The PA 12 powder was heated at a temperature range between 170°C and 175°C for SLS. The samples were heated for several hours based on the scale and complexity of the SLS printing process and cooled for approximately 24 hours before retrieving the finished product. The process was carried out in a nitrogen blanket to prevent oxidation. Typically for SLS printing the recovered material is refreshed with fresh supplied material as the recovered material tends to have a slightly higher melting point in comparison to fresh PA 12. Similarly, as this recovered material ages an increased molecular weight and decreased melt flow is characteristic to it. The melting point of recycled polyamide 12 was 178 °C and the density was 1.01 g/cm³. The polyamide was sieved before use to remove impurities. 20 wt. % Carbon fiber filled polyamide 6 extruded pellets were provided to us by BASF.

2.3.2. Characterization of biocarbon

2.3.2.1. Elemental Analysis of Biocarbon

The biocarbon fibers were characterized for carbon (C), Nitrogen (N) and Oxygen (O) using elemental analysis. Dried, ground, and homogenized samples were weighed into tin capsules and analyzed for carbon and nitrogen content on an Elemental Combustion System (Costech 4010, Costech Analytical Technologies, Inc.,

Valencia, CA) in the LEAF core facility at Michigan Technological University. The instrument was calibrated with atropine. Stability was checked with NIST 1547 every 12 samples with a relative standard deviation of 0.03 for N and 0.19 for carbon.

2.3.2.2. Ash Content Analysis

The ash content in biocarbon was determined using Thermogravimetric Analysis (TGA). Approximately 8-10 mg of biocarbon samples were heated to 800°C from room temperature at a heating rate of 10°C/min at a constant flow of oxygen at 100 cc/min flow rate. The samples were maintained at 800°C for 30 minutes at isothermal mode. The ash content was determined from the residue based on the weight loss curves. The average of 3 runs is reported in the results.

2.3.2.3. XRD Analysis of Biocarbon

The crystallinity of wood fiber and biocarbon samples were analyzed using X-Ray Diffraction. The analysis was done in XDS 2000 (Scintag Inc., USA) at a scattering angle 2θ , scanned from 5° to 60° (at 1.540562 Å wavelength, continuous scanning). The data was

analyzed in Microsoft excel.

2.3.3. Composite formation

The composite fabrication for this study is done in 5 steps, that are presented in Figure 9. The 5 different steps are explained in detail in this section.

Step 1 – In step one the Douglas fir pulp fibers are deagglomerated, the deagglomeration is carried out in a coffee grinder with modified blades as the blades were covered with duct tape to incur as less damage as possible on the fibers to maintain the aspect ratio. The deagglomerated fibers were carbonized in three heating zone tube furnace (Model 23-891, Lindberg, Watertown, WI, USA) by heating the biomass to 1000°C at a heating rate of 10°C/minute. The pulp fiber biomass was retained at 1000°C for 60 minutes and then cooled down overnight to room temperature. The entire process was carried out in a nitrogen environment with a continuous flow of nitrogen at 1000 cc/minute. The fibers were also carbonized at 800 °C and 600 °C in the same process.

Step 2 – The carbonized biocarbon fibers were characterized for composition using elemental analysis and ICP analysis. X-Ray diffraction analysis was done for the fibers to determine the crystallinity of the biocarbon.

Step 3 – The biocarbon fibers (7.5, 9, 15, 25 and 35wt.%) and the PA 12 were conditioned at 80°C overnight in a hot air oven to remove any moisture in the PA 12 polymer and the biocarbon fibers. After conditioning the biocarbon fibers were dispersed in the PA 12 matrix using the coffee grinder with the modified blade.

Biocarbon fibers were incorporated into the mixture at different concentrations as mentioned. Composites filled with 35 wt.% biocarbon were made with the biocarbon fibers carbonized at 800°C and 600°C. The biocarbon and the PA 12 polymer were mixed in the coffee grinder for 15 seconds. This mixture was then fabricated. A comparison between the biocarbon fibers before dispersion and after dispersion is presented in Figure 8. The Figure shows the aspect ratio of the fibers is maintained to a large extent even after the dispersion in the coffee grinder.

Step 4 – The mixture of biocarbon fibers and PA 12 were fabricated using hot compression molding. The mixture was fabricated into composites in 3 steps heating, holding, and cooling. In the heating step, the mixture was heated to 300°C from room temperature. In the holding step, the samples were held at 300°C for 30 minutes to ensure uniform heating. In the cooling cycle, the samples were cooled down to room temperature. Throughout the process of fabrication, a pressure of 96 psi was applied and maintained on the samples.

Step 5 – The composite discs were retrieved from the molding equipment and the surface was polished using a grinding disc (Leco Spectrum System 1000) at 100-150 rpms to make it rough to enhance contact between the surface and the electrodes for the electrical conductivity measurement. An 8-inch P500 grit Alumina based polishing paper was used with water as polishing media. Each side was polished for about 3-5 minutes to achieve uniform surface texture. The diameter and thickness of the samples were measured and recorded prior to the

characterization.

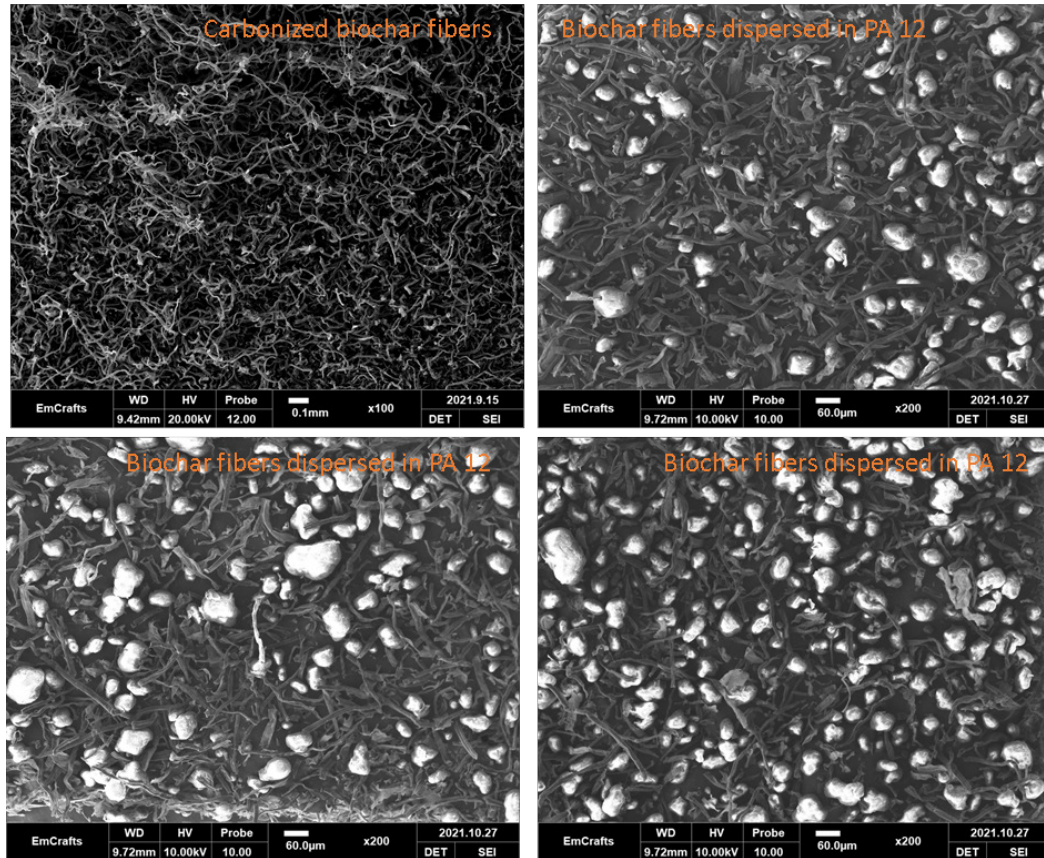


Figure 8. SEM images showing biocarbon fibers before and after dispersion in PA 12 matrix using coffee grinder.

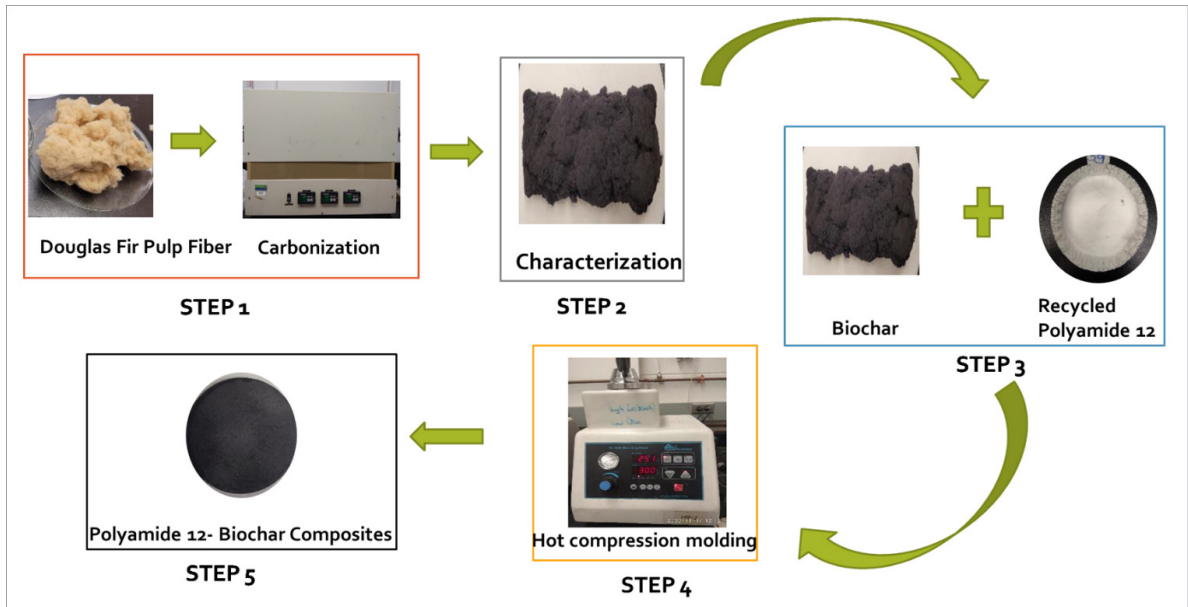


Figure 9. Composite fabrication process for development of biocarbon filled PA 12 composites.

2.3.4. Electrical conductivity measurement

The composite samples were characterized for electrical conductivity using a measuring device designed in the lab in Michigan Technological University (Figure 10). The samples are placed between the electrodes and current and voltage is applied to the samples. DC current is applied using a power source (Siglent Technologies SPD1305X Programmable DC Power Supply 1 Channel, 30 V / 5 A, 150W), the current and voltage readings are taken using (Siglent SDM3065X 6 ½ digit Digital Multimeter) for current and (Siglent Technologies SDM3055 5.5 Digit Digital Multimeter) for voltage. The current and

voltage input values were regulated to keep them at minimum to prevent overheating of sample while obtaining accurate values for measurement. Eight measurements were taken for each sample and 5 replicates were characterized for each loading rate. Average and standard deviation was calculated for each set of samples.

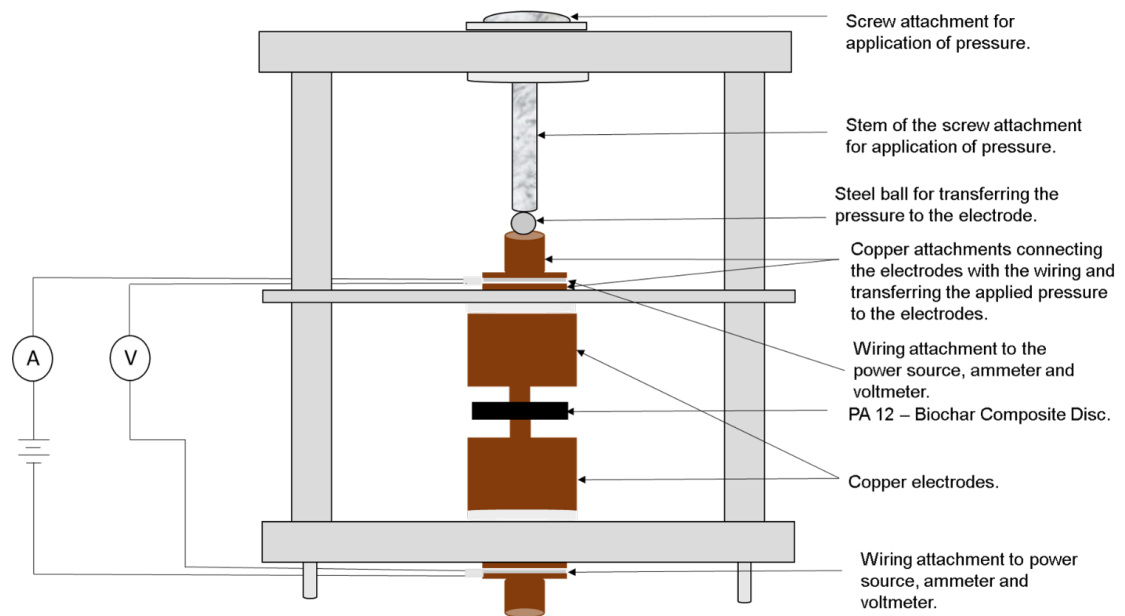


Figure 10. The setup used to characterize the composites for electrical conductivity.

The resistivity of the samples was calculated using the formula described in equation (1) the electrical conductivity was calculated using equation (2) (31).

$$\rho = \frac{RA}{l} \quad (1)$$

ρ = Resistivity of sample in Ω cm.

R = Resistance of sample in Ω .

A = Area of the electrodes in contact with the sample in m^2 .

l = Thickness of the sample in m.

$$\sigma = \frac{1}{\rho} \quad (2)$$

σ = Conductivity (S/m)

ρ = Resistivity (Ω cm)

2.3.5. Dynamic Mechanical Analysis

The DMA analysis of pure polymer and biocarbon filled composites was done in tensile mode for 20mm long 4mm wide 1mm thick samples using DMA 850 (TA Instruments, USA). The experiment was carried out by heating the samples from ambient temperature at 25 °C to 150 °C, at a strain amplitude of 0.01% and frequency of 1 Hz. The glass transition temperature (T_g) of the samples was calculated from the peak of tan delta peaks.

2.3.6. Thermal Properties

Thermogravimetric Analysis (TGA) of the composites was performed to determine the effect of biocarbon addition on the thermal properties of the composites. The analysis was performed using a TA Q500 TGA instrument.

Approximately 10 mg of sample was procured from different spots of a composite sample and was placed in platinum sample pans and heated from room temperature 25 °C to 500 °C at a heating rate of 10 °C/min in a nitrogen atmosphere. The samples were maintained at 500 °C for 30 minutes. The thermal behavior of pure polyamide 12 and the composites were compared to determine the effect on biocarbon on the thermal stability of the composites.

2.3.7. Scanning Electron Microscopy Analysis

Scanning Electron Microscopy was used to analyze the morphology of the composites. The pieces were broken using pliers and then were coated with platinum/palladium using sputter coating to make the surface conductive for better imaging. The SEM was done using EmCrafts tabletop SEM instrument. The imaging was done at 5 kV, 200x magnification.

2.4. Results and Discussion

2.4.1. Elemental and Ash content Analysis

The elemental analysis of Douglas fir biocarbon fibers carbonized at 1000 °C showed 88% carbon content in the biocarbon and 0.7% nitrogen content. The oxygen content was determined to be 2.2 %. The carbon content in the biocarbon is influenced by carbonization temperature and it is believed with

higher carbonization temperature a higher carbon content can be achieved. The ash content of the biocarbon samples was determined to be 2.7 ± 0.7 %.

2.4.2. XRD Analysis

The Figure 11 here shows the comparison between the XRD pattern of Douglas fir pulp fiber and biocarbon fibers. The broad peak between 15° – 16° and the sharp peak at 22.5° for Douglas fir pulp fiber are believed to be cellulosic peaks. These peak patterns could be indicative of the presence of a high cellulose content in the feed stock. On the contrary, in biocarbon these peaks are absent. The lack of significant peaks for biocarbon are indicative of the amorphous nature of biocarbon. The short and broad peak obtained at approximately 23.5° for biocarbon could be due to the presence of turbostratic structure obtained by carbonization at high temperature like 1000°C (100,143,144). The transition from crystalline to amorphous could be a result of high temperature carbonization. The high temperature of the carbonization process could have destroyed the original cellulose structure forming a non-crystalline structure.

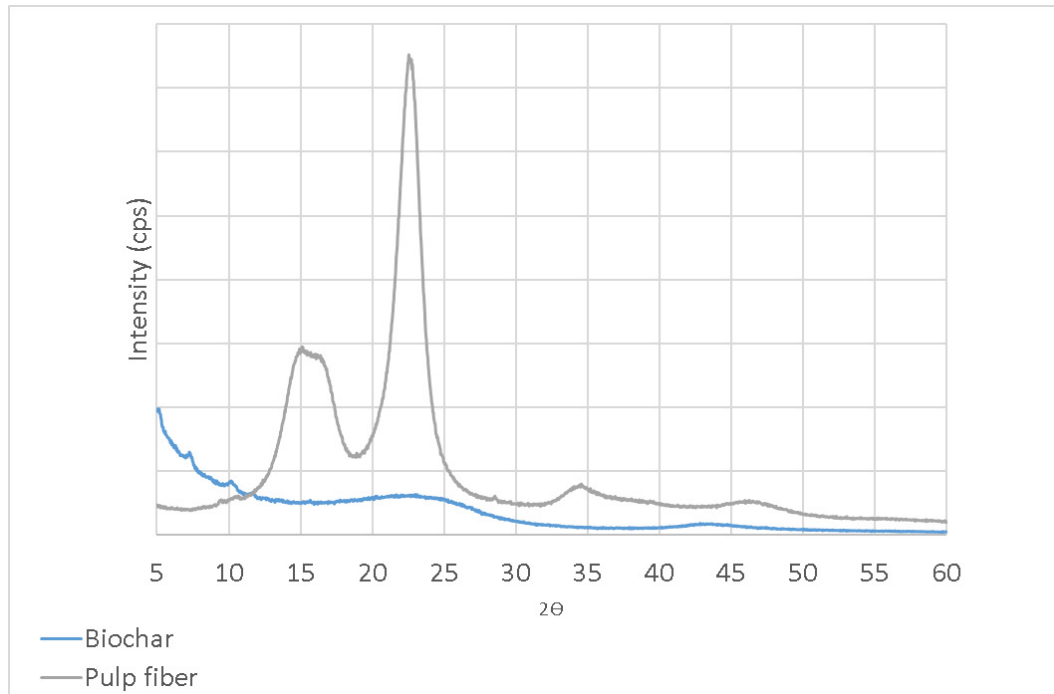


Figure 11. XRD pattern of pulp fiber vs biocarbon.

2.4.3. Electrical property of composites

Improved electrical properties were observed in the composites compared to pure polyamide 12 that has log electrical conductivity of -14 S/cm. At low biocarbon loading level of 7.5wt % the log conductivity of the composite samples was reported to be -6.69S/cm ($4.98 \times 10^6 \Omega \text{ cm}$) indicating drastic drop in electrical properties compared to pure polymer. The electrical conductivity was reported to have further improved with increasing filler concentration in the composites. At 35% filler concentration the conductivity value of the composites was -0.31 S/cm ($2.05 \Omega \text{ cm}$). Composites filled with 40% and 20% carbon fiber have electrical resistivity of $10.08 \Omega \text{ cm}$ (-1.03 S/cm) and $5.04 \times 10^8 \Omega \text{ cm}$ (-8.7 S/cm) respectively(145), the electrical properties of the carbon fiber composites

is significantly lower compared to biocarbon fiber filled composites. This is an indicator of the effectiveness of biocarbon as a conductive filler. Several factors affect the electrical properties of biocarbon which in turn affects the overall composite properties. A major factor contributing to the electrical conductivity of biocarbon is the carbonization temperature. Several studies have reported good electrical conductivity in biocarbon carbonized at $\geq 1000^{\circ}\text{C}$ (31,42,104,105). The carbonization of feedstock at a high temperature results in a turbostratic structure in biocarbon (23,24). The importance of carbonization temperature on the electrical conductivity of the composites can be further supported by the resistivity values for composites filled with biocarbon carbonized at 800°C and 600°C . The composites filled with 35 wt.% biocarbon fibers carbonized at 800°C were observed to have log electrical conductivity of -1.275 S/cm that is 10 times lower than the conductivity value reported for composites filled with biocarbon carbonized at 1000°C . Similarly, log conductivity value of -5.83 S/cm was recorded for the composites filled with 35wt % biocarbon fibers carbonized at 600°C . The observed conductivity value is several orders lower than the composites filled with biocarbon carbonized at 1000°C at the same filler concentration. The turbostratic structure of biocarbon is responsible for the conductivity of biocarbon. The loading rate is another factor, as it can be observed in the study that with increasing filler concentration results in improved composite electrical properties, similar trend is also observed in other studies conducted using biocarbon as an electrically conductive filler (31,42). Morphology of filler is also a contributing factor to the electrical conductivity of

composite (125). The fibrous morphology of the biocarbon fibers incorporated in the polyamide12 matrix in the study has contributed to the improved electrical properties even at low filler concentration. As it can be seen in Figure 1, the biocarbon fibers have retained their length to a large extent even after processing, this definitely is a contributing factor to the formation of a conductive network facilitating improved electrical properties. The electrical resistivity of biocarbon filled composites was compared to 20 wt.% carbon fiber filled polyamide 6 extruded composites that were received from BASF. The 20 wt.% carbon fiber filled composites, had a log electrical conductivity of -1.44 S/cm that lies between the conductivity values of biocarbon composites filled with 25 wt.% biocarbon having a log conductivity of -1.07 S/cm and 15 wt.% biocarbon filled composites having a log electrical conductivity of -1.92 S/cm. The electrical conductivity values of biocarbon fiber filled composites are similar or even better than composites filled with carbon fiber. These results are indicative of the effective performance of biocarbon fibers as electrically conductive fillers in composites. The electrical conductivity trend of biocarbon filled composites is presented in Figure 12, it can be seen that the conductivity values increase as the concentration of biocarbon filler increases and the percolation point on the curve is 7.5 wt.% biocarbon concentration as there is a steep rise in the conductivity of the composites from this point.

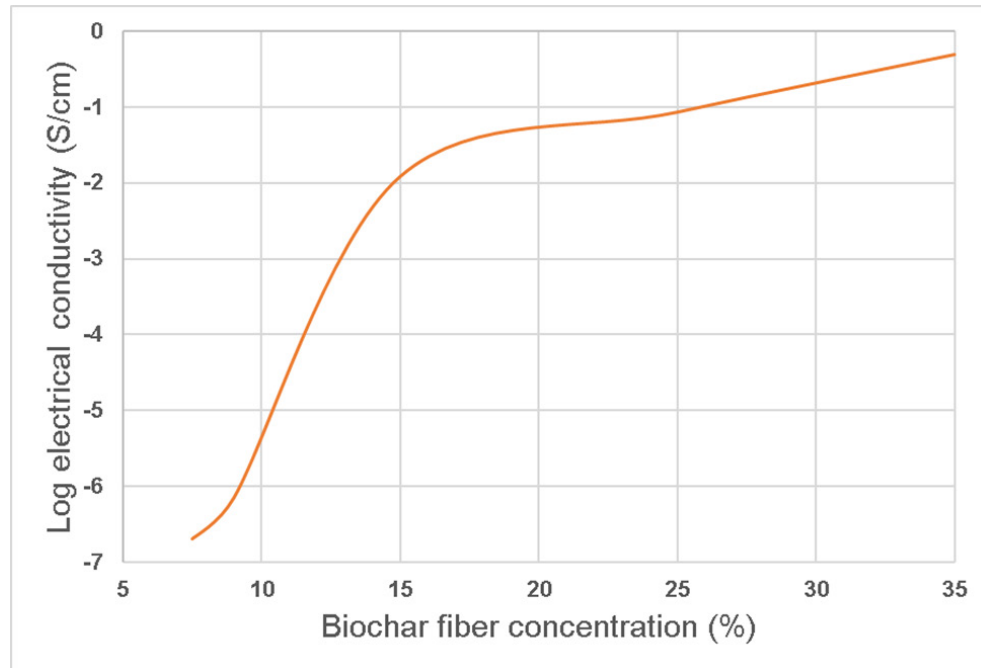
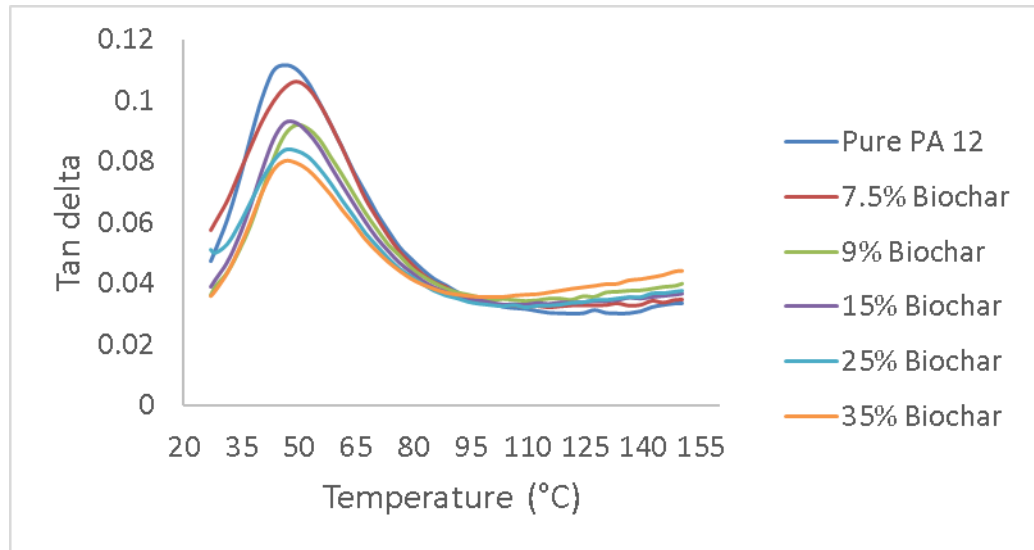


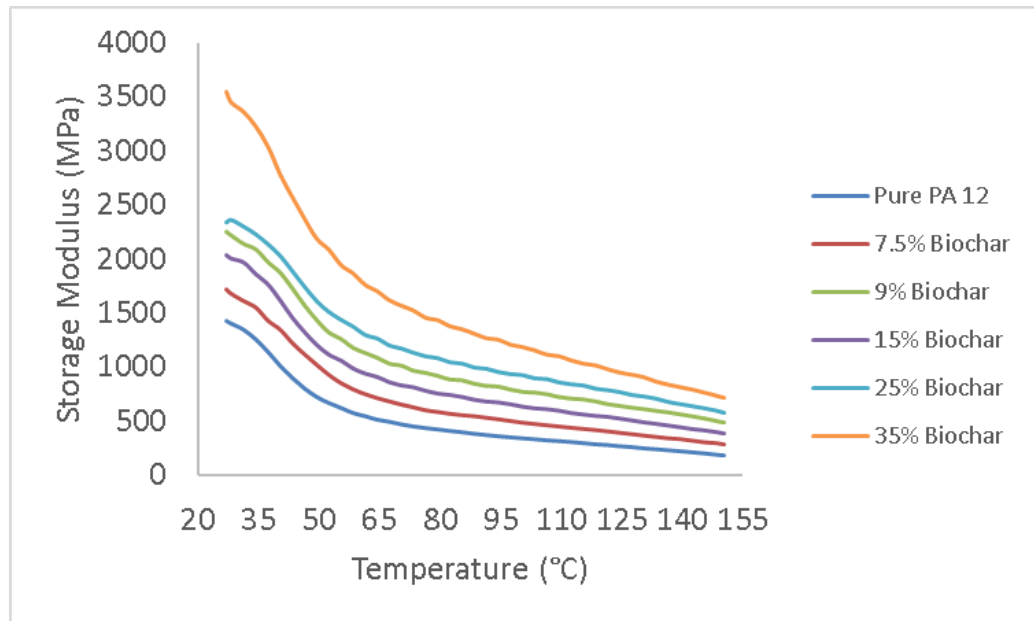
Figure 12. The electrical conductivity trend of biocarbon filled PA 12 composites.

2.4.4. Dynamic Mechanical Analysis

The results from dynamic mechanical analysis of pure PA 12 and biocarbon filled composites showed that the glass transition temperature (T_g) of PA 12 at 46.27 °C and for the composites at 47 °C indicating no significant effect of biocarbon fillers on the T_g of composites. The tan delta peaks (Figure 13 (a)) shows declining magnitude with increase in filler concentration, suggesting a decrease in energy absorption capacity of the composite compared to pure PA 12. On the other hand, the storage modulus values (Figure 13 (b)) show steady increase with increasing filler content, indicated by increased stiffness in the composites. This improvement was expected with incorporation of filler.



(a) Tan delta curves



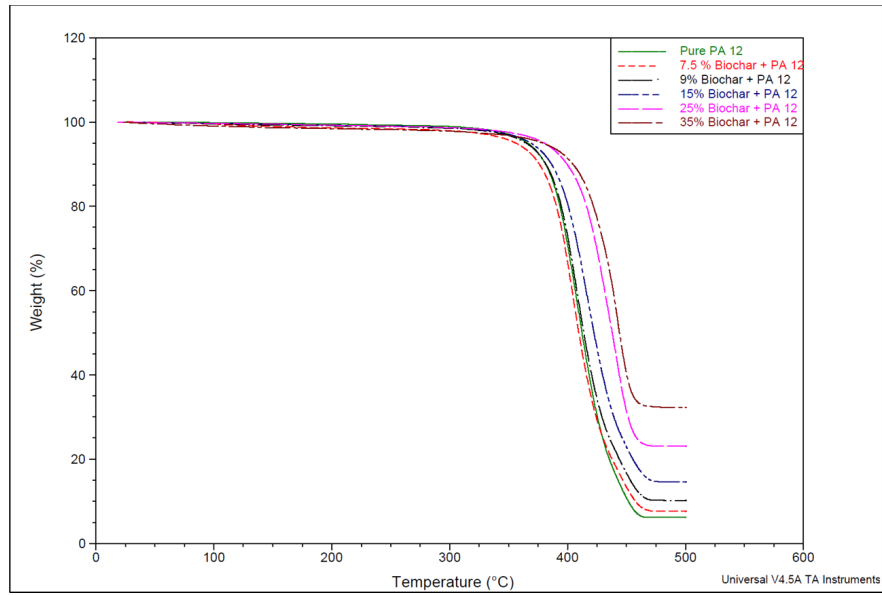
(b) Storage modulus curves

Figure 13. The dynamic mechanical analysis curves of biocarbon fiber filled composites (a) tan delta curves, (b) storage modulus curve.

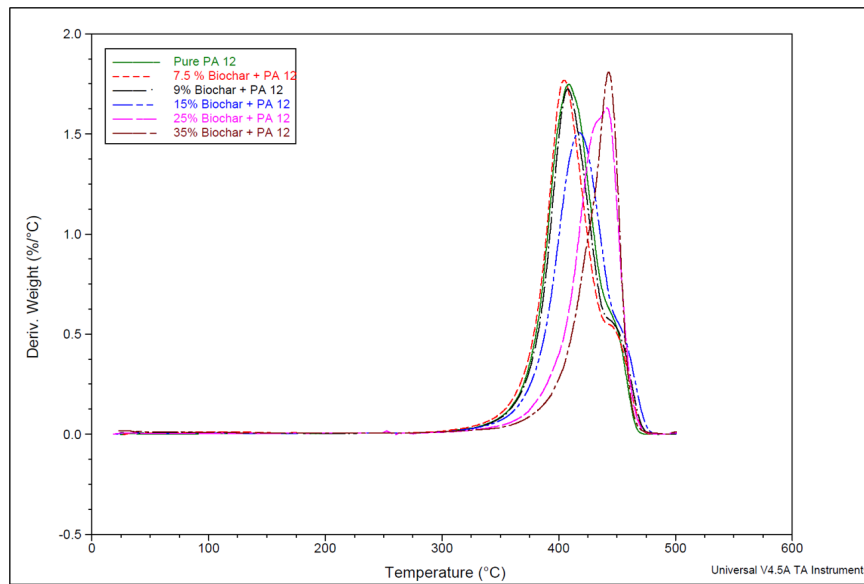
2.4.5. Thermal properties

The TGA weight loss curves (Figure 14 (a)) indicated a shift in the degradation temperature of the composites compared to pure polyamide 12 polymer. The thermal degradation takes place at 378.10°C for polyamide 12 while for the composites lower loading rates 7.5 wt.% and 9 wt.% have temperatures close to the thermal degradation temperature of polyamide around 381°C. There is a significant shift in higher loading rate towards higher degradation temperatures. The temperatures for 25 wt.% and 35 wt.% filler loading composites are close to 400 °C, precisely 391.28 °C for composites filled with 25 wt.% biocarbon and 396.72°C for composites filled with 35 wt.% biocarbon fibers respectively. This indicates enhanced thermal stability in composites introduced by incorporation of thermally stable biocarbon. A negligible amount ~1% of residue was obtained after the entire degradation cycle of polyamide 12, while in case of composites significant amount of residue was obtained on completion of the analysis. The amount of biocarbon residue increased with filler concentration of the composites. This is an indicator of improved thermal properties of composites as well. The residue is also indicative of the material loss during composite processing. The higher the filler retention the lower the material loss throughout the processing phase in the sample specimen(s). The differential thermogravimetry (DTG) curves (Figure 14 (b)) shows the maximum degradation temperature. The maximum degradation temperature of PA 12 was reported to be 407.26°C. Composites with lower

biocarbon fiber loading rates 7.5 wt.% and 9 wt.% the maximum degradation temperature is similar to polyamide 12 around 407 °C however a shift towards right is observed with increasing filler loading rates. 15 wt.% biocarbon filled composites mark the beginning of improved thermal properties as the maximum degradation temperature increased to 417.55 °C. The improvement was significant for 25 wt.% and 35 wt.% samples as a significant increase in maximum degradation temperature with values over 440 °C for both the composite samples. This shift elucidates the improved thermal properties and thermal stability in the composites on addition of biocarbon filler to the polymer matrix. In pure PA 12 a two-step degradation takes place as shown in the Figure 14 (b). This phenomenon is not observed as the filler concentration in the composites increase, as incorporation of biocarbon has resulted in improved thermal stability in the composites fortifying the thermal degradation process.



(a) TGA mass loss curves



(b) DTG curves

Figure 14. The thermogravimetric analysis curves of biocarbon fiber filled composites (a) mass loss curves (b) DTG curves.

2.4.6. SEM Analysis

The Figure 15 here shows the SEM images of the biocarbon fiber filled composites. In the first image 15 (a) no biocarbon fibers were located, it could be due to the low concentration of the filler in the said composite. In Figure 15 (b) a biocarbon fiber can be clearly seen in the image. The fiber length is still maintained after fabrication, contributing to the composite properties, here also one fiber was located in the matrix. In the Figures 15 (c) and (d) more than one fiber can be seen in the fiber pull out images. As the concentration is increasing the fibers are getting more localized in the matrix. In Figure 15 (e) a lot more fibers are localized in the matrix compared to lower biocarbon fiber concentrations explaining the very good electrical and mechanical properties exhibited by the composites filled with 35 wt.% biocarbon fibers.

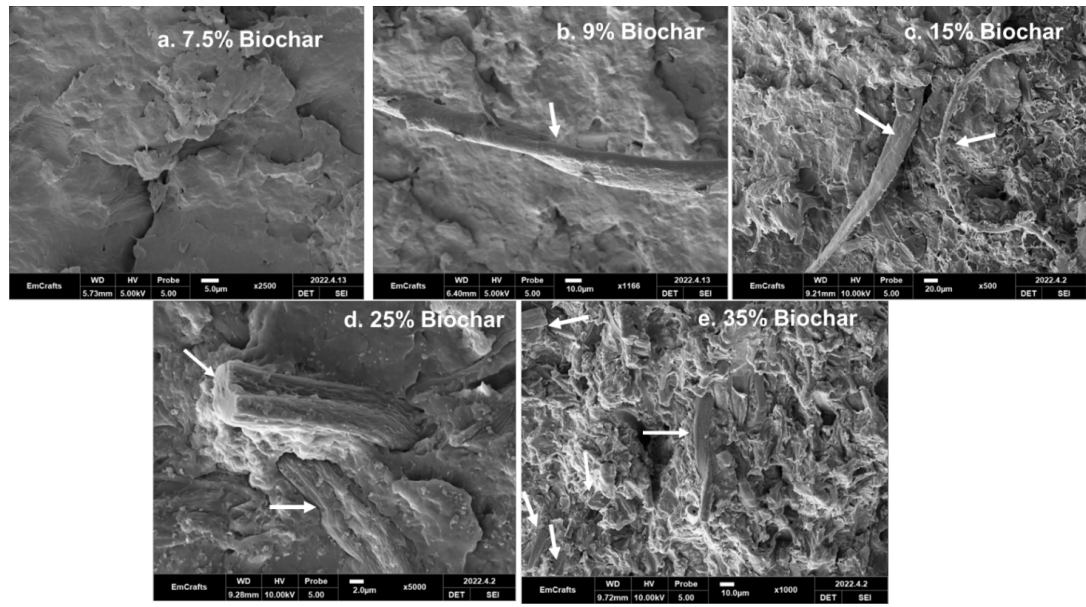


Figure 15. SEM images of biocarbon fibers and biocarbon-polyamide 12 composites, (a) 7.5% biocarbon filled composites, (b) 9% Biocarbon filled composites, (c) 15% Biocarbon filled composites, (d) 25% biocarbon filled composites (e) 35% biocarbon filled composites. The biocarbon fibers are indicated by the arrows on the images.

2.5. Conclusion

Incorporation of biocarbon as an electrically conductive filler has shown promising results. The resistivity value has shown a significant drop even at low filler concentrations as 7.5 wt.%. The carbonization temperature and morphology of the filler are two important factors in enhancing the electrical conductivity of biocarbon and hence improving the electrical properties of the composites. The thermal properties have also shown improvement by indicating higher thermal

stability on incorporation of biocarbon to pure polyamide12 polymer matrix. These positive results definitely indicate the potential of biocarbon as an electrically conductive filler to be used in manufacture of automobile parts. The use of biocarbon fibers is pretty unique since all the studies done previously have utilized biocarbon particles and/or powder. Utilization of recycled PA 12 from SLS waste definitely enhances the sustainability of the process and paves way for utilization of similar waste products maybe from automotive waste. Post end of life cycle automotive parts can be recycled providing raw material for further application as raw material. The recycling and reutilization of waste will make the process circular eliminating waste generation and improving the carbon footprint in the entire lifecycle of the vehicle. The utilization of biocarbon fiber filler, that is one of its kind, can provide the manufacturers with a cost effective sustainable conductive filler alternative improving the economic returns while reducing the environmental cost for both the manufacturer and the consumer.

3. Chapter 3- Development of Theoretical Modelling Framework for Biocarbon fiber filled Composites

3.1. Abstract

Theoretical modelling in material sciences is used to predict the characteristics of a composite prior to its characterization. This enables the researcher to get an idea of how effective the filler is in giving the desired results. Modelling of electrical conductivity of electrically conductive composites have been successful in predicting the efficiency of the conductive filler in the resultant composites. However, theoretical modelling is limited to metals or synthetic filler materials. In this study an attempt is made to develop a modelling framework for electrically conductive biocarbon filler in polyamide (PA 12) composites. The study is built up on existing modelling framework developed by Clingerman et.al using carbon fiber filled composites. In the modelling framework study certain values were taken from the existing reference study model and a few values were taken from literature for biocarbon specifically, to carry out the calculations. Due to unsuccessful fit between the experimental and theoretical curves the inputs and constants in the modelling framework were iterated and the input values with the closest fit with experimental data were replaced in the modelling calculations. The gap between the experimental and theoretical curves was reduced

significantly yet a perfect fit was not achieved. However, this attempt serves as a steppingstone for further in-depth study of biocarbon fiber filled system.

Keywords:

Biocarbon; Sustainable Composites; Carbon Fiber; Modelling; Electrical Conductivity, electrically conductive composites.

3.2. Introduction:

In electrically conductive composites the volume fraction of filler in the composite plays a very important part in the conductivity of the composite. At lower filler loadings the conductivity of the composite is quite similar to conductivity of pure polymer(146). At a certain loading value of filler there is a sudden surge in the conductivity of the polymer composite, this critical value of filler content is known as percolation threshold. The percolation threshold is the quantity of filler that is needed to make a non-conductive matrix conductive by formation of conducting networks in the composite system(106).

3.3. Percolation theory

The transition of an insulator into a conductor can be explained by the percolation theory. The percolation theory states that at a lower filler concentration the conducting clusters are isolated in the polymer matrix, however as the concentration of the filler increases the distance between the

conducting clusters reduce and they start forming network that results in a sharp rise in the conductivity of the otherwise non-conductive system(147) as shown in Figure 16.

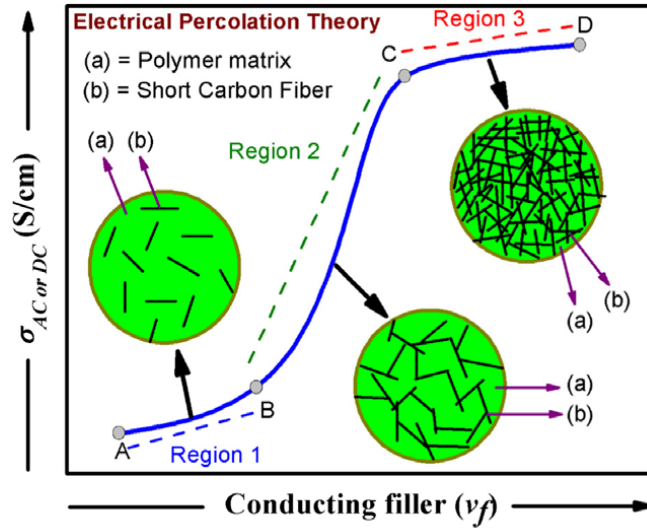


Figure 16. S shaped curve depicting the percolation behaviour in polymer/conducting filler (Carbon fiber) composites (148).

Electrical conductivity in composites occur due to the passage of electrons through the interparticle spaces on the conductive filler network (147). The percolation theory can be explained using the power law (147,149)

$$\sigma = \sigma_e(\phi - \phi_c)^s \text{ when } \phi > \phi_c \quad (1)$$

σ is the conductivity of the bulk resistant material, σ_e is the effective conductivity of the filler/inclusion. Φ is the volume fraction of the filler/inclusion, ϕ_c is the volume fraction at percolation threshold and s is the critical exponent. The power law equation has been used as the basis for development of many other prediction models, used to predict the electrical conductivity of filled composites.

Bueche, 1972 (149) developed a modelling study on conductive filler filled composites. In the study he explained the phenomenon of percolation threshold and electrical conductivity on basis of a gelation phenomena. He explained that at when percolation threshold is overcome in the polymer matrix, at this filler concentration infinite chains of particles appear in the system and with increased particle concentration the fraction of particles in the infinite chain also increases (149). He further explained that this formation of the infinite chain is the phenomena of gelation which is the result of polymerization of small multifunctional molecules. The resistivity of the system can be expressed by this equation 2 (149);

$$\rho = \frac{\rho_m \rho_f}{(1 - \phi)\rho_f + \phi \nu \rho_m} \quad (2)$$

In this equation ρ_m is the resistivity of the matrix, ρ_f is the resistivity of filler, ρ is the resistivity of the composite, ϕ is the volume fraction of filler or conductive

phase, v is the fraction of filler in the infinite cluster, this is a function of number of contacts per particle and the probability of contact [1,9].

Modelling for the prediction of electrical conductivity of conductive filler filled composites is generally based around the volume fraction of filler in the composite (146). Along with volume fraction there are several other factors that have an impact on the percolation threshold and the conductivity of composites. Many physical factors of filler and matrix including structural properties, interfacial properties and constituent conductivity (146).

McLachlan, Blaszkiewicz, & Newnham, 1990 (151) developed a model based on General Effective Media (GEM) equation, to model the electrical conductivity of a composite system having conductive fillers embedded in a non-conductive or poorly conductive matrix. They stated that the GEM equation fits the electrical conductivity as a function of volume fraction data for the composites (151). This model is an example of improved statistical model taking into account the conductivities of the constituent materials (146). The equation is ;

$$\frac{(1 - \phi) \left(\rho_m^{\frac{1}{t}} - \rho_h^{\frac{1}{t}} \right)}{\rho_m^{\frac{1}{t}} + \left(\frac{1 - \phi_c}{\phi_c} \right) \rho_h^{\frac{1}{t}}} + \frac{(\phi) \left(\rho_m^{\frac{1}{t}} - \rho_l^{\frac{1}{t}} \right)}{\rho_m^{\frac{1}{t}} + \left(\frac{1 - \phi_c}{\phi_c} \right) \rho_l^{\frac{1}{t}}} = 0 \quad (3)$$

Here ρ_m is the resistivity of the composite, ρ_h is the resistivity of the composite component with high resistivity, ρ_l is the resistivity of the composite component with low resistivity, ϕ is the volume fraction, ϕ_c is the percolation threshold and t is the critical exponent [1, 9]. The value of t can be determined by calculation or by curve fitting methods (146).

3.3.1. Thermodynamic Models

Mamunya, Davidenko, & Lebedev, 1997 (152) focused on additional factors, along with the volume fraction of filler in the matrix to model the electrical conductivity of conductive filler filled polymer composites. They included the melt viscosities of polymer and filler and the surface energies of the two. Clingerman et al., 2002 (146), have categorised this modelling method in the thermodynamic models owing to the inclusion of these properties. Along with the volume fraction of filler, this model addresses the interaction between the polymer and the filler as well on the percolation behavior of the conductive composites (146). The conductivity of the composite, above percolation threshold can be given by the equation (4) that is dependent on the variables k and K derived using equations 5 and 6 (152);

$$\log \sigma = \log \sigma_c + (\log \sigma_m - \log \sigma_c) \left(\frac{\phi - \phi_c}{F - \phi_c} \right)^k \quad (4)$$

$$k = \frac{K\phi_c}{(\phi - \phi_c)^n} \quad (5)$$

$$K = A - B\gamma_{pf} \quad (6)$$

Here, σ is the conductivity of the composite, σ_c is the conductivity at percolation threshold, σ_m is the conductivity at F , F is the maximum packing fraction, ϕ is the volume fraction, ϕ_c is the percolation threshold, γ_{pf} is the interfacial tension in the composite A , B and n are constants. The value of exponent k is dependent on the percolation threshold, volume fraction and interfacial tension (146). The interfacial tension is calculated using the Fowkes equation [1, 11];

$$\gamma_{pf} = \gamma_p + \gamma_f - 2(\gamma_p\gamma_f)^{0.5} \quad (7)$$

The maximum packing fraction or filler volume fraction F is the packing density coefficient for the filler within the volume of composite at a particular type of packing (152). The value of F can be calculated using the equation 8 (152);

$$F = \frac{V_a}{V_a + V_b} \quad (8)$$

In the equation V_a is the volume fraction of filler and V_b is the space occupied by the matrix. The value of F is dependent on the filler particle morphology. Like for monodispersed spherical particles the value of F is 0.64 (152). For fillers like carbon fibers the aspect ratio AR is taken into consideration for calculation of F . For carbon fiber specifically F can be calculated by the equation (146);

$$F = \frac{5}{\frac{75}{10 + AR} + AR} \quad (9)$$

Clingerman et al. 2003 (125) updated the Mamunya et al. 1997 (152) model. The changes were done in the equation used to calculate the surface energy, in the updated model the developed and equation based on the equation derived by Owens and Wendt 1969;

$$\gamma_{pf} = \gamma_p + \gamma_f - 2(\gamma_p^d \gamma_f^d)^{0.5} - 2(\gamma_p^p \gamma_f^p)^{0.5} \quad (10)$$

Here γ_f^p is the polar surface energy of the filler, γ_p^p is the polar surface energy of the polymer.

Another modification in the model is the estimation of F which was done experimentally and the values were computed using the equation 11 (125);

$$F = \frac{\text{Mass of filler}}{\text{Vibrated volume} \cdot \text{specific gravity of filler}} \quad (11)$$

The electrical conductivity value at percolation threshold was replaced with conductivity of pure polymer (σ_p) as at percolation threshold, the conductivity is almost similar to the conductivity of pure polymer. The values of A and B were changed to 0.11 and +0.03 respectively. The value of constant n was changed to 0.70. The updated Mamunya model equation can be expressed as equations 12, 13 and 14 (125);

$$\log \sigma = \log \sigma_p + (\log \sigma_m - \log \sigma_c) \left(\frac{\phi - \phi_c}{F - \phi_c} \right)^k \quad (12)$$

$$k = \frac{K \phi_c}{(\phi - \phi_c)^{0.7}} \quad (13)$$

$$K = 0.11 + 0.03 \gamma_{pf} \quad (14)$$

A good agreement was observed between the predicted values from the model and the experimental values.

A series of modelling studies were done by Sumita, Abe, Kayaki, & Miyasaka, 1986 (155). In their studies they focused on the surface energies of the polymer and the filler and took into consideration the interfacial tension along with the melt viscosities of the composite matrix. In their models Sumita et al. assumed that network formation in the composite takes place at a mixture independent overall surface energy value g^* , they stated that on the basis of g^* the volume percolation concentration of the composite can be determined, a higher percolation volume concentration is associated with lower surface energies and

vice-versa [14, 15]. They also stated that filler particle diameter and melt viscosity of the polymer making up the matrix affect the percolation volume concentration, according to their study smaller diameter of filler favors higher percolation volume concentration and the percolation volume concentration/critical volume increases with increasing melt viscosity of the matrix polymer [14, 15]. The final equation that was derived by Sumita et al. 1986 (155) through the study conducted by incorporating carbon black in different polymer matrices can be written as expressed in equation 15 (155);

$$\frac{1 - V_f^*}{V_f^*} = \frac{3}{R \times g^*} \left\{ K_{\infty} - (K_{\infty} - K_0)^{-ct/\eta} \right\} \quad (15)$$

K_{∞} is the interfacial energy of the composite per unit area in equilibrium state. In the study the value of K_{∞} is derived by Fowkes equation (153,155);

$$K_{\infty} = \gamma_p + \gamma_f - 2(\gamma_p \gamma_f)^{0.5} \quad (16)$$

Substituting the value of K_{∞} in equation 10 (155) gives us;

$$\frac{1 - V_f^*}{V_f^*} = \frac{3}{R \times g^*} \left\{ \left[\gamma_p + \gamma_f - 2(\gamma_p \gamma_f)^{0.5} \right] \times 1 - e^{-ct/\eta} + K_0^{-ct/\eta} \right\} \quad (17)$$

In this equation V_f^* is the percolation volume concentration of filler, γ_p is the surface energy of the polymer, γ_f is the surface energy of the filler, g^* is the universal free energy responsible for the onset of network formation, K_0 is the surface energy at $t = 0$, that is at the beginning of the mixing process, c is a

constant for the speed for evolution of interfacial free energy, t is thime taken to mix the two components, η is the viscosity of the polymer matrix during the mixing process, R is the diameter of the filler (carbon black in the study) [14, 15]. A good agreement was observed between the model and experimental values in the study of Sumita et al. (156).

3.3.2. Geometric models of Percolation

This class of percolation models were designed to predict the electrical conductivity behavior of sintered composites (156). This model assumes that for dry premixed mixtures of conducting filler and insulating matrix, on sintering the matrix is deformed into cubical strutures and the conductive filler are arranged in a regular pattern on their surfaces [1, 15].

Słupkowski 1984 (157), in their study described the elctrical conductivity of mixtures consisting of conducting and non-conducting powders, and the dependence of conductivity on particle dimensions. The equaltion to calculate the conductivity of the mixtures was given by equation 18 (157) ;

$$\sigma = 2\pi\sigma_f \frac{d([x] + P)}{D \ln\{1 + 1/(([x] + 1)\alpha)\}} \quad (18)$$

Here σ is the conductivity of the mixture, σ_f is the conductivity of the conductive powder, D is the diameter of the insulating particles, d is the diameter of

conductive particles, P is the probability of occurrence of conductive networks, the value of which depends on the statistic laws used to determine [x] [15,16].

$$[x] = \left[\left(\frac{1}{1 - V_f} \right)^{1/3} - 1 \right] \frac{D}{2d} \quad (19)$$

[x] is the total number of sublayers filled with conductive particles and V_f is the volume fraction of conductive particles [15,16].

Malliaris & Turner, 1971 (158) proposed a well known model in this category. In their study they developed two different equations to describe volume percolation concentration (156). In the study they developed two equations, one for $V_{A\text{ as}}$ as expressed in equation 20 (a) to determine the concentration at the onset of network formation, the second equation for V_B as expressed in equation 20 (b) for determination of concentration in the end when a drastic increase in conductivity is observed [15,17].

$$V_B = 100 \left[\frac{1}{1 + \left(\frac{\Theta D}{4d} \right)} \right] \quad (20a)$$

$$V_A = 0.5 p_c V_B \quad (20b)$$

In the equation 20 (a) V_A is the concentration of conductive filler during network formation and in equation 20 (b) V_B is the filler concentration in the end of drastic increase of conductivity. Θ is the estimate of the arrangement of conductive particles on the surface on insulating particles, the value of Θ is different for

different arrangements, D is the diameter of insulating particles and d is the diameter of conductive particles and p_c is the first non-zero probability of the occurrence of a continuous band of conductive particles on the surface of insulating particles [15,17]. A good agreement between the model and experimental values was not obtained in the study and their assumptions were insufficient to determine the conductivity and percolation threshold in binary mixtures of conductive and insulating particles [15,17].

3.3.3. Structure oriented model

Previous models discussed above addressed various physical properties of the filler and the matrix. One property that affects the final electrical conductivity of the composite is the structure of the filler. Properties like aspect ratio and filler orientation in the composite affects the electrical conductivity of the composite (146). Processing techniques have a huge impact on these properties of the filler in the composite.

Two models were proposed by Weber and Kamal 1997 (159) based on the study conducted on composites formulated by incorporating nickel coated graphite fibers in isotactic polypropylene. They considered filler concentration, dimension of filler, aspect ratio and orientation of filler in an end to end model with an assumption that the fibers were connected end to end and were aligned in the direction of electrical conductivity test [12, 18]. Another model was developed taking into account fiber-fiber contacts, fiber length and the alignment of fiber in

an angle Θ to the direction of electrical conductivity test, this was expressed in the equations 21 (a, b and c) [12, 18];

$$\rho_{c,long} = \frac{\pi d^2 \rho_f X}{4 \phi_p d_c l \cos^2 \Theta} \quad (21 a)$$

$$X = \frac{1}{0.59 + 0.15m} \quad (21 b)$$

$$\beta = \frac{\phi - \phi_c}{\phi_t - \phi_c} \quad (21 c)$$

In the equations $\rho_{c,long}$ is the longitudinal composite electrical resistivity, ρ_f is the fiber electrical resistivity, X is the function of number of contacts, d_c is the fiber diameter, l is the fiber length, m is the number of contacts, ϕ_p is the volume fraction of fibers participating in conductive strings, Θ is the angle orientation and ϕ_t is the threshold value at which fibers participate in strings (125).

The structure oriented models take into account the filler morphology and orientation but do not integrate surface energy in the modelling.

The objective of this study is to model the electrical properties of biocarbon filled polymer composites to determine the fit between the theoretical electrical conductivity values with the experimentally determined electrical conductivity values. Electrical conductivity modelling of synthetic carbon-based fillers has been done and reported; however, no such study has been reported using natural lignocellulose-based electrically conductive fillers. In our study we are exploring the applicability of such a specific model on modelling our biocarbon

fiber filled composites. A major aspect that we are focusing on is the fibrous structure of biocarbon fibers which is similar to carbon fibers morphologically, we are using the carbon fiber data as reference while modelling the electrical properties of biocarbon fiber filled composites.

3.4. Material and Methods

3.4.1. Biocarbon and polyamide

The biocarbon used in this study was produced in the lab in Michigan Technological University. The Douglas fir pulp feedstock was procured from Domtar paper org. The pulp was deagglomerated prior to carbonization. The carbonization was done in a three-heating zone tube furnace (Model 23-891, Lindberg, Watertown, WI, USA). The final temperature was set to 1000°C at a heating rate of 10°C. A steady flow of nitrogen was maintained at 1000cc/min throughout the process of carbonization. The samples were maintained at 1000°C for 60 minutes.

Recycled polyamide 12 recovered from selective laser sintering (SLS) method was used as matrix. It was provided to us by Ford Motor company. The melting point of polyamide 12 was 178°C and the density was 1.01 g/cm³.

3.4.2. Composite formation

The composite samples are developed with different biocarbon concentrations presented in table V. Biocarbon and nylon were conditioned overnight at 80°C overnight to remove moisture. The biocarbon fibers were dispersed in the nylon matrix in a coffee grinder with modified blades. The blades of the coffee grinder were wrapped with duct tape to mask the edges of the metal blades. This was done to ensure minimal damage to the biocarbon fiber aspect ratio. The composites were fabricated using hot compression mounting method. The samples were molded at 300° C at 96 psi pressure. The composite samples were maintained at the temperature and pressure for 30 minutes and then cooled. The composites discs surface was polished using grinding discs, to make it rough for better contact with the electrodes for characterization. Figure 17 shows the process of fabrication of composite samples.

Table V: Composite composition with different filler loading rates.

Concentration of Biocarbon Filler (%)	Concentration of Polyamide (PA) 12 (%)
7.5	92.5
9	91
15	85
25	75
35	65

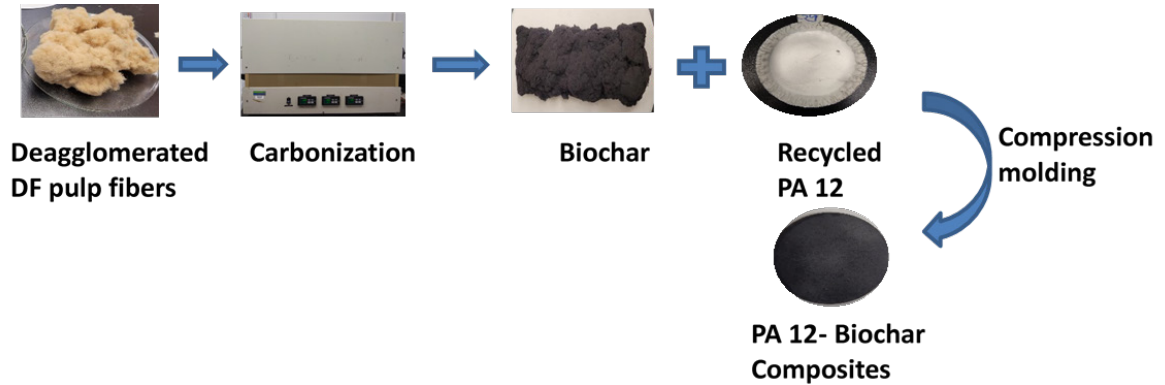


Figure 17. Composite fabrication process for development of biocarbon filled PA 12 composites.

3.4.3. Electrical conductivity measurement

The composite samples were characterized for through plane electrical resistivity using a measuring device designed in the lab in Michigan Technological University (Figure 18). The samples were placed between the electrodes and DC current was applied perpendicularly using a power source (Powerbes DC power supply SPS W1203, having output of 120V and 3A), the current and voltage were measured using (Sigilent SDM3065X 6 ½ digit Digital Multimeter) for current and (Sigilent Technologies SDM3055 5.5 Digit Digital Multimeter) for voltage. The volume resistivity of the composites was calculated using the formula expressed in equation 22 (25).

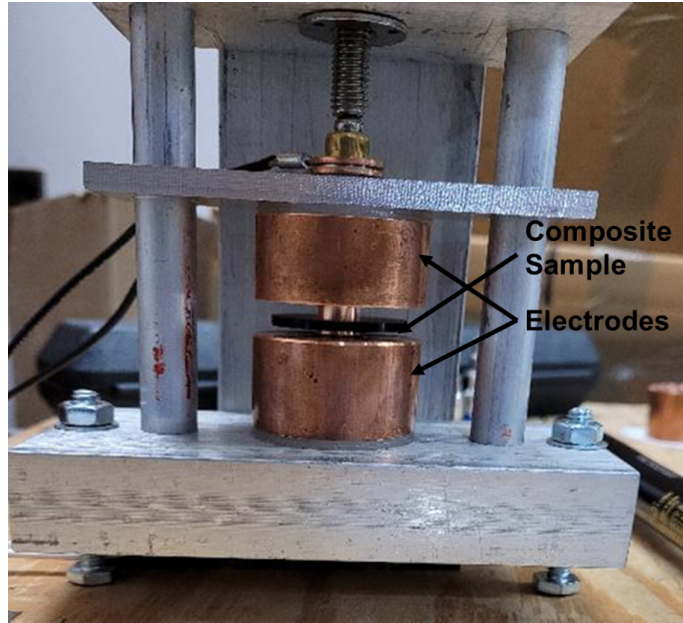


Figure 18. The equipment set up used to measure the electrical conductivity of PA 12-Biocarbon composites. The composite sample is placed between two electrodes while the measurements are done.

$$\rho = \frac{RA}{l} \quad (22)$$

ρ = Resistivity (Ωcm)

R = Resistance of sample (Ω)

A = Area (cm^2)

l = Thickness of the sample (cm)

The conductivity is based on resistivity values and can be determined by using the formula expressed in equation 23.

$$\sigma = \frac{1}{\rho} \quad (23)$$

σ = Conductivity (S/m)

ρ = Resistivity (Ωcm)

3.5. Results

3.5.1. Electrical conductivity

The electrical properties of biocarbon filled composites are presented as log electrical conductivity. The electrical conductivity of the composites improved drastically compared to pure polymer having electrical conductivity of -14 S/cm . At lowest filler concentration, 7.5 wt.% the electrical conductivity of the composite was recorded to be -3.853 S/cm that is much higher than the electrical conductivity value of pure PA 12. The electrical conductivity trend as shown in Figure 19, shows a steady increase in the conductivity values with increasing biocarbon concentration making 7.5 wt.% the percolation point for the composites. The improvement electrical properties of the composites can be attributed to the fibrous morphology of biocarbon fibers as shown in Figure 20 that enable network formation in the composite increasing the electrical conductivity. At highest filler concentration of 35 wt.% the electrical conductivity of the composites was reported to be -0.3296 S/cm ,

this value is several orders higher than the electrical conductivity reported for pure polymer. At higher filler concentrations the biocarbon fibers are more localized in the matrix resulting in better network formation leading to the improved electrical properties. Another factor contributing to the improved electrical properties is the carbonization temperature of biocarbon. It has been reported in literature that biomass carbonized at $\geq 600^{\circ}\text{C}$ temperature tends to have electrical conductivity, that improves with temperature(104,105),(42,134). Biocarbon has characteristic turbostratic structure that can facilitate electrical conductivity. Higher carbonization temperature makes the structure more organized resulting in improved properties with higher temperatures.

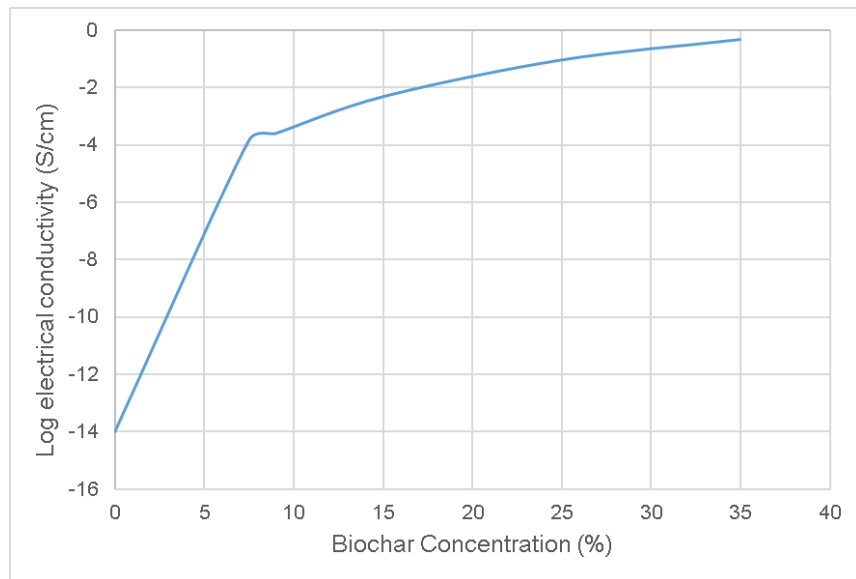


Figure 19. Electrical conductivity trend of PA 12-biocarbon filled composites.

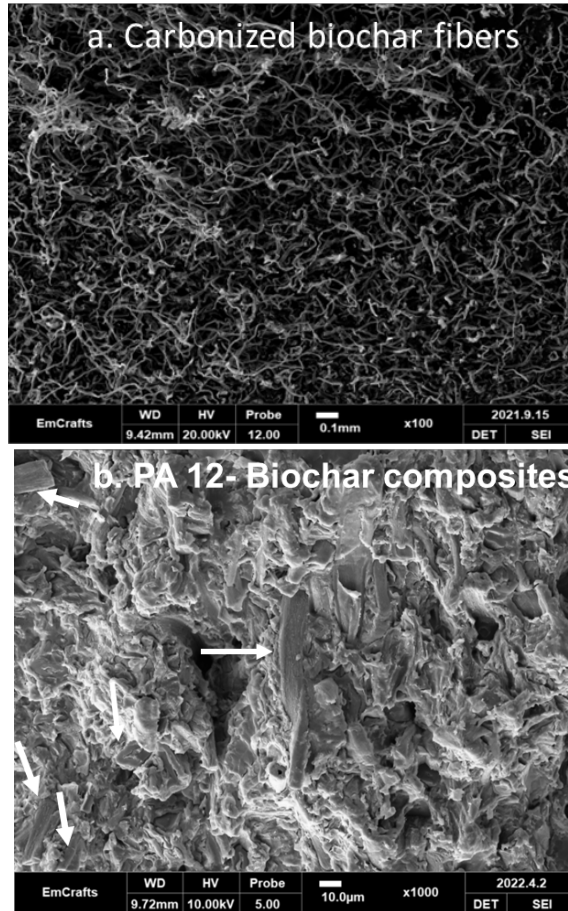


Figure 20. SEM images of biocarbon carbonized at 1000°C and fractured composite surface, (a) shows the fibrous morphology of the Douglas fir fibers maintained even after carbonization, (b) the arrows indicated the localized biocarbon fibers that are still in fiber form even after composite processing.

3.6. Modelling electrical conductivity of the composites

The modelling in this study was based on a preexisting study developed by Clingerman et al. 2003 (125). In their study they developed a model based on the existing Mamunya model, that is a thermodynamic model considering the surface energy and morphology of the electrically conductive filler incorporated in the composite. The original and the updated model derived by Clingerman et al is also discussed in detail in the introduction. In the study developed by Clingerman et al. 2003 (125) they modelled the electrical properties of three different fillers namely synthetic graphite, carbon black and carbon fiber (125). In our study we have built the model using the data for presented in their study carbon fiber-based modelling as our reference, owing to morphological similarities in biocarbon fibers and carbon fibers.

3.6.1. Volume Fraction and conductivity of biocarbon filled composites.

Volume fraction of filler in the composite is an important factor in the modelling process as the volume fraction is the variable factor in the modelling calculation that is different for every individual composite. The volume fraction values corresponding to the weight fractions and the associated electrical conductivities are listed in table VI.

Table VI: Electrical conductivity of biocarbon filled composites.

Biocarbon Concentration (%)	Volume Fraction of Biocarbon	Log Electrical conductivity (S/cm)
7.5	0.0397	-3.853
9	0.0480	-3.6025
15	0.0826	-2.324
25	0.1453	-1.043
35	0.215	0.3296

3.6.2. Modelling of biocarbon filled composites using combination of original and updated Mamunya model

This modelling method incorporates surface energy of the composite derived from surface energies of the components, along with the morphology in addition to volume fraction and conductivity. The surface energy values for PA 12 (γ_p) were found from literature to be 40.7 mJ/m² (160) and the surface energy value for biocarbon (γ_f) was found to be 24.1 mJ/m² (161). Based on these values the surface energy of composites (γ_{pf}) was determined using equation 7 (125),

$$\gamma_{pf} = \gamma_p + \gamma_f - 2(\gamma_p\gamma_f)^{0.5} \quad (7)$$

The surface energy value for composites was calculated to be 2.162 mJ/m². The fibrous morphology of fibers is incorporated into the model by an expression F, F was calculated in the study using the equation 24 (125),

$$F = \frac{\text{Mass of filler}}{\text{Vibrated volume} \cdot \text{specific gravity of filler}} \quad (24)$$

In the study done by Clingerman et al. 2003 (125) F was determined for carbon fiber to be 0.225, in our study we have assumed F to be 0.225 as well owing to similar morphological features of biocarbon fibers and carbon fibers. The values incorporated for constants A, B and n were 0.11, 0.03 and 0.7 respectively in the reference study and the same values were used in the modelling of biocarbon fibers as well. In updated Mamunya modelling done by Clingerman et al. 2003 (125) the value for constants A and B was determined by a linear regression between the constant K and the surface energy of the composite (γ_{pf}) (125). The process of derivation of the constant n was not discussed in the original study as well as in the study by Clingerman et al. 2003. All these values along with electrical conductivity at percolation threshold that was determined to be at volume fraction 0.0397 (75 wt.%) and at maximum filler concentration at volume fraction 0.215 (35 wt.%) were incorporated in the equations 25, 26 and 27 to determine the theoretical conductivity values for biocarbon filled composites.

$$\log \sigma = \log \sigma_p + (\log \sigma_m - \log \sigma_c) \left(\frac{\phi - \phi_c}{F - \phi_c} \right)^k \quad (25)$$

$$k = \frac{K \phi_c}{(\phi - \phi_c)^{0.7}} \quad (26)$$

$$K = 0.11 + 0.03 \gamma_{pf} \quad (27)$$

Here, σ is the conductivity of the composite, σ_c is the conductivity at percolation threshold, σ_m is the conductivity at F , F is the maximum packing fraction, ϕ is the volume fraction, ϕ_c is the percolation threshold, γ_{pf} is the interfacial tension in the composite A , B and n are constants. The value of exponent k is dependent on the percolation threshold, volume fraction and interfacial tension (146). The list of inputs and the calculated values are presented in the table VII. The experimental values and the modelling values for conductivity were plotted in Figure 22 to Figure out the fit between the two. It was observed that there is a significant distance between the experimental values and the theoretical values, except for the values at percolation and maximum filler concentration.

Table VII. Inputs and calculated electrical conductivity values for modelling of biocarbon filled composites

Loading Rate of biochar (%)	VF at F (maximum packing) ϕ	VF at percolation ϕ_c	n	K	k	F	Conductivity at percolation ($\log \sigma_c$) S/cm	Conductivity at F ($\log \sigma F$) S/cm	Log σ
7.5	0.0252	0.0252	0.7	0.175	4.07	0.225	-3.853	-0.32926	-3.85
9	0.0335	0.0252	0.7	0.175	0.126	0.225	-3.853	-0.32926	-1.49
15	0.0494	0.0252	0.7	0.175	0.059	0.225	-3.853	-0.32926	-0.74
25	0.084	0.0252	0.7	0.175	0.032	0.225	-3.853	-0.32926	-0.46
35	0.144	0.0252	0.7	0.175	0.0195	0.225	-3.853	-0.32926	-0.36

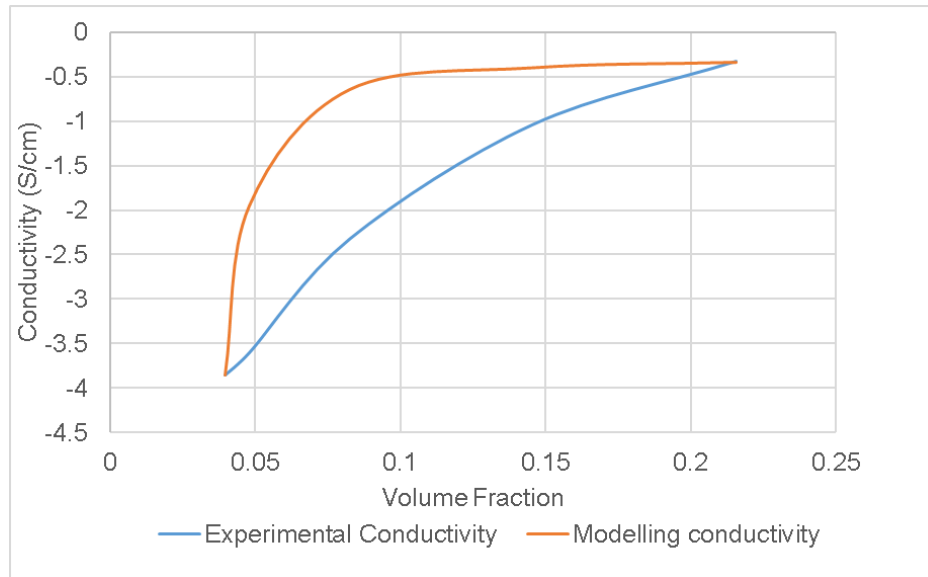


Figure 21. The curves representing experimental and theoretical conductivity values for biocarbon filled composites.

3.6.3. Updated modelling framework

In order to improve the fit between the experimental and theoretical conductivities we came up with a trial-and-error method. In this method the value of the constant/variable in the previous calculation will be subject to addition and subtraction by a certain value setting the upper limit and higher limit of the constant/variable in a meaningful range. This was done to find the values that give us theoretical electrical conductivity values closest to the experimental values and to close the gap between the two. The values for constants A, B and n, the values for surface energy and the value for F were subjected to this iteration.

3.6.4. Updated A, B and n

The values for A, B and n were subject to addition and subtraction to find a value that closes the gap between the experimental and theoretical conductivity values. The value for A was initially taken as 0.11, and 10 values in multiples of 5 were added to it making the final value 0.61. The value of B that was taken initially was 0.03 and it was subjected to ± 0.005 till the upper limit and lower limit values obtained were 0.075 and 0.005 respectively. The value of n incorporated in the calculations initially was 0.7 and was subjected to ± 0.05 , the upper limit was set at 1 and the lower limit was 0.4. These values were individually substituted in the calculations and the curves were plotted to determine the value

giving the closest curve with the experimental data. The curves are presented in Figures 23,24 and 25.

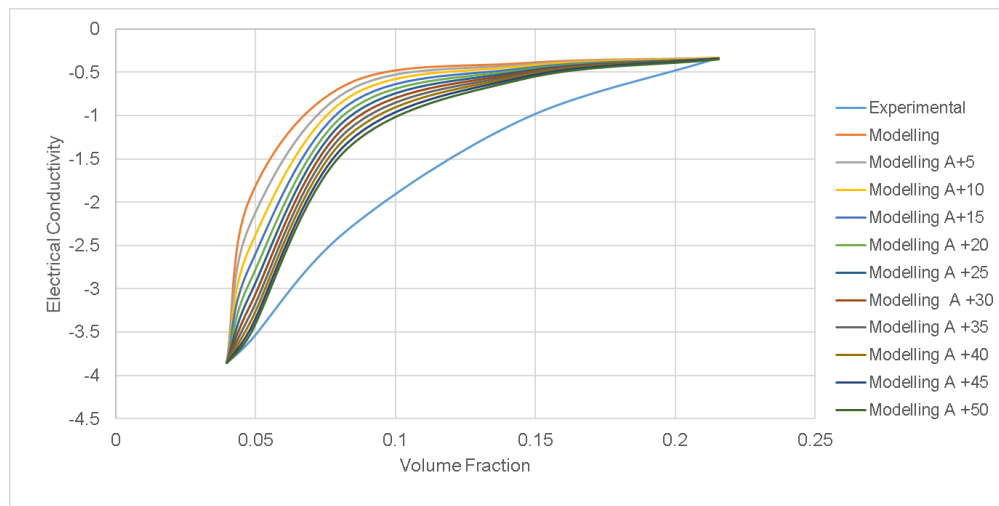


Figure 22. Presenting the iterations for the constant A, from the iterations it can be seen the curve representing A + 50 is the closest to experimental values curve.

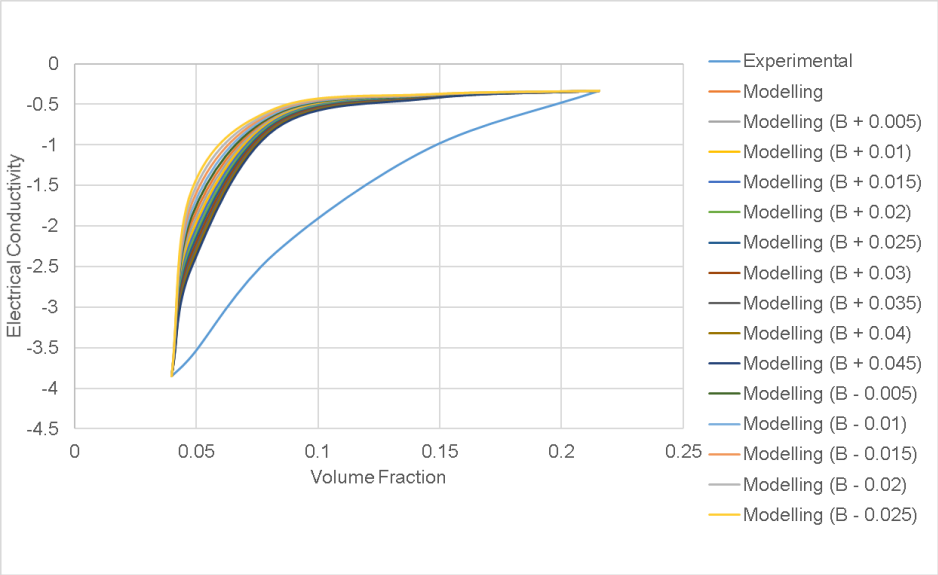


Figure 23. The curves presenting the iterations for constant B and the curve plotted with $B+0.045$ is the closest to experimental values curve.

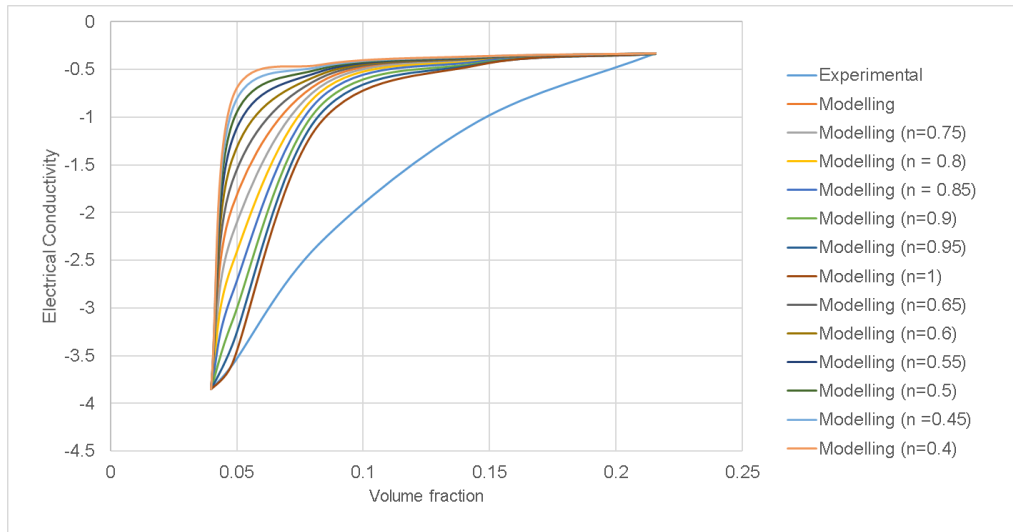


Figure 24. The curves presenting iterations for constant n, the curve with n value 1 is the closest to the experimental values curve.

3.6.5. Iterations for surface energy

The surface energy values for both biocarbon and PA 12 were subject to iterations and the values obtained were replaced in the modelling calculations to determine the value that can close the gap between the experimental and theoretical conductivity values. The surface energy values are used to calculate the constant K in the modelling expression. The surface energy value for PA 12 was taken to be 40.7 mJ/m^2 , this value was subjected to ± 5 and was stopped at maximum value 65.7 mJ/m^2 and the lowest value was set at 15.7 mJ/m^2 . Similarly, the surface energy for biocarbon was incorporated as 24.1 mJ/m^2 and was subjected to ± 5 and the maximum value was 49.1 mJ/m^2 and lowest value

was 0.1 mJ/m². These updated values were incorporated into calculating K that was included in the modelling calculations. The curves for updated values of K are presented in Figure 26.

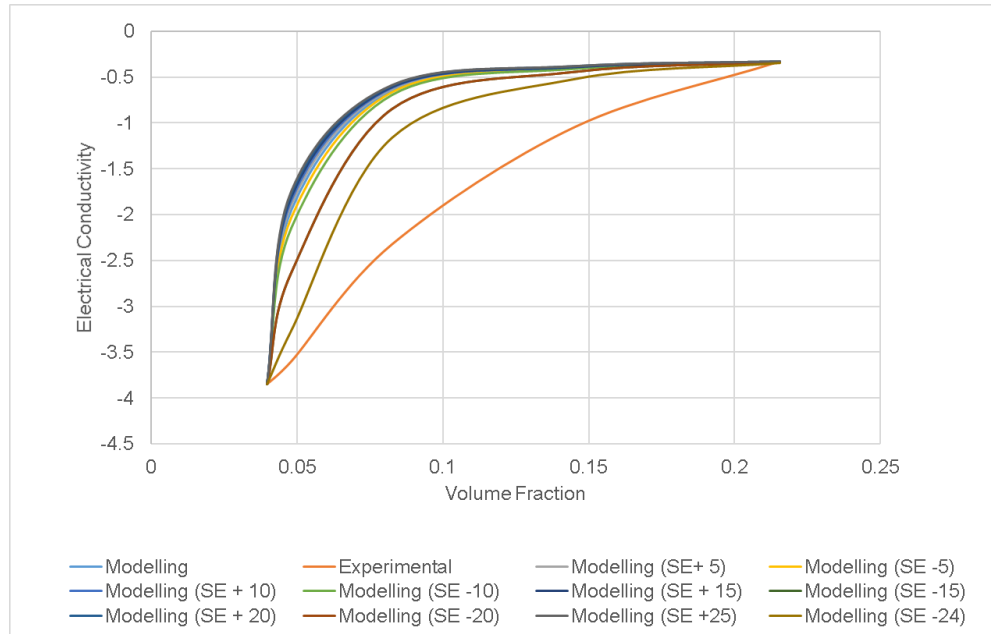


Figure 25. The curves presenting the iterations for surface energy values for composite components, the curve developed using SE-24 is the closest to experimental values.

3.6.6. Iterations for F

F is the component that incorporates the value for morphology of filler in the modelling calculations. The value of F was initially taken as 0.225, it was updated by ± 0.05 . the maximum value derived was 0.375 and the minimum value was 0.175. The curves for updated F values are presented in Figure 27. As we can

see the modelling curves are stretched beyond the maximum experimental conductivity value and the fit is not great. The F values were further iterated by ± 0.01 to the original value and then the calculations were done with all the other updated values. The results are presented in curves in Figure 28. No difference can be observed between the modelling curve values and the iterated curve values.

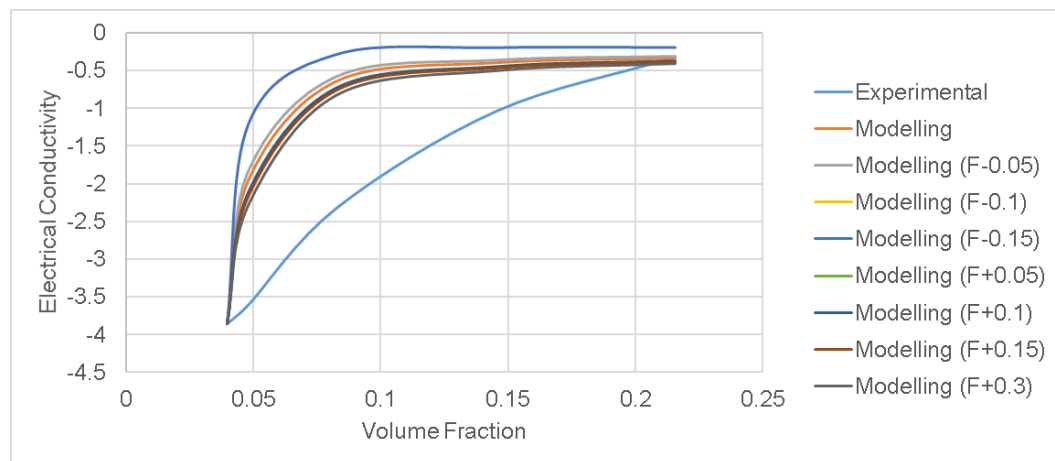


Figure 26. The curves representing iterations for F, the curve developed with F+0.3 is the closest to the experimental curve.

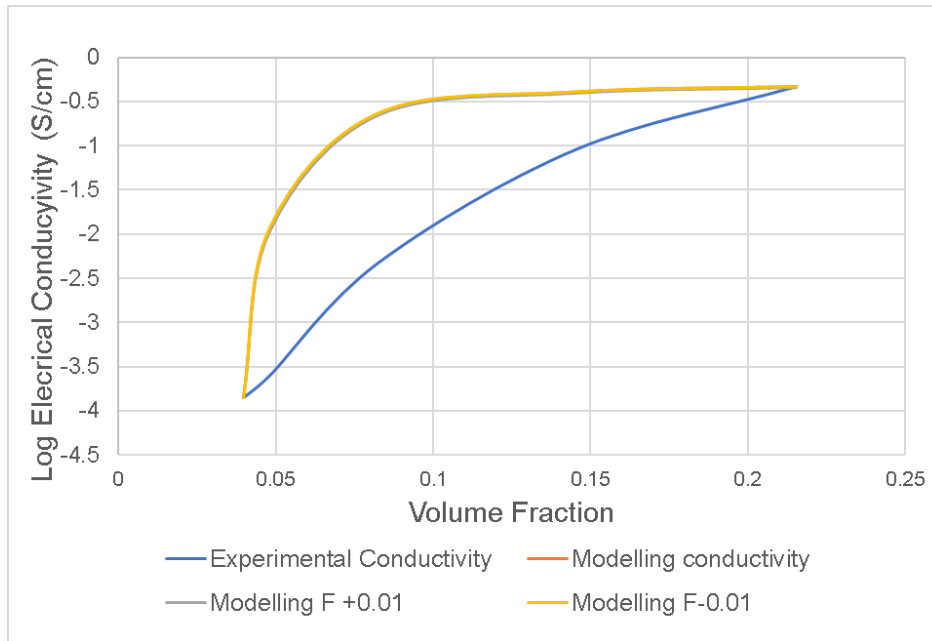


Figure 27. The curves representing the iterations for F. No clear distinction can be seen in the modelling curve and the iterated curves.

3.6.7. The modelling curve with updated inputs

All the values derived from these iterations were combined and the calculations were done using these new inputs. As a clear distinction between the iterated values for F was not obtained, the value for F+0.01 and F-0.01 was incorporated in the updated model to Figure out the best fit with all the other updated input values. It can be seen in Figure 29 that the best fit was obtained with the value F-0.01

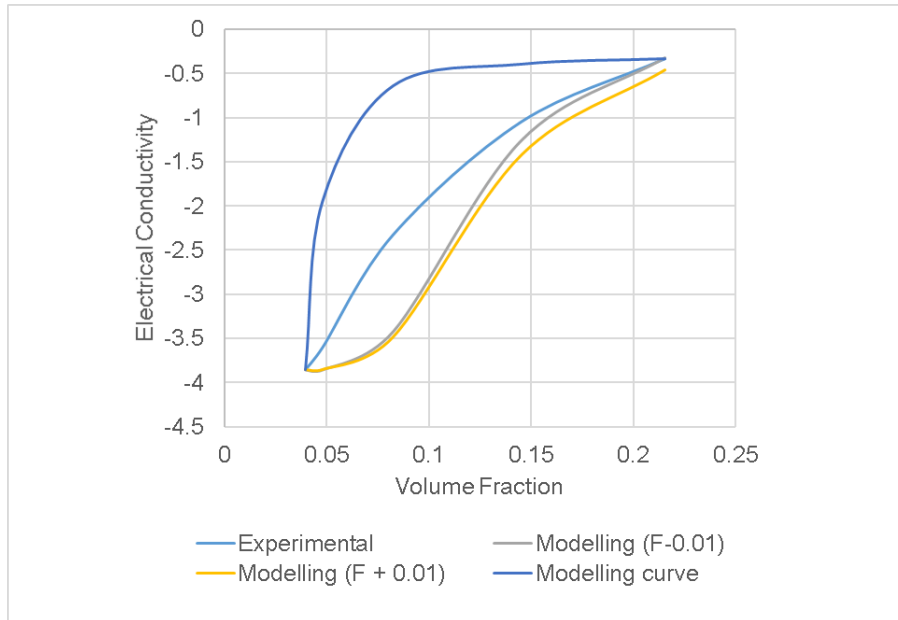


Figure 28. The curves presenting all updated values with iterations for F, it can be observed the value for F-0.01 is closest to the experimental curve.

The final input values for the updated model are presented in table VIII. It was observed that with these iterated values the gap between the experimental and theoretical values was significantly reduced as shown in Figure 30. The gap between the experimental and the modelling curve is significantly reduced when compared to the initial model. However, a perfect fit between the experimental and theoretical values was not achieved. The gap between the theoretical and experimental curve is very less for the fillers having higher biocarbon concentration and higher electrical conductivity, compared to the composites with lower biocarbon concentration. This could be due to the higher volume fraction and/or the higher electrical conductivity values of these composites that was able to close this gap. Based on the shape of the modelling curve at the

percolation point, the shift of the percolation point to the left in the experimental curves can probably improve the fit of the experimental and theoretical curves at the lower filler concentrations as well.

Table VIII. The updated input and calculated values for modelling of biocarbon filled composites.

Loading Rate	VF at F (maximum packing) ϕ	VF at percolation ϕ_c	n	K	k	F	Conductivity at percolation (log σ_c) S/cm	Conductivity at F (log σ_F) S/cm	Log σ
7.5	0.039	0.0397	1	1.607051	9116.571	0.215	-3.853	-0.32926	-3.853
9	0.048	0.0397	1	1.607051	7.672958	0.215	-3.853	-0.32926	-3.853
15	0.082	0.0397	1	1.607051	1.488454	0.215	-3.853	-0.32926	-3.4197
25	0.145324	0.0397	1	1.607051	0.604238	0.215	-3.853	-0.32926	-1.2585
35	0.215483	0.0397	1	1.607051	0.363059	0.215	-3.853	-0.32926	-0.3257

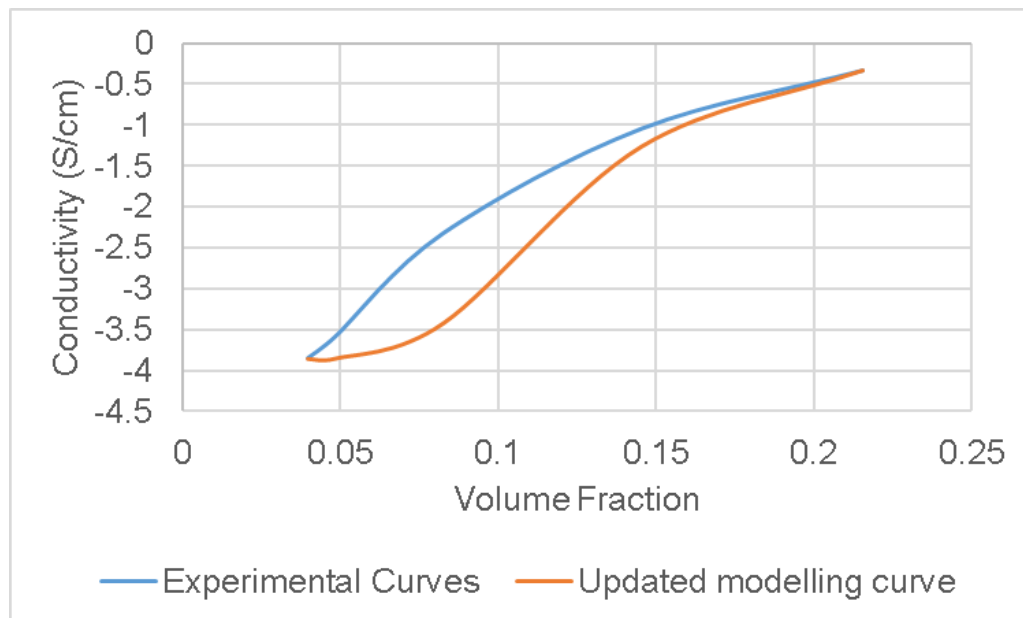


Figure 29. The curves presenting the experimental values and the updated modelling values.

3.7. Conclusion

This study was developed to develop a modelling framework for natural biocarbon filled composites using carbon fiber-based model as a reference. A good fit was not obtained initially using the data from literature and reference model. After a series of iterations for the different constants and variables the gap between the theoretical and experimental electrical conductivity curve was closed significantly. However, a perfect fit between the experimental and theoretical curves was still not achieved. As this study was built on a reference based on synthetic filler, certain nuances like difference in raw material feedstock leading to difference between the properties and characteristics of natural and synthetic filler could have contributed to the lack of fit between the theoretical and experimental conductivity curves. As there is a lack of modelling studies done incorporating biobased filler materials, this study can act as a steppingstone for further development of modelling methods that can be specific only to natural fibrous fillers or even more specifically biocarbon fibres as they are gaining traction as a potential replacement for traditional fillers like carbon fibre, graphene, etc.

4. Chapter 4 - A comparative study on the effect of morphology of fillers on the properties of biocarbon filled polyamide 12 composites.

4.1. Abstract

Polymers based composites used in automotive manufacturing have contributed significantly to light weighting. Composites properties are greatly dependent on filler properties that determine the properties of the end product. In this study recycled PA 12 composites were filled with biocarbon fiber and biocarbon powder at different concentrations to study the impact of filler morphology on composite properties. It was observed that for both sets of composites the electrical properties improved compared to pure PA12 that has a resistivity of - 14 S/cm. The composites filled with biocarbon fiber filler had significantly high electrical conductivity values. At 7.5 wt.% the biocarbon fiber samples reported log electrical conductivity of – 3.85 S/cm while biocarbon powder samples reported log conductivity values of -7.455 S/cm. Similarly at 35 wt.% the biocarbon fiber filled composites reported log electrical conductivity of – 0.33 S/cm while the biocarbon powder filled composites log conductivity was -2.54 S/cm. The pronounced difference in electrical conductivity can be attributed to the morphology of biocarbon incorporated in the composites. The thermal properties for both the composites showed improved thermal stability, more prominent in biocarbon powder filled composites compared to biocarbon fiber

filled composites. An increase in thermal stability of the composites was observed on incorporation of filler and an increasing trend was observed with increasing filler concentration as well for both the composites. The mechanical properties showed improvement on incorporation of biocarbon as the storage modulus increased from 1500 MPa for pure PA 12 to ~ 3500 MPa on incorporation of biocarbon filler. The storage modulus values were also better for biocarbon fiber filled composites. The composite samples were scaled up to 1 kg with 15 wt.% biocarbon fiber concentration. The electrical properties of the composites were reported to be – 7.54 S/cm. The tensile and flexural modulus for the composites were reported to be 2280 ± 75.2 MPa and 2071.12 ± 36.1 MPa respectively, indicating improved electrical and mechanical properties compared to pure PA 12.

4.2. Introduction

Sustainable automotive manufacturing looks for ways to improve the carbon footprint generated in the lifetime of a vehicle. The sustainability goal can be achieved by improved fuel efficiency and reduced greenhouse gas emissions. Reduced weight of automobiles can facilitate achievement of these goals. Lightweighting of vehicles is taken up as a sustainable approach by automotive manufacturers to attain the sustainability goals without compromising on the quality of the product (19). Polymer based products including unfilled and filled composites with inorganic fillers and fibres have created a niche in replacing conventionally used materials making about 15% of the entire vehicle. They comprise a significant amount of the interiors and even the fuel line making a significant difference in automobile weight. This replacement has definitely made it possible to move closer to the sustainability goals established by the automotive manufacturers, however, the polymer composites are filled with inorganic fillers and fibres such as talc, calcium carbonate, clay and glass fibres (127,128) making the end product bulky. Another issue encountered with these composites is poor electrical conductivity leading to electrostatic accumulation that could be a problem. To overcome these shortcomings composites filled with light weight electrically conductive fillers forming electrically conductive polymer composites are now being considered ideal. Electrically conductive polymer composites(ECPCs) are polymer composites with a conductive filler material

(25,101–103). Electrically conductive composites can be developed by incorporation of various electrically conductive fillers in the matrix. Carbon based fillers like carbon nanotubes, carbon fibers, carbon black etc., have been reported to be used as filler and the composites have shown good conductivity values (135,136). The synthetic carbon-based fillers are highly energy and cost intensive, a potential replacement for these fillers is biocarbon.

Biocarbon is the carbon rich solid material that is left after the thermochemical conversion of biomass in an oxygen limited environment (1). Carbonization is a process in which the progressive conversion of a three dimensional organic macromolecular system like wood, into a macro-atomic network of carbon atoms (23). In the process of carbonization, the biomass is heated to a certain temperature usually at a slow heating rate in an inert atmosphere using gasses like nitrogen argon etc. Biocarbon has been largely implemented in soil amendment and soil quality enhancement. Biocarbon has been reported to have improved the soil nutrient quality, has a positive effect on the soil microorganisms, owing to its high surface area and nutrient content it does a great job in soil quality improvement (162–164). In the recent decade biocarbon is seen to be gaining a lot of traction as a reinforcing filler improving the mechanical and thermal properties in polymer composites. Das et al. 2016 (5) have reported improved tensile modulus of 3.82 GPa and improved thermal stability in polypropylene filled with biocarbon developed from pine wood recovered from landfills (5). Behazin, Mohanty, and Misra 2017 (79) incorporated ball milled switch grass (*miscanthus*) based biocarbon into a toughened

polypropylene matrix and observed 120% improvement in mechanical properties in the composites (79). Biocarbon carbonized at temperatures higher than 600°C develop electrical conductivity and can be incorporated as an electrically conductive filler in polymer composites. Nan et al. 2016 (31) developed electrically conductive polyvinyl Alcohol (PVA) composites by incorporating wood biocarbon developed from three different species, carbonized at different temperatures and reported the improvement of mechanical properties as the tensile modulus values improved by 429% at 10% biocarbon incorporation along with electrical conductivity of 1.833×10^{-3} S/cm comparable to composites filled with carbon nanotubes (31). Giorelli and Bartoli 2019 developed biocarbon from coffee grounds by carbonizing the biomass at different temperatures and incorporated this biocarbon into epoxy matrix and reported electrical conductivity of 2.02 S/m in composites filled with 20 wt.% biocarbon carbonized at 1000°C. C. Das et al. 2021 (134) have a detailed review discussing effective incorporation of biocarbon as reinforcing and electrically conductive filler in various polymer composites. Addition of biocarbon as a filler in composites not only makes the composite sustainable, it opens up doors for value added application of agricultural and forest materials. As biocarbon can be made from any kind of lignocellulosic biomass it creates a platform to utilize waste generated from agricultural waste, sawmills, wood processing industries, furniture manufacturing industries etc., (6,14,68,165–167). Reuse of lignocellulosic feedstock as raw material for biocarbon production can close loops and help towards lowering greenhouse gas emissions.

One of the widely used polymers in automotive manufacturing is polyamide (PA) 12. It has exception resistance to most of acids and alkalis, it has poor oil absorption, resistant to reducing and oxidizing agents, has very low degradation by light exposure and low flammability (168). The above-mentioned properties of polyamide 12 make it a suitable raw material to be used as composite matrix for manufacturing under the hood components and in the fueling system of automobiles. Virgin plastic is usually the preferred choice owing to its superior properties, however with increased focus on sustainable manufacturing practices a lot of focus is on recycling polymers and reusing them as raw materials. Waste polyamide 12 recovered from selective laser sintering manufacturing of composites has been successfully implemented as a raw material for development of composites. Very little to insignificant difference between the properties of composites developed with virgin PA 12 and the composites made with recycled PA 12 were observed (169,170). This opens up the possibility of a closed loop manufacturing system that can facilitate the recycling of scrap polymer based automotive parts making the process highly sustainable.

Aspect ratio of filler is a crucial factor when considering electrical properties as popular fillers like carbon fibers and carbon nanotubes have a high aspect ratio owing to their fibrous morphology and are attributed with excellent electrical properties. Higher aspect ratio of conductive filler can facilitate improved electrical properties in the composites (171–173). This study was developed with the hypothesis that wood based biocarbon filler developed using pulp fiber has

better electrical conductivity compared to biocarbon powder developed from hardwood feedstock. In this study biocarbon developed from two different kinds of wood feed stock (milled wood particles and wood pulp fibers) were compared based upon their performance as electrically conductive filler. The objective of the study was to determine whether the hypothesis of higher conductivity is achieved with a filler with higher aspect ratio or not was analyzed by carbonizing the biocarbon at same temperature and developing composites and subjecting them to electrical conductivity analysis. Along with electrical conductivity, the thermal properties of the composites were also studied, and the results are presented in the study.

4.3. Materials and methods

4.3.1. Biocarbon, Carbon fiber and recycled Polyamide 12

Biocarbon filler incorporated in this study was developed from two different biomass feedstocks namely milled hardwood hickory and Douglas fir pulp. The milled wood feedstock was prepared by milling hickory wood chunks in a Wiley mill Figure 31. The pulp used in the study is Douglas fir pulp that was provided to us by Domtar paper company. The pulp was deagglomerated using water and then dried in a hot air oven at 90°C overnight. The dried pulp was further deagglomerated into a fluffy form that was used as feedstock Figure 32. Both the milled wood and pulp fiber feedstock were carbonized at 1000° C in a tube

furnace with three zone heating (Model 23-891, Lindberg, Watertown, WI, USA). The carbonization was done in a steady flow of nitrogen at 1000 cc/min to keep the system inert and also facilitate some transfer of heat in the carbonization tube. The feedstock was retained at 1000° C to ensure uniform heating throughout all zones and all the samples. 23 wt.% of biocarbon was retained post carbonization from milled wood feedstock and 16 wt.% of biocarbon was retained from the Douglas fir pulp feedstock.



Figure 30. Milled wood used as feedstock for biocarbon production.



Figure 31. Deagglomerated Douglas fir pulp used as feedstock for biocarbon production.

Carbon fiber (Ultramid® Advanced N3HC8) used in this study was provided by BASF, having a bulk density of 1320 kg/m^3 and electrical conductivity of 0.2 S/m .

Recycled polyamide (PA) 12 powder (Figure 3) was used as matrix in this study and was provided to us by Ford Motor Company. The PA 12 was waste that was recovered from selective laser sintering process. It was heated at a temperature range between 170°C to 175°C for SLS for several hours that is normally subject to the nature of the finished product that determines the complexity and scale of the process. Post process the setup is cooled for about 24 hours before the finished product was retrieved. To prevent oxidation the process was carried out

in a nitrogen blanket to keep the system inert. The melting point of recycled polyamide 12 was 178 °C and the density was 1.01 g/cm³.

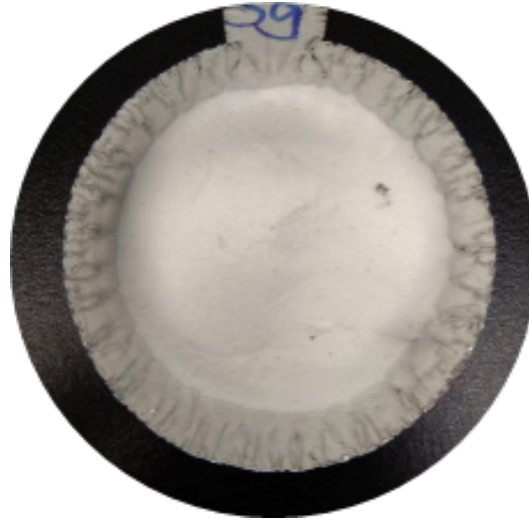


Figure 32. Recycled PA 12 powder used as matrix in biocarbon filled composites.

4.3.2. Composite Fabrication

The composites with the two different biocarbon were developed in several steps, the steps are discussed below. The entire process is presented in Figure 34.

Preparation of biocarbon filler – The biocarbon particles developed from hickory wood were milled in a ball mill for 1 hour to reduce the particles into powder. The powder was characterized for carbon content and particle size. The biocarbon fibers were also characterized for carbon content and aspect ratio of

fibers.

Dispersion of biocarbon filler in PA 12 matrix- Both the biocarbon fillers were incorporated at 7.5, 9, 15, 25 and 35 wt.% in the PA 12 matrix. The biocarbon powder and polyamide 12 were suspended in ethanol and ultrasonicated using Elma ultrasonic cleaner. The samples were subjected to 37 KHz ultrasonic frequency for 60 minutes. The dispersed samples were dried at 80°C in a hot air oven overnight to remove the ethanol and condition the samples prior to sample fabrication. The biocarbon fiber was dispersed in the PA 12 matrix using a coffee grinder. The blades of the coffee grinder were modified by duct tape wrapping, to mask the edges of the blades. The masked blades minimize the effect of blade on the biocarbon fibers aspect ratio.

Composite Fabrication - Hot compression molding method was used to fabricate all the composite samples. The fabrication was done in 3 steps, heating, holding and cooling. The composite mixture was heated from ambient temperature to 300°C. The temperature was selected based on previous runs that were done at lower temperatures and proper curing of the composites was not achieved, but a properly cured composite was obtained at 300° C. Post heating the samples were held at 300° C for about 30 minutes to ensure uniform heating and curing of the composite discs. After 30 minutes the samples were cooled to room temperature using running water around the die. Post the cooling cycle the pressure in the set up was released and the composite discs were recovered. The composite disc surface was polished using a grinding disc (Leco

Spectrum System 1000) at 100-150 rpms. The abrasive medium used was an 8-inch P500 grit Alumina based polishing paper, water was used as the polishing media. Each face of the disc was polished between 1-3 minutes to roughen the surface for better contact with the electrodes for characterization.

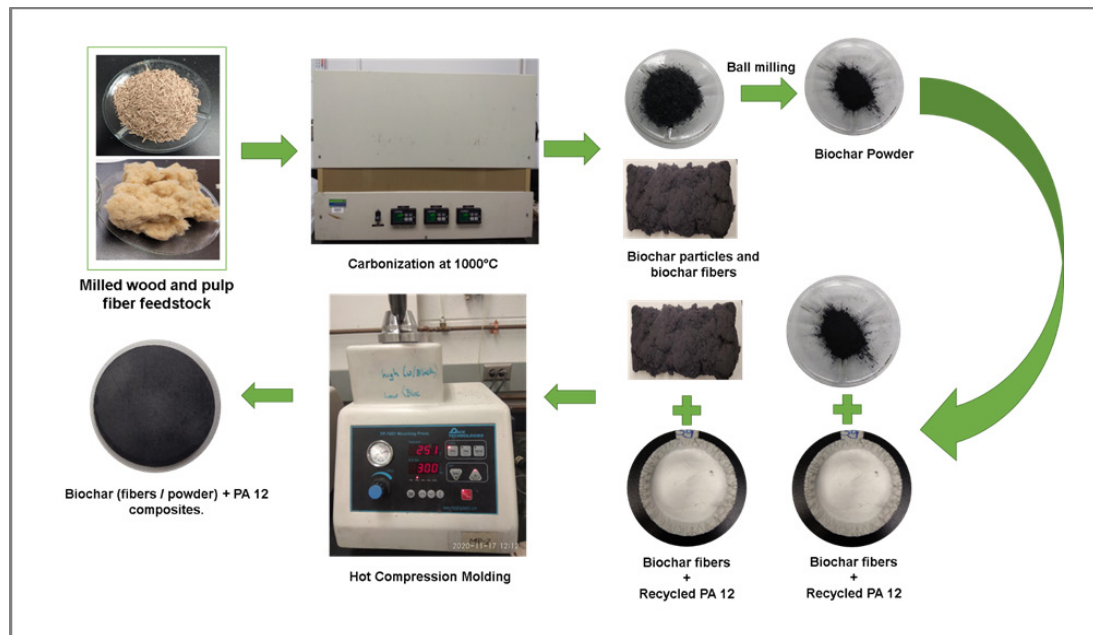


Figure 33. Process flow for the fabrication of PA 12-biocarbon composites.

4.3.3. Elemental analysis and morphology of filler

Biocarbon powder and fibers were characterized for carbon (C) and nitrogen (N) content using elemental analysis. Dried, ground, and homogenized biocarbon fiber and biocarbon particle samples were weighed into tin capsules and analyzed for carbon content on an Elemental Combustion System (Costech

4010, Costech Analytical Technologies, Inc., Valencia, CA) in the LEAF core facility at Michigan Technological University. The instrument was calibrated with atropine. Stability was checked with NIST 1547 every 12 samples with a relative standard deviation of 0.03 for N and 0.19 for carbon.

The particle size of biocarbon powder filler was determined using laser diffraction method. The sample was dispersed in water and laser beams were incident on the dispersed particles. Based on the diffraction of the incident laser beam the volume percent of biocarbon particles in different particle size groups was determined. This distribution data was later analyzed using Microsoft Excel software.

The dispersed mixture of biocarbon and biocarbon fibers was used to determine the aspect ratio of biocarbon fibers in the composite. Once the biocarbon was dispersed in the PA 12 powder using coffee grinder, they were analyzed using scanning electron microscopy (SEM) using Emcrafts tabletop SEM. The imaging of the fibers was done at 5 kV with 200x magnification. The aspect ratio of the fibers was calculated by measuring the length and breadth of the fibers using ImageJ software.

4.3.4. Electrical conductivity measurement of composites

The composite samples were characterized for electrical conductivity using a measuring device designed in the lab in Michigan Technological University

(Figure 36). This device was developed based on the ASTM standards D257-14 and D4496 -13. The principle of this device is measurement of resistivity of sample under known pressure value. The samples were placed between the electrodes and 20-inch pounds torque was applied on the samples. DC current input was facilitated using a power source (Powerbes DC power supply SPS W1203, with output of 120V and 3A), the current and voltage were recorded using (Sigilent SDM3065X 6 ½ digit Digital Multimeter) for current and (Sigilent Technologies SDM3055 5.5 Digit Digital Multimeter) for voltage respectively. The current and voltage input values were set at the lowest possible values to prevent sample any damage to the samples over the course of measurement. 8 different points on the surface of the composite disc were measured for each sample and 4 to 5 replicates were characterized for each filler concentration in both the composite sample sets. Average and standard deviation were calculated for each set of samples.

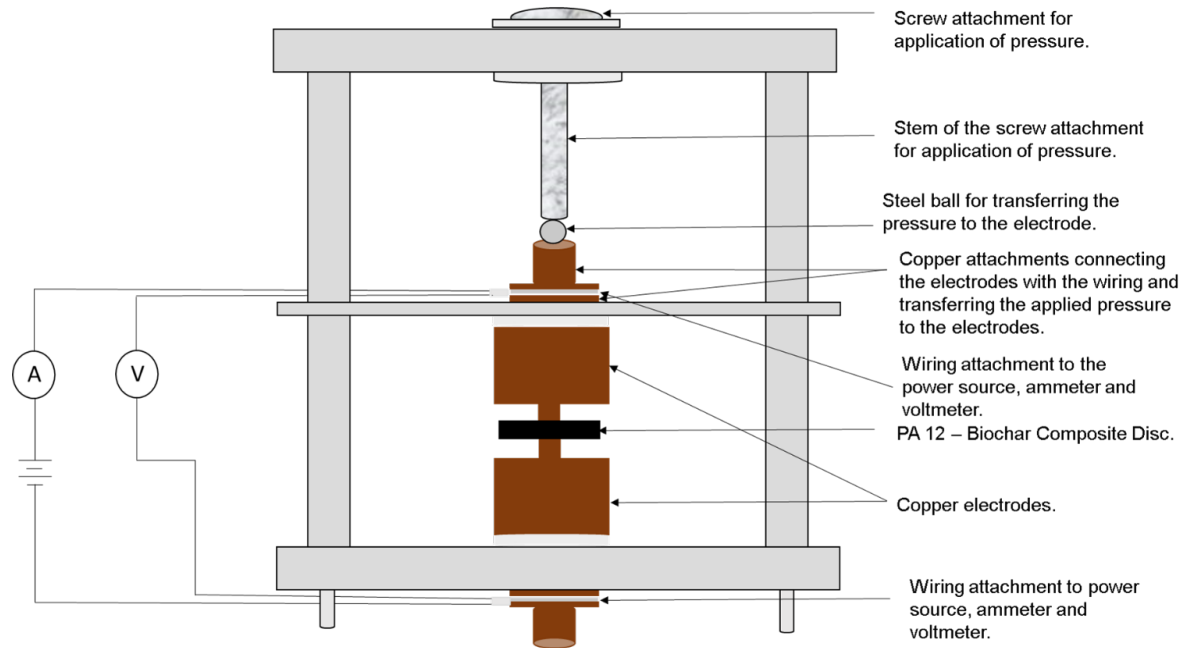


Figure 34. The equipment used to measure the electrical resistivity of PA 12-Biochar composites.

The resistivity of the samples was calculated using the formula described in equation 1 (31) and conductivity was calculated using equation 2,

$$\rho = \frac{RA}{l} \quad (1)$$

ρ = Resistivity of sample in Ω cm.

R = Resistance of sample in Ω .

A = Area of the electrodes in contact with the sample in m^2 .

l = Thickness of the sample in m.

$$\sigma = \frac{1}{\rho} \quad (2)$$

σ = Conductivity (S/m)

ρ = Resistivity (Ωcm)

4.3.5. Thermal Properties of composites

The thermal stability of biocarbon addition to the composite was analyzed using Thermogravimetric Analysis (TGA). Samples were obtained from different spots of a composite disc to get determine the effect on the composite sample as a whole. Three replicates of each sample were analyzed. Approximately 10mg of sample was analyzed using TA Q500 TGA. The composite samples were heated from room temperature to 500 °C at a heating rate of 10°C/ minute, the samples were maintained at 500 °C for 30minutes. The TGA runs were performed in nitrogen atmosphere. The TGA data was analyzed using TA Universal software (TA Instruments, USA).

4.3.6. Mechanical Properties

The DMA of pure polymer and biocarbon filled composites was done in tensile mode for 20mm long 4mm wide 1mm thick samples. The experiment was carried out by heating the samples from ambient temperature at 25 °C to 150 °C, at a strain amplitude of 0.01% and frequency of 1 Hz. The glass transition temperature (Tg) of the samples was calculated from the peak of tan delta peaks.

4.4. Results and discussion

4.4.1. Morphology of biocarbon fillers and carbon content

The graph here in Figure 36 shows the particle size distribution of the milled wood biocarbon, ball milled for 1 hour. The distribution of the particles appears to be normal, and large volume of particles is distributed between 4.7, 3.3 and 2.4 μm . Biocarbon powder was viewed under optical microscope at 40X magnification, the particles as it can be seen in Figure 38, are very small as they have been milled for 60 minutes in a ball mill resulting in the current particle size. The average particle size of biocarbon powder particles was determined to be $5.03 \pm 3.5 \mu\text{m}$.

The aspect ratio of 200 biocarbon fibers was calculated dividing the average length of fibers by the average diameter of the fibers respectively and was determined to be 25. The average length of the fibers was $181.9 \pm 115 \mu\text{m}$, and the average diameter of the fibers was $7.27 \pm 1.45 \mu\text{m}$. The frequency distribution of the aspect ratio of 200 fibers is presented in Figure 37. As per the distribution of aspect ratio maximum aspect ratio vales are between 10-20 followed by 20-35. Even though the fibers underwent a fair amount of breakage post processing in the coffee grinder, the aspect ratio indicates the length of the fibers was still maintained. This shows the effectiveness of the modification of the coffee grinder blades in preserving the aspect ratio of the biocarbon fibers. The

fibrous structure of biocarbon fibers post carbonization can be seen in the SEM image in Figure 39 (a) and the morphology of biocarbon fibers after dispersion in the PA 12 matrix can be seen in Figure 39 (b).

The carbon and nitrogen content of the biocarbon fibers was determined to be 88 wt.% and 0.7 wt.% respectively. Biocarbon powder samples contained 92 wt.% and 0.5 wt.% nitrogen. The percentage of the elements was calculated against the weight of samples used for the analysis.

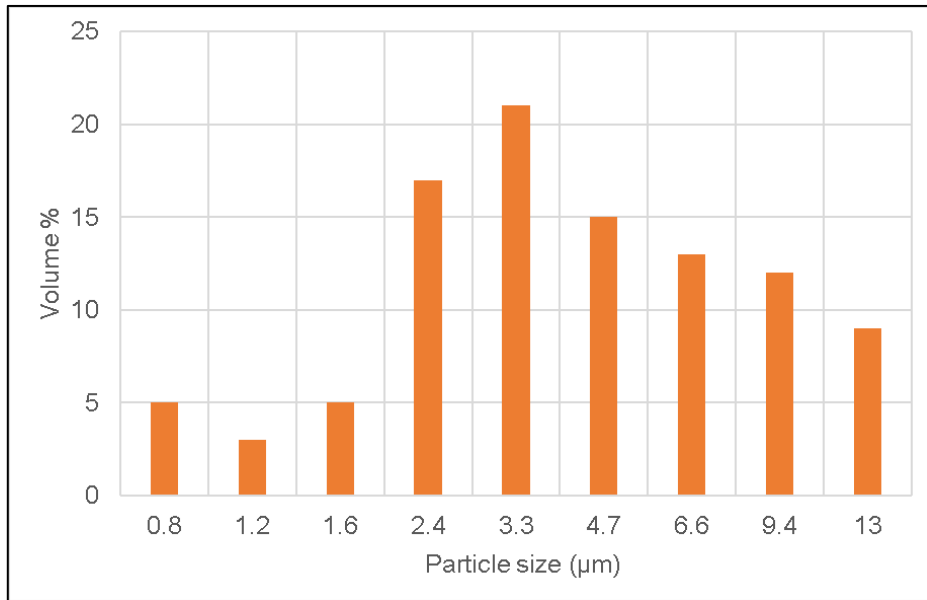


Figure 35. The particle size distribution of biocarbon powder shows 3.3 µm had the maximum volume.

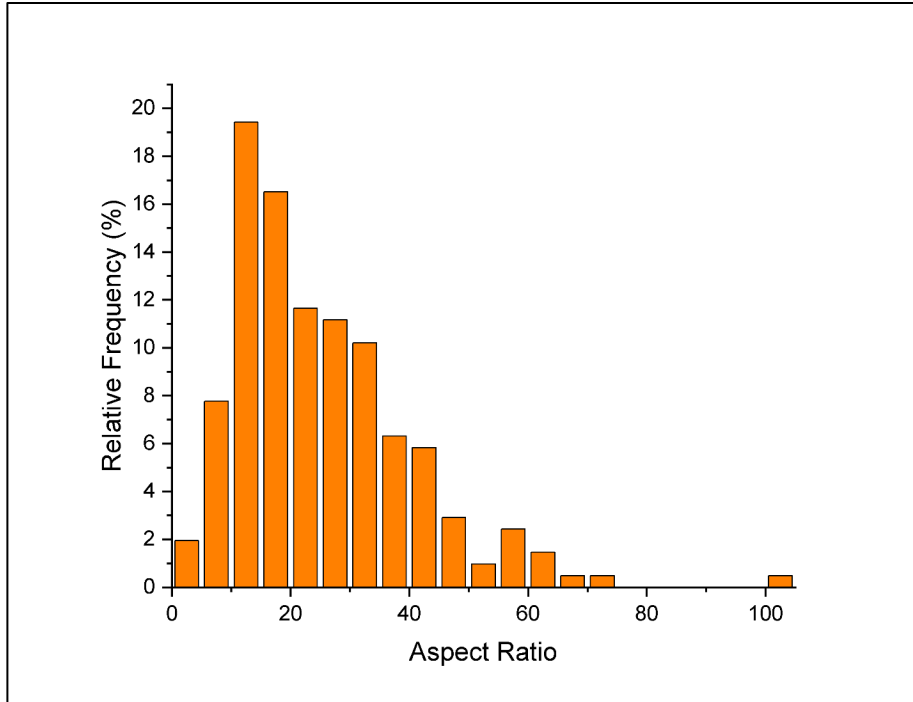


Figure 36. The frequency distribution of aspect ratio of 200 biocarbon fibers.

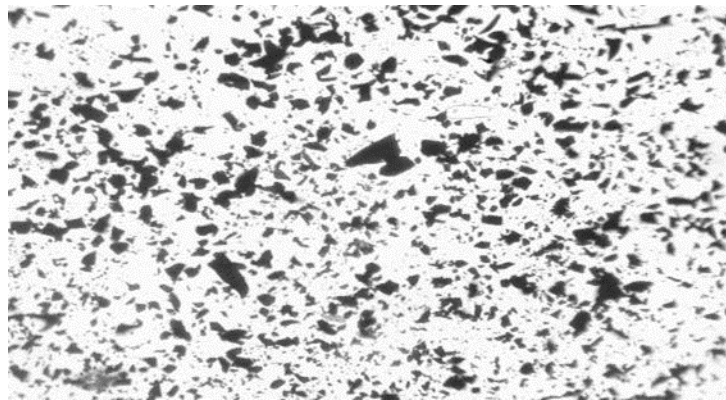
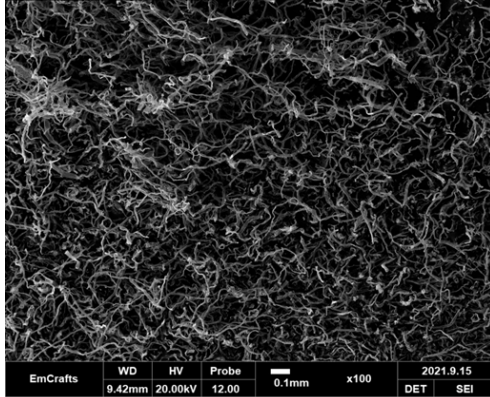


Figure 37. Biocarbon particles observed under optical microscope set to 40X magnification.



a. Carbonized biochar fibers



b. Biochar dispersed in PA 12

Figure 38. (a) Biocarbon fiber after carbonization as seen using SEM at 100X magnification; (b) Biocarbon fibers dispersed in PA 12 matrix, as seen under an optical microscope set to 40X magnification.

4.4.2. Electrical Properties

The addition of biocarbon filler in both fiber form and powder form improved the electrical properties of the composites considerably. The log electrical conductivity of pure PA 12 was -15 S/cm (174) and it increased considerably with increasing filler concentration. The biocarbon fiber filled samples, reported log electrical conductivity of - 3.85 S/cm for biocarbon fiber composite samples and -7.475 S/cm for biocarbon powder filled samples at 7.5 wt.%, this shows a substantial improvement in the electrical properties of composites even at a low filler concentration. The resistivity kept dropping with increasing filler concentration and at the highest filler concentration of 35 wt.% the electrical conductivity of the composites was - 0.33 S/cm of the biocarbon fiber composite samples and -2.541 S/cm for biocarbon powder filled samples. In both cases the electrical conductivity goes up with addition of filler and increases continuously as the filler concentration progressively increases. The improved electrical properties can be attributed to several factors, one of the major factors being temperature of carbonization. Several studies have reported carbonization treatment temperatures $\geq 1000^{\circ}\text{C}$ has resulted in the formation of electrically conductive biocarbon and have also reported successful implementation of the biocarbon as an electrically conductive filler in polymer composites (24,31,42,104,105). Higher temperatures of carbonization result in the formation of turbostratic structure in the filler. The turbostratic structure in a material is

characterized by the presence of discontinuous highly ordered crystalline phases, its these phases that make the filler electrically conductive (23,24). Morphology of filler is another very important factor that determines the electrical properties of the composites. As discussed earlier it is seen that higher aspect ratio is often related to better electrical properties(171–173). In this study, both the biocarbon fillers improve the electrical property of the composites, however, the log electrical conductivity values reported for composites filled with biocarbon fiber fillers are significantly higher compared to conductivity values of composites filled with biocarbon powder, at the same loading rates. The only factor differentiating the two fillers is the morphologies of the filler. The fibrous structure of biocarbon fibers having aspect ratio of is drastically different from the particles having average particle size of 5.03 μm . The biocarbon fibers are significantly longer compared to the broken bits of biocarbon particles as seen in the morphology analysis. Hence the difference in electrical properties of the resultant composites filled can be attributed to the morphology of filler incorporated. The electrical conductivity trends of biocarbon fiber filled composites and biocarbon powder filled composites are presented in Figure 40. The electrical property of the composites is also impacted by the concentration of filler. As we can see in table in both cases the electrical conductivity of the composites significantly increase with increasing filler concentration, this is in accordance with previously reported studies (31,42).

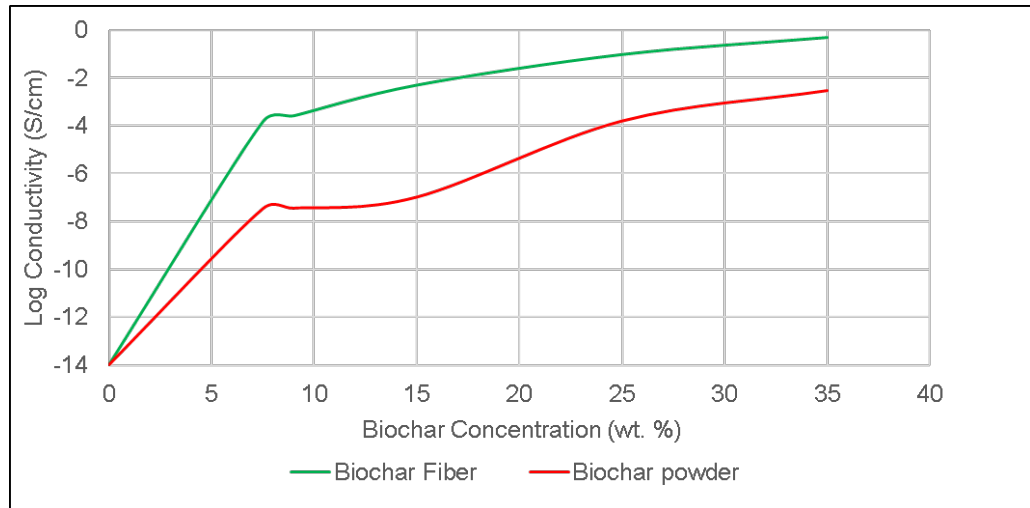


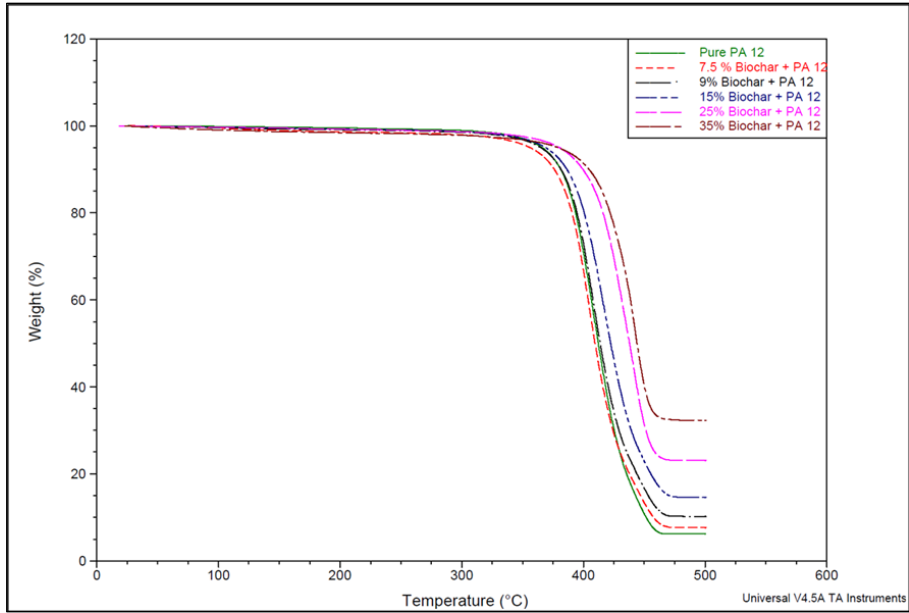
Figure 39. Electrical conductivity trends of biocarbon fiber filled composites and biocarbon powder filled composites.

4.4.3. Thermal Properties

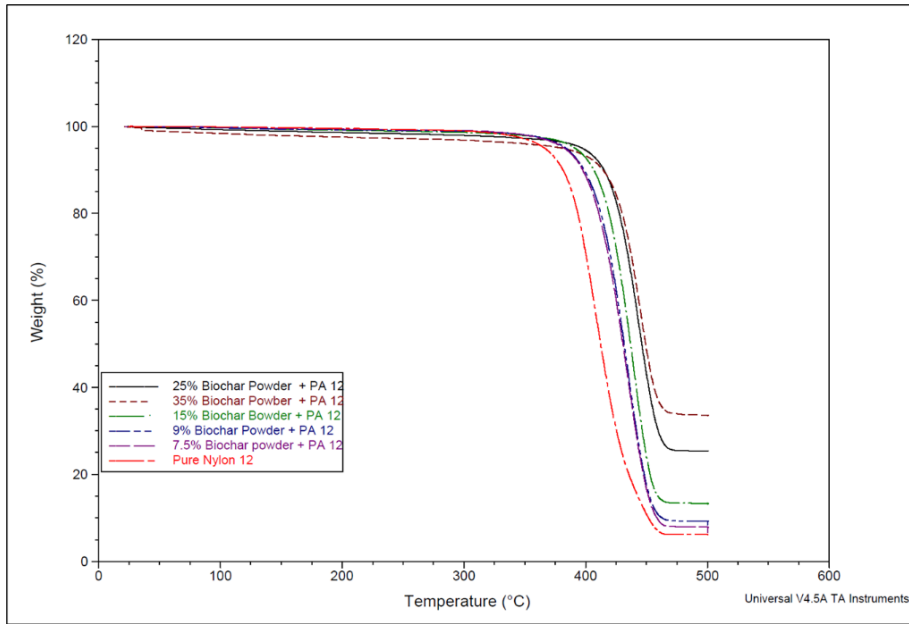
The Figures (41) a and b show the weight loss curves of pure polyamide 12 and the composites filled biocarbon (a) is for biocarbon fibers and (b) is for biocarbon powder. There is a shift in the degradation temperature of the composites on addition of biocarbon irrespective of the type of filler. The initiation of thermal degradation happens at about 378.10 °C for pure PA 12, while for biocarbon fiber filled composites the temperature shifts

to 381.75 °C at 9 wt.% filler concentration and at the temperature shift keeps progressing as filler concentration increases as at 35 wt.% the composites the onset of thermal degradation temperature went up to 396.72 °C. Similar trends are also observed for biocarbon powder samples, the onset of thermal degradation takes place at 388.84 °C at a filler concentration of 7.5 wt.%, the trend kept increasing with filler concentration and the onset of thermal degradation increased to 411.13 °C at 35 wt.% biocarbon powder filler concentration. This shift is due to the improved thermal stability of the composites that is attributed to the thermally stable biocarbon obtained by carbonization at such high treatment temperature (5). The derivative TGA curves shown in Figure 42 (a) for biocarbon fiber filled composites and (b) for biocarbon powder filled composites, also show a shift towards right for the highest degradation temperature for both sets of composites. The maximum degradation temperature of pure PA 12 was 407.26 °C that went up to 417.55 °C at 15 wt.% biocarbon fiber incorporation and kept increasing. At 35 wt.% biocarbon fiber concentration the maximum degradation temperature recorded was 442.74 °C. The biocarbon powder samples also had an increase in the maximum degradation temperatures, at 7.5 wt.% filler concentration the maximum degradation temperature reported was 433.79°C. Similar to the mass loss curves the maximum degradation temperature increased with filler concentration, at 35 wt.% biocarbon powder concentration the maximum degradation temperature was 445.49

°C. Incorporation of biocarbon filler improves the thermal stability in both cases; however, incorporation of biocarbon powder showcases this improvement even at lower concentrations. The effect of thermally stable nature of biocarbon is more pronounced in powder form compared to fiber form. The particle size of the biocarbon powder provides more surface area allowing better heat transfer throughout in the composite and better interaction between the polymer and filler leading to slightly better thermal properties. Increased thermal stability in the composites can facilitate application of these composites as raw materials for components requiring higher temperature resistance in automobile manufacturing.

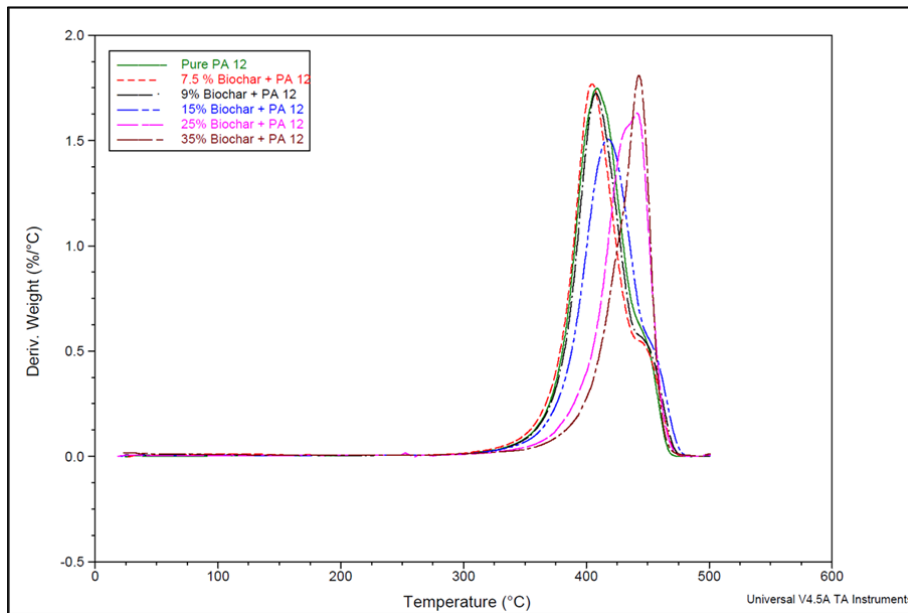


(a) Biocarbon Fiber

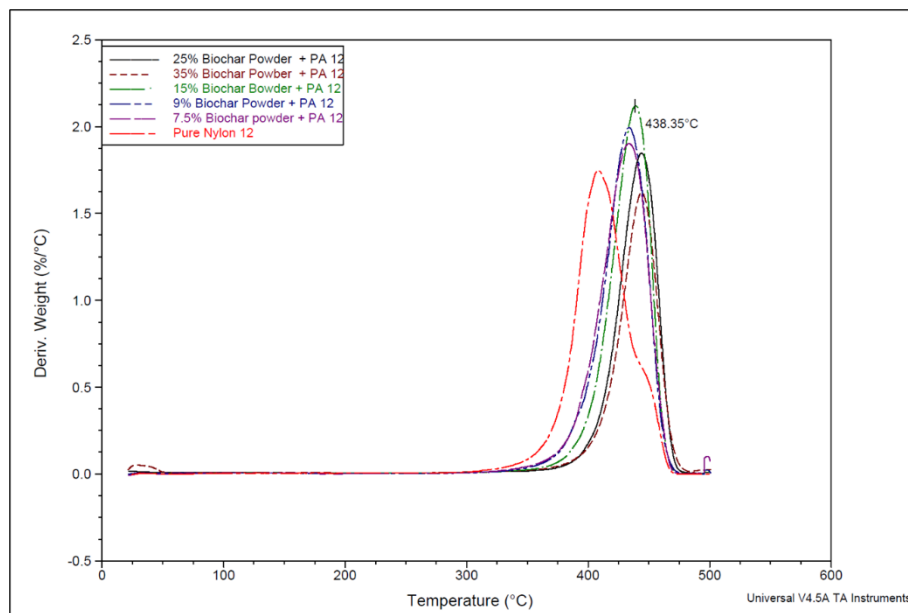


(b) Biocarbon Powder

Figure 40. TGA weight loss curves of biocarbon filler filled PA 12 composites (a) weight loss curves of biocarbon fiber filled PA 12 composites, (b) weight loss curves of Biocarbon powder filled PA 12 composites.



(a) Biocarbon fiber



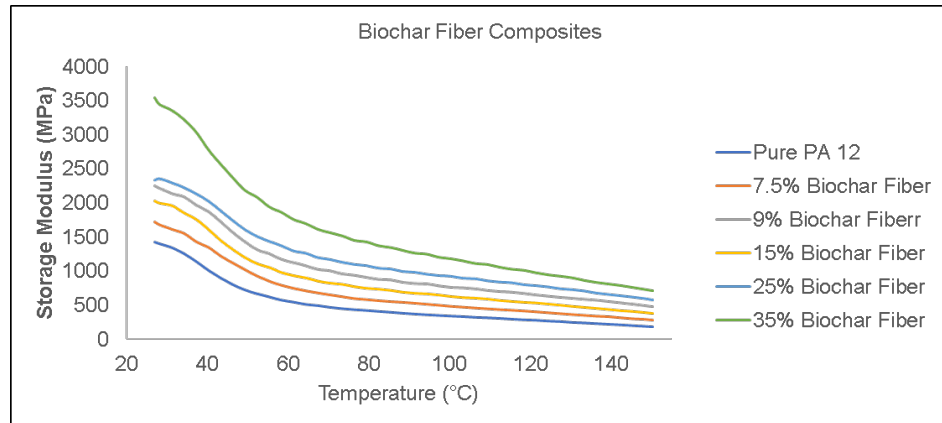
(b) Biocarbon powder

Figure 41. Derivative thermogravimetry (DTG) curves of (a) biocarbon fiber filled PA 12 composites, (b) Biocarbon powder filled PA 12 composites.

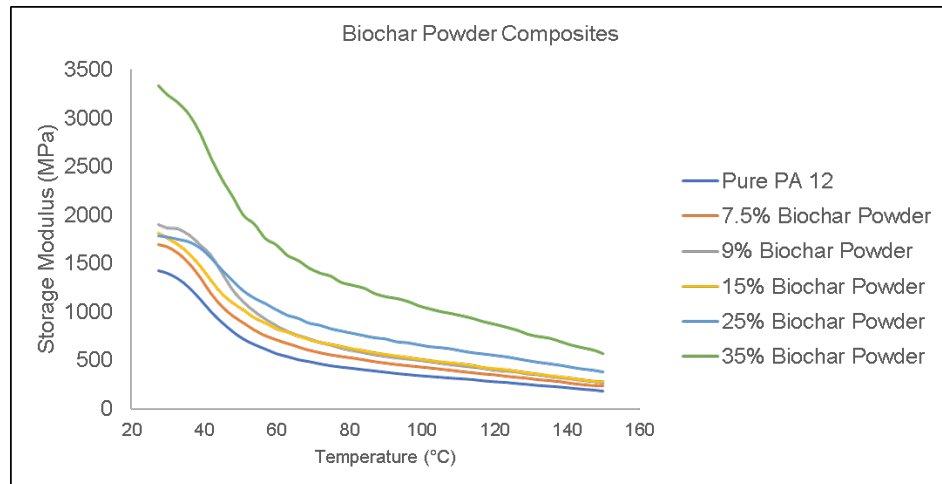
4.4.4. Mechanical Properties

The storage modulus values obtained from DMA show improved mechanical properties for both biocarbon fiber and biocarbon powder filled composite samples. The storage modulus values of the composites filled with 35 wt.% biocarbon filler shows a storage modulus of 3547 MPa for biocarbon fiber filled composites, and 3300 MPa for biocarbon powder filled composites. This improvement is significant as the storage modulus value of pure PA 12 samples is ~ 1500 MPa. The biocarbon fiber filled samples show a steady increase in the storage modulus values with increasing filler concentration as can be seen in Figure 43 (a). The biocarbon powder samples also show an increase in storage modulus with increasing biocarbon content as seen in Figure 43 (b), but the composites filled with 9 wt.%, 15 wt.% and 25 wt.% of biocarbon powder have reported almost similar storage modulus value ~ 1900 MPa. In both cases the storage modulus of 9 wt.% biocarbon is better than 15 wt.% biocarbon concentration. The 9 wt.% biocarbon fiber filled samples reported storage modulus value of ~ 2300 MPa while the storage modulus value was ~ 2000 MPa for 15 wt.% biocarbon fiber samples. Similarly, in biocarbon fiber filled samples the storage modulus for 9 wt.% biocarbon content samples was ~ 1900 MPa while the composites filled with 15 wt.% biocarbon powder recorded storage modulus

values of ~ 1800 MPa. This is consistent in both the composite samples and is quite interesting as the general trend is improved storage modulus with increased filler concentration. The storage modulus values of the composites filled with lower biocarbon concentrations are higher for biocarbon fiber filled composites compared to biocarbon powder filled composites as the storage modulus values are over 2000 MPa for all the biocarbon concentrations. This could be due to the fibrous morphology of the biocarbon fibers providing better reinforcement to the composites compared to biocarbon powder.



(a) Biocarbon Fibers

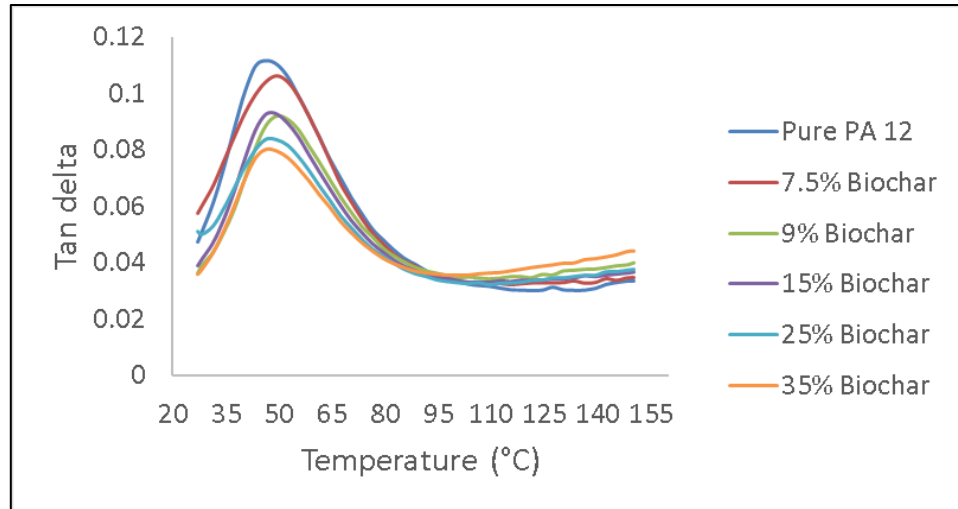


(b) Biocarbon Powder

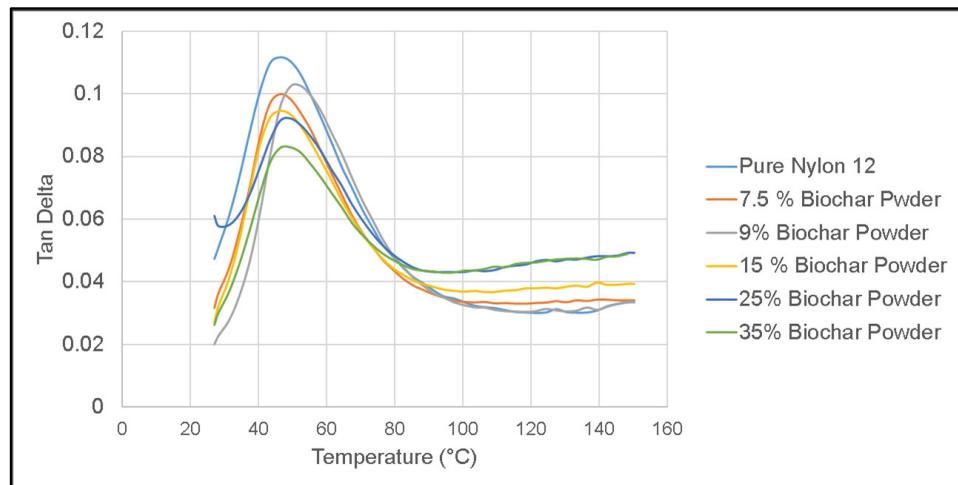
Figure 42. Storage modulus curves of (a) biocarbon fiber filled PA 12 composites, (b) Biocarbon powder filled PA 12 composites.

The tan delta curves for the composites are shown in Figure 44. The biocarbon fiber filled composite and the biocarbon powder filled composites reported glass transition temperature (T_g) values of 47 °C and 48.07 °C respectively, that are not very different from the T_g of

pure polyamide 12 that was determined to be 46.27 °C. In both cases the tan delta values show a decline with increasing filler concentration. The lower tan delta values are a result of reduced energy absorption in the composites compared to pure PA 12 as the elasticity of the polymer reduced with filler incorporation and energy is stored rather than being dissipated (44,175).



(a) Biocarbon Fibers



(b) Biocarbon powder

Figure 43. Tan delta curves of (a) PA 12-biocomposites (b) PA 12-biocomposites with biochar powder filled composites.

4.5. Scaling up of composites

An attempt at scaling up was made by developing composites on a large-scale using melt compounding of the composites followed by composite fabrication using hot compression molding to characterize the composites for electrical properties and injection molding to characterize the mechanical properties of the composites. The biocarbon fiber composites were filled with 15 wt.% biocarbon and the total composite manufacturing was scaled up to 1 kg. Similar approach was taken for producing carbon fiber filled composites as well. The melt compounding of the fillers and the recycled PA 12 was done using twin screw extruder (Barbender Instruments, Inc., New Jersey). The melt compounding was done at 200°C for biocarbon fiber filled composites and 235°C for carbon fiber filled composites at a screw rate of 120 rpm/minute. The composite samples for electrical conductivity characterization the composite discs were made using hot compression molding of the extruded bits. The electrical properties characterization was done using the method described above in the chapter. The samples were characterized for mechanical properties precisely for tensile properties and flexural properties based on ASTM standards D638 and D790 using Instron frame (model 5967, Instron Corporation , USA).The flexural tests were conducted at room temperature and a strain between 1 – 5 % was applied on the samples with 5 % being the maximum strain. The tensile test was done at room temperature at a displacement rate of 5 mm/minute. The samples for mechanical characterization were fabricated using injection molding using

Victory 85 injection molding equipment (Engel Global, USA) at 220°C at 70 rpm screw speed, 5 seconds holding time and 25 second cooling time, five replicated were tested for each sample.

4.5.1. Results

4.5.1.1. Electrical Conductivity

The electrical properties of recycled pure PA 12, biocarbon fiber filled composites and carbon fiber filled composites is presented in table IX. It can be seen that the on incorporation of filler the log electrical conductivity of the composites improve drastically on filler incorporation. The biocarbon electrical conductivity of biocarbon fiber filled composites was -7.544 S/cm that was half of the conductivity value reported for pure polymer that was -14 S/cm. The electrical conductivity value reported for carbon fiber filled composites was -2.684 S/cm that is considerably higher than the electrical conductivity of pure PA 12. The biocarbon composites fabricated using melt compounding for filler dispersion have a relatively lower electrical conductivity value compared to carbon fiber composites fabricated the same way. The electrical conductivity for these composites is also significantly lower compared to biocarbon fiber composites that were dispersed using coffee grinder as seen in the table IX. This could be the result of reduction in aspect ratio of the biocarbon fibers during melt compounding in a twin screw extruder as the process is quite abrasive compared

to dispersion in a coffee grinder. The biocarbon fibers being produced from pulp are significantly more brittle compared to carbon fibers that are produced from polymer hence the melt compounding process is more abrasive for biocarbon composites compared to carbon fiber composites. However, the electrical conductivity values reported for the extruded composites is in the electrostatic dissipative range and can be used for electrostatic dissipative applications. In order to improve the electrical conductivity a less abrasive method like dispersion of filler using a single screw extruder can be done to preserve the aspect ratio of the filler better.

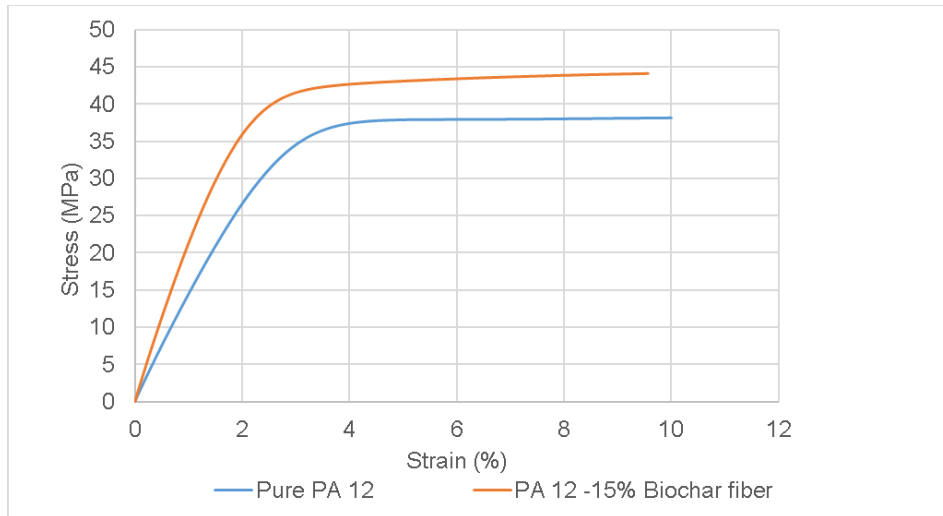
Table IX. Electrical conductivities of pure PA 12, biocarbon fiber filled composites and carbon fiber filled composites.

Filler	Log Electrical Conductivity (S/cm)
Pure PA 12	-14
PA 12 + 15% Biocarbon fibers (extruded)	-7.544
PA 12 + 15% Biocarbon fibers	-2.32
PA 12 + 15% Carbon fibers	-2.684

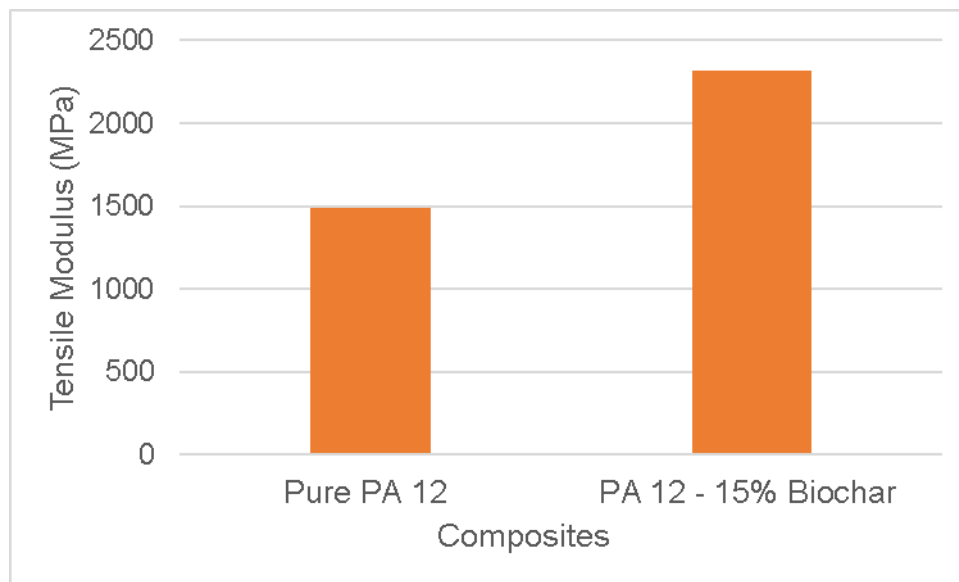
4.5.1.2. Mechanical properties

Tensile test

The tensile test results were reported as average of five samples, for the pure PA 12 and the composites show that the tensile strength of the composites filled with 15 wt.% biocarbon have improved on incorporation of filler compared to pure PA 12 as seen in Figure 45 (a). The average maximum tensile stress reported for pure PA 12 was 38.1 ± 0.29 MPa while for the biocarbon filled composites the maximum tensile stress reported was 44 ± 0.31 MPa that is significantly higher. The modulus values of pure PA 12 and biocarbon fiber filled composites are shown in Figure 45 (b). It can be seen that on incorporation of biocarbon the modulus values of the composites increased significantly compared to pure PA 12. The modulus value reported for pure PA 12 was 1460 ± 25.9 MPa while for the composites the modulus value was 2280 ± 75.2 MPa showing the drastic improvement on incorporation of filler. These properties are in agreement with previous studies(5,37). It can be seen that for both PA 12 and the composites the curve becomes steady at maximum strain and does not break at maximum strain.



(a) Tensile Strength



(b) Tensile Modulus

Figure 44. Tensile properties of pure PA 12 and 15 wt.% biocarbon fiber filled composites.

Flexural Test

The flexural curves for pure PA 12, and biocarbon fiber filled composites are presented in Figure 46. It can be seen that biocarbon fiber filled composites have better flexural properties compared to pure PA 12. The maximum flexural stress for biocarbon fiber filled composites was 66.2 ± 0.73 MPa, and for pure PA 12 it was reported to be 50.71 ± 1.06 MPa. The flexural modulus for biocarbon fiber filled composites was 2071.12 ± 36.1 MPa while pure PA 12 the modulus values were 1309.51 ± 47.32 MPa. The modulus value shows that the flexural properties improved on addition of fillers compared to pure PA 12. This improvement can be attributed to the enhanced stress transfer from the matrix to the filler enhancing the mechanical properties of the composites (5).

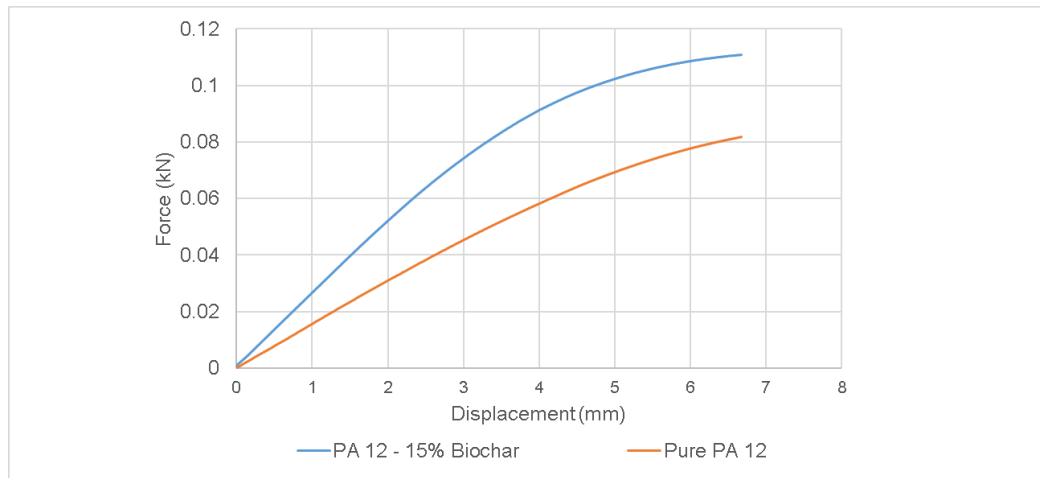


Figure 45. Flexural properties of pure PA 12 and 15 wt.% biocarbon fiber filled PA 12 composites.

4.5. Conclusion

Addition of biocarbon in polyamide 12 matrix definitely led to an improvement in the electrical and thermal properties of the composites. The difference in the electrical properties of the two different sets of composites indicate the importance of morphology of filler. It validates the fact that a higher filler aspect ratio or longer filler morphology is beneficial in obtaining better electrical properties compared to short or more globular shaped fillers. This could be due to a better network formation of filler leading to better electron transport through the otherwise non-conductive matrix. Incorporation of biocarbon in the filler also improves the thermal property of the composites which increases the applicability of the resultant composites. Biocarbon powder showed a better performance in improving thermal properties of the composites; however, better electrical conductivity of biocarbon fiber fillers gives it an upper hand making it the choicer filler. Nevertheless, the ability of biocarbon in making thermally stable electrically conductive composites makes it a lucrative alternative to currently used synthetic carbon-based fillers that are highly energy intensive and not very cost effective unlike biocarbon, that is sustainable and much more economical. The electrical properties of the scaled-up composites were in the electrostatic dissipative range, this could have been due to the reduced aspect ratio of the biocarbon fibers as the composite material was processed in a twin screw extruder. An improvement in the tensile and flexural properties was seen

on incorporation of 15 wt.% biocarbon fibers to recycled PA 12 matrix as the filler reinforces the matrix enhancing its stress bearing capacity.

5. Chapter 5 - Cradle to grave life cycle analysis of biocarbon fiber filled composites used to manufacture an automotive component

5.1. Abstract

A cradle to grave life cycle analysis was conducted on biocarbon fiber filled composites. Recycled polyamide 12 waste recovered from selective laser sintering method was filled with softwood biocarbon fibers and the functional unit of the study was amount of conductive filled required to make an electrically conductive composite for fuel filter housing for pickup trucks. The global warming potential in units of kg CO₂ equivalent, the cumulative energy demand (CED) and impact of composites on several categories like eutrophication, ozone depletion, ecotoxicity, carcinogenic, acidification etc., were modeled using SimaPro. The emissions produced by the biocarbon filled composites were estimated to be 124 kg CO₂ equivalent. The highest emissions were recorded for the use phase of the composite and the lowest emissions were estimated for the biocarbon manufacturing phase and the end-of-life phase of the composites. The environmental impact analysis also showed the highest impact potential for the use phase of the composites.

5.2. Introduction

Automobile emissions have been major contributors to introducing greenhouse gasses into the environment. The automobile design specifically weight and horse power contribute largely to the emissions produced by them (176). A typical passenger vehicle produces emissions of about 4.6 metric tons annually, calculated based on the CO₂ emitted on burning one gallon of gasoline which is equivalent to 8, 887 grams (17). However, EPA reported a reduction of 28% in emissions and a 30% increase in fuel economy since 2004 till 2018 (176) and the suggested further improvements in this trend in the upcoming years. This improvement is possible due to the sustainable approaches taken up by automotive industry to cut down emissions and improve fuel efficiency. Approaches like light weighting of vehicles has been taken up by most of the automotive manufacturers to improve the carbon footprint of producers and consumers alike. Substitution of traditional metal automotive components with light weight plastic composite-based components is the approach taken up for light weighting. However, plastics being bad conductors of electricity tend to accumulate electrostatic charge and can lead to problems that requires the development of electrically conductive polymer composites. Studies have reported the use of carbon-based fillers like carbon nanotubes, carbon fibers etc., in development of electrically conductive composites (125,135,136,146). However, the manufacturing process of these fillers is highly energy and cost intensive (177)(178). Biocarbon is a sustainable biomass derived carbon filler

that has been incorporated as reinforcement of polymer composites. Biocarbon is showing great promise as an electrically conductive filler (134). Biocarbon itself is very sustainable given its carbon negative nature due to its carbon sequestration ability (179). However, the environmental effect of development of composites and also the impacts of the use of the composites also needs to be determined.

Life Cycle Analysis/Assessment (LCA) is a powerful tool that can be used to determine the environmental effects of a product or a study. LCA is an assessment tool that can be used to determine the impact a product or a process has on the environment throughout its life cycle that is from cradle to grave (180). It evaluated the environmental impact of a process or a unit by consolidating the environmental impacts starting from procurement of raw material, manufacturing and distribution, use and then end of life by disposal or recycling (181). The cradle to grave approach is the most commonly known, however there are several approaches like cradle to gate, cradle to cradle that is determined based on the phases involved in the life cycle of a product or a process. Figure 49 shows the different phases involved in the life cycle analysis framework, modified from (182).

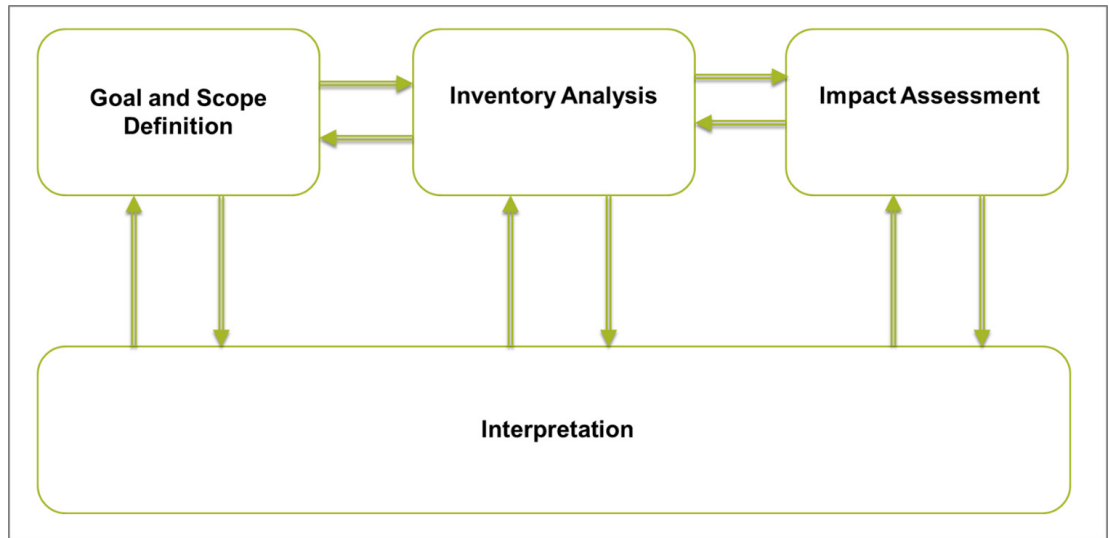


Figure 46. Life Cycle Analysis Framework (based on ISO 14040, 1997) modified from Rebitzer et al. 2004 (182).

5.3. Goal and Scope

A fuel filter housing is a three part component that has a fuel filter head, a water in fuel sensor and a fuel filter, they are traditionally made from metal but with sustainability as priority they are available made from polymer based composites (183). The fuel if filtered through this assembly while refueling of the vehicle, electrostatic accumulation around this component can lead to problems like charging, burn injuries etc., Hence it is important to have electrically conductive fuel filter housing assembly to prevent any issues like charging, burn accidents, electric shock etc., This study is designed to model the environmental impact of biocarbon filled electrically conductive composites. This study takes up the

cradle to grave approach in modelling the life cycle analysis and impact analysis of the composite used as raw material to manufacture a fuel filter housing.

5.4. Objectives

1. To determine the environmental impact of biocarbon filled nylon composites by modelling a cradle to grave life cycle assessment model using a standardized format like ISO 14044 (2006) for the amount of filler required to have an electrically conductive composite material to model an automobile component.
2. To determine the global warming potential GWP of biocarbon-nylon composite as per IPCC GWP 100a guidelines.
3. Determine the cumulative energy demand (CED) in the entire lifecycle of the composites.
4. Determination of the impact of the composites on the several impacts included in TRACI applicable to North America for impact assessment (184,185).

5.5. Functional Unit

The functional unit for life cycle analysis is the quantified unit that is used as a basis to estimate all the impacts (186). A functional unit also helps in developing

a common ground on which the entire analysis is built irrespective of the differences in the kinds of materials or processes compared to each other. The functional unit for this study is set as the amount of conductive filler required to fabricate a composite with log electrical conductivity value of - 2 S/cm. The composite would serve as raw material for manufacture of the fuel filter housing. The electrical conductivity value was decided based on lab studies done here at Michigan Technological University. In the study biocarbon fiber filled composite discs were compared to carbon fiber filled composites. According to the results of this study the required electrical conductivity can be achieved by incorporating 15 wt.% of biocarbon fiber. The weight of the fuel filter housing was determined to be 2.26 kg (5 pounds) (187). The amount of recycled polyamide (PA) 12 and fillers was calculated based on the required filler level to achieve the expected electrical conductivity.

5.6. Lifecycle System Boundaries

The life cycle boundary also known as the life cycle inventory of a system includes all the processes and operations along with the input and output flows from and to nature (188,189) . The system boundaries of all the processes involved in the production of PA 12 – biocarbon composite is presented in Figure 50.

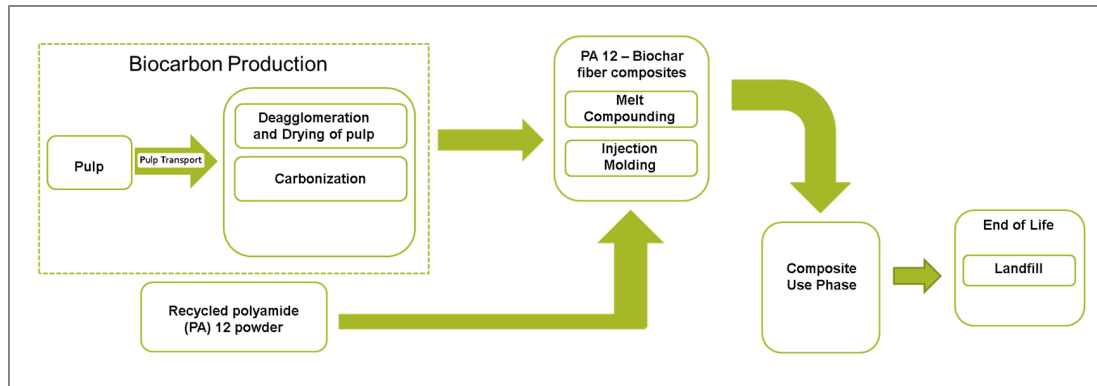


Figure 47. The system boundaries of PA 12-biocomposite fiber composites.

5.6.1. Manufacturing biocomposite filler

In our study biocomposite fibers were produced from Douglas fir, that is a softwood species and the pulp produced from it has superior aspect ratio and length (190). The pulp used in the study was produced through Kraft pulping process. In this process the wood is subjected to pulping in a highly alkaline solution, using sodium hydroxide (NaOH) and sodium sulfide (Na₂S). The pulp raw material for biocomposite production process in the LCA assessment was taken from Ecoinvent 3 database. The pulp received from the supplier was in the form of sheets that needed to be deagglomerated prior to carbonization. The deagglomeration was done in water using a mechanical mixer. In lab it was done in a 2-gallon bucket where 250 grams of pulp was deagglomerated in 1 hour. The scaling up of the process was done by assuming the deagglomeration to be done in a 55-gallon drum that could hold about 200 kgs of pulp in water and then deagglomerated using a 1.12 KW industrial scale mechanical mixer (191). The time taken to deagglomerate 2 kg of pulp was assumed to be 1 hour given the scale and

equipment efficiency. In the lab scale production of biocarbon, the deagglomerated pulp was dried a hot air oven at 90°C overnight (~10 hours). The scaling up was done using a 85-liter, 115 W industrial scale hot air oven (192). The energy was calculated in megajoules (MJ) by using the total time taken that is 10 hours and equipment power. Prior to carbonization, the dried pulp was fluffed to separate the fibers, in the lab it was being done using a 12-gallon shop vac, that took about 1 hour to fluff 250 grams of pulp. To produce the require amount of biocarbon that is 0.33 kg, 2 kilograms of pulp was needed based on 16 wt.% biocarbon retention. Hence the process was scaled up to a 16 gallon, 6.5 HP shop vac (193). Assuming that a 16-gallon shop vac could process 500 grams of pulp each time, the total time taken to full 2 kilograms of pulp was estimated to be 4 hours in total. The energy was calculated in megajoules (MJ) using the time taken and energy of the shop vac.

In the lab here at Michigan Technological University, the carbonization of pulp was done at 1000°C in a nitrogen environment, using a laboratory scale tube furnace. The biocarbon production for the electrically conductive composites was produced using a larger industrial scale furnace. A 202-liter capacity chamber furnace with maximum temperature range of 1200°C and maximum power of 24kW was assumed to be used (194). As the biocarbon yield of pulp was determined to be 16%, the time taken to produce the required amount of biocarbon (337 g) was assumed to be 2 hours based upon the lab scale data that takes 2.5 hours for a complete a carbonization run, as the capacity and power of the equipment is higher the time taken was assumed to be 2 hours for

the scaled-up process. The total energy expenditure was calculated based on the power of the furnace and the total time taken to produce the required amount of biocarbon.

5.6.2. Transport

It is assumed that the biocarbon fibers were produced from pulp in the facility where the composites were being manufactured. Hence the pulp was transported from the pulp and paper mill. Similarly, the carbon fibers were procured from certain supplier. In certain cases transportation can have a large impact on the greenhouse emissions and environmental impacts of the finished product (184). In order to normalize the impact of transport it was assumed that the pulp was obtained from suppliers located in 1000 km radius from the composite manufacturing facility. The transportation-based emissions were calculated to transport 2 kilograms of pulp from production facility.

5.6.3. Recycled polyamide (PA) 12

The recycled polyamide (PA) 12 used in this study was retrieved from selective laser sintering (SLS) process. The polyamide (PA) 12 powder was recovered as waste and recycled as a polymer matrix in our process. As there is no data available for PA 12 in the Ecoinvent 3 database, the data was created in the data base using existing polyamide 6,6 data and by creating altering the emission

data associated with it to match up to polyamide 12 to incorporate the environmental burdens associated with polyamide 12 in this study. The emissions value was adjusted to 15.39 kg CO₂ equivalent by retrieving the data from previous studies (195,196). In this study the environmental burdens associated with SLS of PA 12 are excluded as the PA 12 used as matrix material in this study was recovered as waste hence it carries no environmental burdens of the previous process (195). In the future if the demand for recycled PA 12 increases adding to its value, the associated environmental burdens can be taken into consideration while using it as a raw material (195).

5.6.4. Electrically conductive composite manufacturing

The composite manufacturing was done using two steps, the first step was melted compounding of filler and polymer to disperse the filler in the matrix followed by injection molding of the compounded material into fuel filter housing component. The concentration of biocarbon filler in the composites was 15 wt.% (0.33 kg). The process parameters for both melt compounding and injection molding were taken from the Ecoinvent database in SimaPro by selecting appropriate processing methods (197). The lifecycle inventory data for production of both biocarbon fiber filled composites is compiled in table XIV.

Table X. Lifecycle inventory data for manufacturing recycled PA 12-biocarbon fiber composites. (*energy consumption is calculated based on power consumption and time taken to complete the process)

Bn

Process/Operations	Data	Source
Pulp	2 kg	LCA assembly
Recycled PA 12	1.921 kg	Author defined
Transport	2 tkm	
Deagglomeration (energy)	4.032 MJ	Estimated*
Drying (energy)	4.14 MJ	Estimated*
Pulp fluffing (energy)	69.7 MJ	Estimated*
Carbonization (energy)	172.8 MJ	Estimated*
Melt Compounding	Data from SimaPro	Ecoinvent
Injection Molding	Data from Simapro	Ecoinvent

5.6.5. Use phase

The fuel consumption for the distance travelled in the lifetime of the vehicle was calculated using equation (2) (184,195,198,199).

$$FC = MIF \times m \times d \quad (2)$$

Here FC is the fuel consumption in liters, MIF is the mass induced fuel consumption in liters (L), m is the mass of the composite and d is the total distance traveled in the lifetime of the vehicle. The value for MIF was taken from literature to be 0.285 L/ 100kg×100km, that was estimated for Ford F-150 trucks (195). The total distance travelled by the vehicle in its lifetime was also taken from literature to be 285,000 kms (195,200). Based on the calculations the mass-based fuel consumption for the composites was determined to be 18.35L. The greenhouse gas emissions and the environmental impacts for the use phase of the composites were determined based on this calculated fuel consumption value.

5.6.6. End of life scenario of the composites

The most common methods of plastic waste disposal in USA are landfill and incineration (201). As most of the waste is landfilled in USA, it was assumed that at the end of the life phase the composites were shredded and then landfilled (195,202). The landfilling was done based on United States landfilling methods, the landfilling of PA 12 that comprises 85 wt.% of the composite was assumed to be equivalent to landfilling of mixed plastics and for biocarbon fibers that comprises 15 wt.% of the composite, it was assumed to be equivalent to landfilling of wood products.

5.6.7. Life cycle analysis and impact assessment

The impact assessment was modelled using SimaPro software (177,184,203). The impact assessment for potential contribution of the biocarbon fiber filled composites to global warming potential, ozone layer depletion, eutrophication, acidification, smog, respiratory diseases and carcinogenic was estimated using TRACI (US 2008) assessment method. The cumulative greenhouse gas emission expressed as kg CO₂ equivalent was estimated using the IPCC GWP 100 assessment method. The cumulative energy demand of the processes was calculated using the cumulative energy demand (CED) assessment method.

5.7. Results

5.7.1. Greenhouse gas emissions and cumulative energy demand

The greenhouse gas emissions associated with recycled PA 12-biocarbon fiber composites was 124 kg of CO₂ equivalent for the entire life cycle of the composite. The emissions associated to each phase is presented in table XI. It can be seen that the highest emissions are produced in the use phase. These emissions are associated to the fuel use used in the entire lifecycle of the vehicle. This is followed by the composite manufacturing, in this phase the emissions generated are associated to the recycled PA 12 and the composite manufacturing processes extrusion and injection molding. The biocarbon

manufacturing phase has emissions allocated to the pulp raw material, emissions generated in transportation of pulp and emissions associated with preparing and carbonization of pulp. The least emissions are associated to the end-of-life phase. Among the three stages biocarbon manufacturing phase has the lowest emissions indicating that the process is sustainable. The relatively high emissions in the use phase can be controlled by mindful automotive usage and use of alternative fuel like biobased fuels.

Table XI. Emissions produced in the different phases in the lifecycle of biocarbon filled recycled PA 12 composites.

Life cycle stage	Emissions (kg CO ₂ equivalent)
Biocarbon manufacturing	13.2
Biocarbon-recycled PA 12 composite manufacturing	31.9
Composite use phase	73.8
Composite end of life phase	2.68

The cumulative energy demands (CED) of biocarbon fiber filled composites in the different life cycle stages namely biocarbon manufacturing, composite manufacturing and the use phase of the composite is shown in Figure 48. It can be seen in the figure that non-renewable fossil fuel demand is the highest in the use phase as the vehicle runs on fossil fuel, the composite manufacturing phase

has the highest nuclear energy demand. The three different renewable sources have a high demand in the biocarbon manufacturing phase. The cumulative energy demand of the entire life cycle of the composites including the end-of-life phase is presented in Figure 49. It can be seen that the energy demand for the end-of-life phase of the composites is negligible compared to the manufacturing and use phase. This is in correspondence with the emissions associated to each life cycle stage.

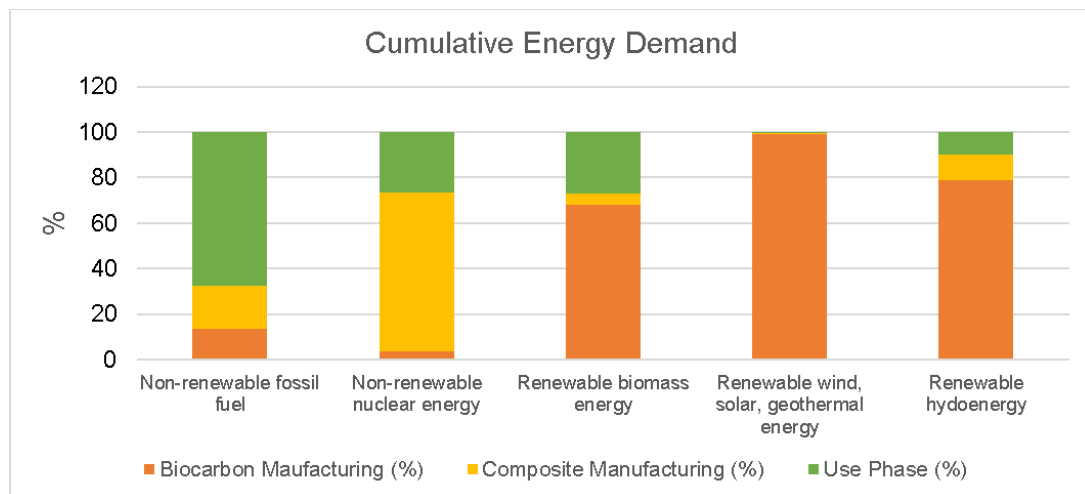


Figure 48. Cumulative energy demand for recycled PA 12-biocarbon manufacturing and use phase.

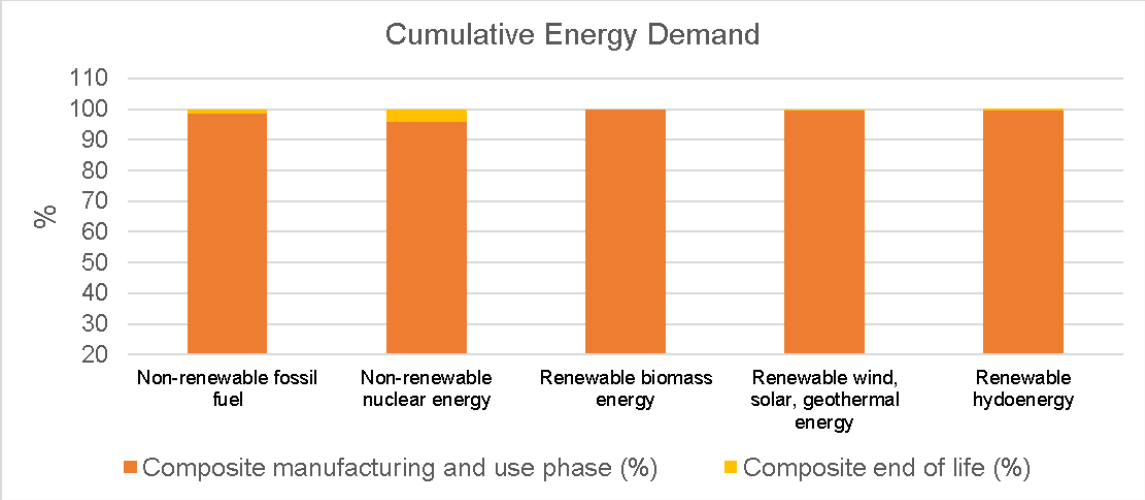


Figure 49. Cumulative energy demand for recycled PA 12-biocarbon composites lifecycle .

5.7.2. Impact Assessment

The impact potential of biocarbon filled PA 12 composites for their complete lifecycle is shown in Figure 50. It can be seen that the end-of-life phase of the composites has negligible contribution to the overall impact of the composites. Most of the impact is from the manufacturing and use phase. A detailed breakdown of the environmental impacts of the manufacturing and use phase is discussed further in this section.

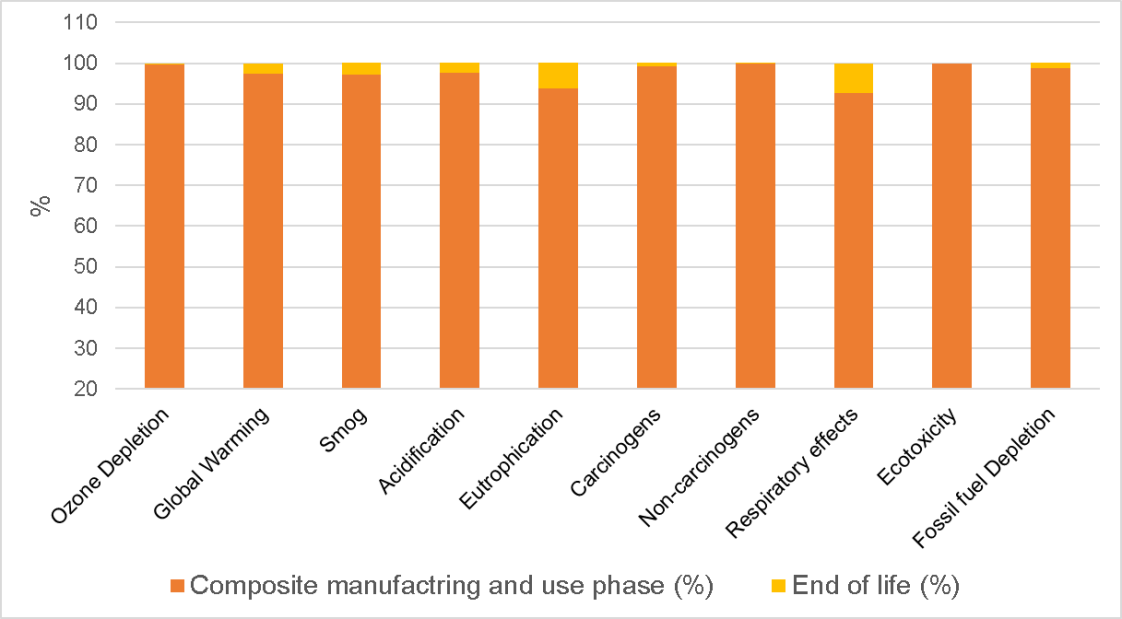


Figure 50. Environmental impact assessment of recycled PA 12-biocarbon composites (manufacturing and use phase)

The impact assessment of biocarbon fiber filled composites manufacturing and use phase can be seen in Figure 51. It can be seen from the figure that the highest environmental impact potential is for the use phase. This can be allocated to the fuel used in the life cycle of the automobile. In case of eutrophication potential, it can be seen that all the three phases have almost equal contribution. Ecotoxicity potential is the highest for biocarbon production phase and can be allocated to pulp production. In pulp production a lot of waste water is generated that is usually released into water bodies and can lead to aquatic toxicity (204,205) as reflected in the environmental impacts. The non-

carcinogens potential is also high for biocarbon manufacturing and the major contributor to this is the electricity used in carbonization. The environmental impacts of composite manufacturing phase are quite similar in most of the impact categories.

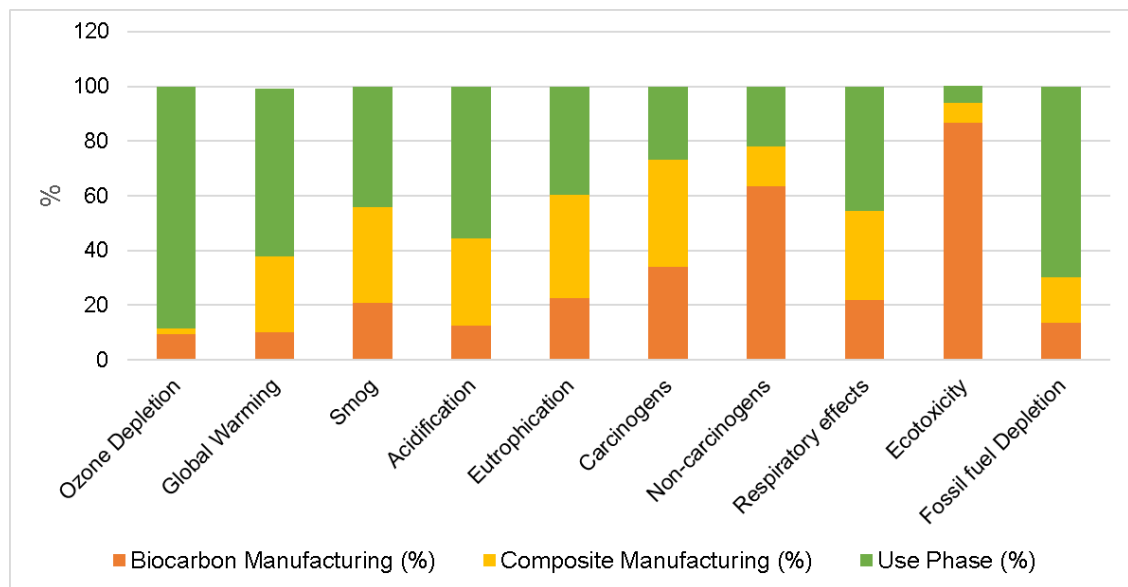


Figure 51. Comparative impact assessment of PA 12-carbon fiber filled composite production and PA 12-biocarbon composite production including end of life scenario.

5.8. Conclusion

The life cycle analysis of recycled PA 12-biocarbon composites was carried out in this study. The total emissions produced in the lifecycle of the composites was estimated to be 124 kg CO₂ equivalent. It was seen that the highest emissions were associated to the use phase of the composite, that can be allocated to the fuel consumption by the automobile in its entire lifecycle. The same is also reflected in the environmental impacts, as the highest contribution potential in most categories was for the use phase of the composites. The biocarbon manufacturing phase had the relatively lower emissions compared to composite manufacturing and use phase of the composites. This shows the biocarbon production is a sustainable process and can improve the overall sustainability of the composites. The pulping process has a high ecotoxicity potential, but treatment of wastewater and other water management practices can help reduce the environmental impact. Overall biocarbon filled composites can be used as an alternative to traditionally used electrically conductive composites. In the future a comparative study between the conventionally used electrically conductive composites and biocarbon filled composites can be done to compare the environmental impacts and determine the more sustainable alternative.

List of References

1. IBI IBI. Standardized Product Definition and Product Testing Guidelines for Biochar That Is Used in Soil. Int Biochar Initiat [Internet]. 2015;(November):23. Available from: http://www.biochar-international.org/sites/default/files/Guidelines_for_Biochar_That_Is_Used_in_Soil_Final.pdf
2. Das O, Sarmah AK, Zujovic Z, Bhattacharyya D. Characterisation of waste derived biochar added biocomposites: Chemical and thermal modifications. Sci Total Environ [Internet]. 2016;550:133–42. Available from: <http://dx.doi.org/10.1016/j.scitotenv.2016.01.062>
3. Elnour AY, Alghyamah AA, Shaikh HM, Poulouse AM, Al-Zahrani SM, Anis A, et al. Effect of pyrolysis temperature on biochar microstructural evolution, physicochemical characteristics, and its influence on biochar/polypropylene composites. Appl Sci. 2019;9(6):7–9.
4. Behazin E, Rodriguez-Urbe A, Misra M, Mohanty AK. Long-term performance of β -nucleated toughened polypropylene-biocarbon composites. Compos Part A Appl Sci Manuf [Internet]. 2018;105:274–80. Available from: <https://doi.org/10.1016/j.compositesa.2017.11.014>
5. Das O, Bhattacharyya D, Hui D, Lau K-T. Mechanical and flammability characterisations of biochar/polypropylene biocomposites. Compos Part B Eng [Internet]. 2016 Dec;106:120–8. Available from: <http://dx.doi.org/10.1016/j.compositesb.2016.09.020>
6. Poulouse AM, Elnour AY, Anis A, Shaikh H, Al-Zahrani SM, George J, et al. Date palm biochar-polymer composites: An investigation of electrical, mechanical, thermal and rheological characteristics. Sci Total Environ [Internet]. 2018;619–620:311–8. Available from: <https://doi.org/10.1016/j.scitotenv.2017.11.076>
7. Zhang H, Yao W, Qian S, Sheng K. Fabrication and reinforcement of ternary composites based on polypropylene matrix with bamboo particle/ultrafine bamboo-char. Polym Compos. 2018;39(12):4364–71.
8. Sundarakannan R, Arumugaprabu V, Manikandan V, Vigneshwaran S. Mechanical property analysis of biochar derived from cashew nut shell waste reinforced polymer matrix. Mater Res Express. 2019;6(12).
9. National V. Concept and Practice of the Circular Economy Concept and Practice of the Circular Economy . Athanasios Valavanidis. 2018;(July).
10. Zhang S, Yao W, Zhang H, Sheng K. Polypropylene biocomposites

reinforced with bamboo particles and ultrafine bamboo-char: The effect of blending ratio. *Polym Compos.* 2018;39:E640–6.

11. Bartoli M, Nasir MA, Jagdale P, Passaglia E, Spiniello R, Rosso C, et al. Influence of pyrolytic thermal history on olive pruning biochar and related epoxy composites mechanical properties. *J Compos Mater.* 2020;54(14):1863–73.
12. Idrees M, Jeelani S, Rangari V. Three-Dimensional-Printed Sustainable Biochar-Recycled PET Composites. *ACS Sustain Chem Eng.* 2018;6(11):13940–8.
13. Pudelko A, Postawa P, Stachowiak T, Malińska K, Drózd D. Waste derived biochar as an alternative filler in biocomposites - Mechanical, thermal and morphological properties of biochar added biocomposites. *J Clean Prod.* 2021;278.
14. Das O, Sarmah AK, Bhattacharyya D. Biocomposites from waste derived biochars: Mechanical, thermal, chemical, and morphological properties. *Waste Manag* [Internet]. 2016;49:560–70. Available from: <http://dx.doi.org/10.1016/j.wasman.2015.12.007>
15. Schmidt H-P. 55 Uses of Biochar. *Ithaca J.* 2012;25(1/2012):13–25.
16. Chawla KK. *Composite Materials* [Internet]. *Composite Materials: Science and Engineering*, Third Edition. New York, NY: Springer New York; 2012. Available from: <http://link.springer.com/10.1007/978-0-387-74365-3>
17. US EPA. Greenhouse Gas Emissions from a Typical Passenger Vehicle (EPA-420-F-18-008, April 2018). 2018;(September 2011):1–5. Available from: <https://nepis.epa.gov/Exe/ZyPDF.cgi?Dockkey=P100U8YT.pdf>
18. EPA. The 2020 EPA Automotive Trends Report: Greenhouse Gas Emissions, Fuel Economy, and Technology since 1975 (EPA-420-R-21-003, January 2021). 2021;(January). Available from: www.epa.gov/enforcement/daimler-
19. Kelly JC, Sullivan JL, Burnham A, Elgowainy A. Impacts of Vehicle Weight Reduction via Material Substitution on Life-Cycle Greenhouse Gas Emissions. *Environ Sci Technol.* 2015;49(20):12535–42.
20. Haraguchi K. Biocomposites. In: *Encyclopedia of Polymeric Nanomaterials.* 2014.
21. John MJ, Thomas S. Biofibres and biocomposites. *Carbohydr Polym.* 2008;71(3):343–64.

22. Faruk O, Bledzki AK, Fink HP, Sain M. Biocomposites reinforced with natural fibers: 2000-2010. Vol. 37, Progress in Polymer Science. 2012.
23. Marsh H, Rodríguez-Reinoso F. Activated Carbon (Origins). Act Carbon. 2006;(1997):13–86.
24. Xie X, Goodell B, Qian Y, Peterson M, Jellison J. Significance of the heating rate on the physical properties of carbonized maple wood. Holzforschung [Internet]. 2008 Sep 1;62(5):591–6. Available from: <https://www.degruyter.com/document/doi/10.1515/HF.2008.090/html>
25. Nan N. Development of polyvinyl alcohol/wood-derived carbon thin films : Influence of processing parameters on mechanical , thermal , and electrical properties. Retrieved from West Virginia Univ Libr data. 2016;
26. Ikram S, Das O, Bhattacharyya D. A parametric study of mechanical and flammability properties of biochar reinforced polypropylene composites. Compos Part A Appl Sci Manuf [Internet]. 2016;91:177–88. Available from: <http://dx.doi.org/10.1016/j.compositesa.2016.10.010>
27. Wijitkosum S, Jiwonok P. Elemental composition of biochar obtained from agricultural waste for soil amendment and carbon sequestration. Appl Sci. 2019;9(19).
28. Schaul JS. Polymer processing. Chem Eng News. 1985;63(37):2.
29. Vankayala RR, Lai WJP, Cheng KC, Hwang KC. Enhanced electrical conductivity of nylon 6 composite using polyaniline-coated multi-walled carbon nanotubes as additives. Polymer (Guildf) [Internet]. 2011;52(15):3337–43. Available from: <http://dx.doi.org/10.1016/j.polymer.2011.05.007>
30. Khan A, Savi P, Quaranta S, Rovere M, Giorcelli M, Tagliaferro A, et al. Low-cost carbon fillers to improve mechanical properties and conductivity of epoxy composites. Polymers (Basel). 2017;9(12).
31. Nan N, DeVallance DB, Xie X, Wang J. The effect of bio-carbon addition on the electrical, mechanical, and thermal properties of polyvinyl alcohol/biochar composites. J Compos Mater. 2016;50(9):1161–8.
32. Giorcelli M, Bartoli M. Development of coffee biochar filler for the production of electrical conductive reinforced plastic. Polymers (Basel). 2019;11(12):1–17.
33. Chung CI. Introduction. In: Extrusion of Polymers [Internet]. München: Carl Hanser Verlag GmbH & Co. KG; 2019. p. 1–15. Available from: <https://www.hanser-elibrary.com/doi/10.3139/9781569907382.001>

34. Das R, Pattanayak AJ, Swain SK. Polymer nanocomposites for sensor devices [Internet]. *Polymer-based Nanocomposites for Energy and Environmental Applications: A volume in Woodhead Publishing Series in Composites Science and Engineering*. Elsevier Ltd.; 2018. 206–216 p. Available from: <http://dx.doi.org/10.1016/B978-0-08-102262-7.00007-6>
35. Li S, Li X, Chen C, Wang H, Deng Q, Gong M, et al. Development of electrically conductive nano bamboo charcoal/ultra-high molecular weight polyethylene composites with a segregated network. *Compos Sci Technol* [Internet]. 2016;132:31–7. Available from: <http://dx.doi.org/10.1016/j.compscitech.2016.06.010>
36. Behazin E, Misra M, Mohanty AK. Compatibilization of toughened polypropylene/biocarbon biocomposites: A full factorial design optimization of mechanical properties. *Polym Test* [Internet]. 2017;61:364–72. Available from: <http://dx.doi.org/10.1016/j.polymertesting.2017.05.031>
37. Behazin E, Misra M, Mohanty AK. Sustainable biocarbon from pyrolyzed perennial grasses and their effects on impact modified polypropylene biocomposites. *Compos Part B Eng* [Internet]. 2017;118:116–24. Available from: <http://dx.doi.org/10.1016/j.compositesb.2017.03.003>
38. Ogunsona EO, Misra M, Mohanty AK. Sustainable biocomposites from biobased polyamide 6,10 and biocarbon from pyrolyzed miscanthus fibers. *J Appl Polym Sci*. 2017;134(4):1–11.
39. Ferreira GF, Pierozzi M, Fingolo AC, da Silva WP, Strauss M. Tuning Sugarcane Bagasse Biochar into a Potential Carbon Black Substitute for Polyethylene Composites. *J Polym Environ* [Internet]. 2019;27(8):1735–45. Available from: <https://doi.org/10.1007/s10924-019-01468-1>
40. Das O, Bhattacharyya D, Sarmah AK. Sustainable eco-composites obtained from waste derived biochar: a consideration in performance properties, production costs, and environmental impact. *J Clean Prod* [Internet]. 2016 Aug;129:159–68. Available from: <http://dx.doi.org/10.1016/j.jclepro.2016.04.088>
41. Das O, Sarmah AK, Bhattacharyya D. A novel approach in organic waste utilization through biochar addition in wood/polypropylene composites. *Waste Manag* [Internet]. 2015;38(1):132–40. Available from: <http://dx.doi.org/10.1016/j.wasman.2015.01.015>
42. Li S, Huang A, Chen YJ, Li D, Turng LS. Highly filled biochar/ultra-high molecular weight polyethylene/linear low density polyethylene composites for high-performance electromagnetic interference shielding. *Compos Part B Eng* [Internet]. 2018;153(April):277–84. Available from:

<https://doi.org/10.1016/j.compositesb.2018.07.049>

43. Arrigo R, Bartoli M and, Malucelli G. polymers Poly (lactic Acid)– Biochar Biocomposites : E f f ect of Processing and Filler Content on Rheological ,. 2020;1–13.
44. Zhang Q, Cai H, Ren X, Kong L, Liu J, Jiang X. The dynamic mechanical analysis of highly filled rice husk biochar/High-density polyethylene composites. *Polymers (Basel)*. 2017;9(11).
45. Wang B, Li H, Li L, Chen P, Wang Z, Gu Q. Electrostatic adsorption method for preparing electrically conducting ultrahigh molecular weight polyethylene/graphene nanosheets composites with a segregated network. *Compos Sci Technol [Internet]*. 2013;89(2):180–5. Available from: <http://dx.doi.org/10.1016/j.compscitech.2013.10.002>
46. Liang JZ, Li RKY, Tjong SC. Morphology and Tensile Properties of Glass Bead Filled Low Density Polyethylene Composites. *Polym Test*. 1998;
47. Bai JB, Allaoui A. Effect of the length and the aggregate size of MWNTs on the improvement efficiency of the mechanical and electrical properties of nanocomposites - Experimental investigation. *Compos Part A Appl Sci Manuf*. 2003;34(8):689–94.
48. Allaoui A, Bai S, Cheng HM, Bai JB. Mechanical and electrical properties of a MWNT/epoxy composite. *Compos Sci Technol*. 2002;62(15):1993–8.
49. Ciecierska E, Boczkowska A, Kurzydowski KJ, Rosca ID, Van Hoa S. The effect of carbon nanotubes on epoxy matrix nanocomposites. *J Therm Anal Calorim*. 2013;111(2):1019–24.
50. Gonçalves JAV, Campos DAT, Oliveira GDJ, Da Silva Rosa MDL, Macêdo MA. Mechanical properties of epoxy resin based on granite stone powder from the sergipe fold-and-thrust belt composites. *Mater Res*. 2014;17(4):878–87.
51. Taib MNAM, Julkapli NM. Dimensional stability of natural fiber-based and hybrid composites [Internet]. *Mechanical and Physical Testing of Biocomposites, Fibre-Reinforced Composites and Hybrid Composites*. Elsevier Ltd; 2018. 61–79 p. Available from: <http://dx.doi.org/10.1016/B978-0-08-102292-4.00004-7>
52. Hornsby PR., Hinrichsen E., Tarverdi K. Preparation and properties of polypropylene composites reinforced with wheat and flax straw fibres Part II Analysis of composite microstructure and mechanical properties JMS60060 JMS60060. *J Mater Sci*. 1997;32:1009–15.

53. Sohi SP, Krull E, Lopez-Capel E, Bol R. A review of biochar and its use and function in soil. *Adv Agron.* 2010;105(1):47–82.
54. Wambua P, Ivens J, Verpoest I. Natural fibres: Can they replace glass in fibre reinforced plastics? *Compos Sci Technol.* 2003;63(9):1259–64.
55. Das O, Bhattacharyya D, Sarmah AK. Sustainable eco-composites obtained from waste derived biochar: A consideration in performance properties, production costs, and environmental impact. *J Clean Prod* [Internet]. 2016;129:159–68. Available from: <http://dx.doi.org/10.1016/j.jclepro.2016.04.088>
56. Fu SY, Feng XQ, Lauke B, Mai YW. Effects of particle size, particle/matrix interface adhesion and particle loading on mechanical properties of particulate-polymer composites. *Compos Part B Eng.* 2008;39(6):933–61.
57. Das O, Sarmah AK, Bhattacharyya D. Nanoindentation assisted analysis of biochar added biocomposites. *Compos Part B Eng* [Internet]. 2016;91:219–27. Available from: <http://dx.doi.org/10.1016/j.compositesb.2016.01.057>
58. Zickler GA, Schöberl T, Paris O. Mechanical properties of pyrolysed wood: A nanoindentation study. *Philos Mag.* 2006;86(10):1373–86.
59. Devallance DB, Oporto GS, Quigley P. Investigation of hardwood biochar as a replacement for wood flour in wood-polypropylene composites. *J Elastomers Plast.* 2016;48(6):510–22.
60. Behazin E, Ogunsona E, Rodriguez-Urbe A, Mohanty AK, Misra M, Anyia AO. Mechanical, chemical, and physical properties of wood and perennial grass biochars for possible composite application. *BioResources.* 2016;11(1):1334–48.
61. Dubnikova IL, Berezina SM, Antonov A V. The effect of morphology of ternary-phase polypropylene/glass bead/ethylene-propylene rubber composites on the toughness and brittle-ductile transition. *J Appl Polym Sci.* 2002;85(9):1911–28.
62. Ogunsona EO, Misra M, Mohanty AK. Impact of interfacial adhesion on the microstructure and property variations of biocarbons reinforced nylon 6 biocomposites. *Compos Part A Appl Sci Manuf* [Internet]. 2017;98:32–44. Available from: <http://dx.doi.org/10.1016/j.compositesa.2017.03.011>
63. Giorcelli M, Khan A, Pugno NM, Rosso C, Tagliaferro A. Biochar as a cheap and environmental friendly filler able to improve polymer mechanical properties. *Biomass and Bioenergy* [Internet].

2019;120(February 2018):219–23. Available from:
<https://doi.org/10.1016/j.biombioe.2018.11.036>

64. Godara A, Mezzo L, Luizi F, Warriar A, Lomov S V., van Vuure AW, et al. Influence of carbon nanotube reinforcement on the processing and the mechanical behaviour of carbon fiber/epoxy composites. *Carbon N Y* [Internet]. 2009;47(12):2914–23. Available from:
<http://dx.doi.org/10.1016/j.carbon.2009.06.039>
65. Nagarajan V, Mohanty AK, Misra M. Biocomposites with Size-Fractionated Biocarbon: Influence of the Microstructure on Macroscopic Properties. *ACS Omega*. 2016;1(4):636–47.
66. Vaisman L, Wagner HD, Marom G. The role of surfactants in dispersion of carbon nanotubes. *Adv Colloid Interface Sci*. 2006;128–130(2006):37–46.
67. Bartoli M, Giorcelli M, Rosso C, Rovere M, Jagdale P, Tagliaferro A. Influence of commercial biochar fillers on brittleness/ductility of epoxy resin composites. *Appl Sci*. 2019;9(15).
68. Zhang Q, Xu H, Lu W, Zhang D, Ren X, Yu W, et al. Properties evaluation of biochar/high-density polyethylene composites: Emphasizing the porous structure of biochar by activation. *Sci Total Environ* [Internet]. 2020;737:139770. Available from:
<https://doi.org/10.1016/j.scitotenv.2020.139770>
69. Zhang Q, Zhang D, Lu W, Khan MU, Xu H, Yi W, et al. Production of high-density polyethylene biocomposites from rice husk biochar: Effects of varying pyrolysis temperature. *Sci Total Environ* [Internet]. 2020;738:139910. Available from:
<https://doi.org/10.1016/j.scitotenv.2020.139910>
70. Pillai K V., Rennecker S. Dynamic mechanical analysis of layer-by-layer cellulose nanocomposites. *Ind Crops Prod* [Internet]. 2016;93:267–75. Available from: <http://dx.doi.org/10.1016/j.indcrop.2016.02.037>
71. Zhang Q, Lei H, Cai H, Han X, Lin X, Qian M, et al. Improvement on the properties of microcrystalline cellulose/polylactic acid composites by using activated biochar. *J Clean Prod* [Internet]. 2020;252:119898. Available from: <https://doi.org/10.1016/j.jclepro.2019.119898>
72. Spanoudakis J, Young RJ. Crack propagation in a glass particle-filled epoxy resin - Part 2 Effect of particle-matrix adhesion. *J Mater Sci*. 1984;19(2):487–96.
73. Tandon GP, Weng GJ. The effect of aspect ratio of inclusions on the

- elastic properties of unidirectionally aligned composites. *Polym Compos.* 1984;5(4):327–33.
74. Cantwell WJ, Morton J. The impact resistance of composite materials - a review. *Composites.* 1991;22(5):347–62.
 75. Ho MP, Lau KT, Wang H, Hui D. Improvement on the properties of polylactic acid (PLA) using bamboo charcoal particles. *Compos Part B Eng [Internet].* 2015;81:14–25. Available from: <http://dx.doi.org/10.1016/j.compositesb.2015.05.048>
 76. Roy N, Sengupta R, Bhowmick AK. Modifications of carbon for polymer composites and nanocomposites. *Prog Polym Sci [Internet].* 2012;37(6):781–819. Available from: <http://dx.doi.org/10.1016/j.progpolymsci.2012.02.002>
 77. Li S, Li D. Electrically conductive charcoal powder/ultrahigh molecular weight polyethylene composites. *Mater Lett [Internet].* 2014;137:409–12. Available from: <http://dx.doi.org/10.1016/j.matlet.2014.09.022>
 78. Li S, Li X, Deng Q, Li D. Three kinds of charcoal powder reinforced ultrahigh molecular weight polyethylene composites with excellent mechanical and electrical properties. *Mater Des [Internet].* 2015;85:54–9. Available from: <http://dx.doi.org/10.1016/j.matdes.2015.06.163>
 79. Behazin E, Mohanty AK, Misra M. Sustainable lightweight biocomposites from toughened polypropylene and biocarbon for automotive applications. *21st Int Conf Compos Mater ICCM 2017 [Internet].* 2017;2017-Augus(August):20–5. Available from: <https://www.scopus.com/inward/record.uri?eid=2-s2.0-85053137607&partnerID=40&md5=0a0656fe392bfde05be94e352730e5d8>
 80. Das O, Sarmah AK. Mechanism of waste biomass pyrolysis: Effect of physical and chemical pre-treatments. *Sci Total Environ [Internet].* 2015;537:323–34. Available from: <http://dx.doi.org/10.1016/j.scitotenv.2015.07.076>
 81. Meng X, Zhang Y, Lu J, Zhang Z, Liu L, Chu PK. Effect of bamboo charcoal powder on the curing characteristics, mechanical properties, and thermal properties of styrene-butadiene rubber with bamboo charcoal powder. *J Appl Polym Sci.* 2013;130(6):4534–41.
 82. Abdul Khalil HPS, Firoozian P, Bakare IO, Akil HM, Noor AM. Exploring biomass based carbon black as filler in epoxy composites: Flexural and thermal properties. *Mater Des [Internet].* 2010;31(7):3419–25. Available from: <http://dx.doi.org/10.1016/j.matdes.2010.01.044>

83. Zhang Q, Zhang D, Xu H, Lu W, Ren X, Cai H, et al. Biochar filled high-density polyethylene composites with excellent properties: Towards maximizing the utilization of agricultural wastes. *Ind Crops Prod* [Internet]. 2020;146(October 2019):112185. Available from: <https://doi.org/10.1016/j.indcrop.2020.112185>
84. Lin X, Kong L, Cai H, Zhang Q, Bi D, Yi W. Effects of alkali and alkaline earth metals on the co-pyrolysis of cellulose and high density polyethylene using TGA and Py-GC/MS. *Fuel Process Technol* [Internet]. 2019;191(December 2018):71–8. Available from: <https://doi.org/10.1016/j.fuproc.2019.03.015>
85. Gezahegn S, Lai R, Huang L, Chen L, Huang F, Blozowski N, et al. Porous graphitic biocarbon and reclaimed carbon fiber derived environmentally benign lightweight composites. *Sci Total Environ*. 2019;664:363–73.
86. Yang W, Fortunati E, Dominici F, Kenny JM, Puglia D. Effect of processing conditions and lignin content on thermal, mechanical and degradative behavior of lignin nanoparticles/polylactic (acid) bionanocomposites prepared by melt extrusion and solvent casting. *Eur Polym J* [Internet]. 2015;71:126–39. Available from: <http://dx.doi.org/10.1016/j.eurpolymj.2015.07.051>
87. Moustafa H, Guizani C, Dupont C, Martin V, Jeguirim M, Dufresne A. Utilization of torrefied coffee grounds as reinforcing agent to produce high-quality biodegradable PBAT composites for food packaging applications. *ACS Sustain Chem Eng*. 2017;5(2):1906–16.
88. Oliveira M, Santos E, Araújo A, Fachine GJM, Machado A V., Botelho G. The role of shear and stabilizer on PLA degradation. *Polym Test* [Internet]. 2016;51:109–16. Available from: <http://dx.doi.org/10.1016/j.polymertesting.2016.03.005>
89. Lee J, Kim KH, Kwon EE. Biochar as a Catalyst. *Renew Sustain Energy Rev* [Internet]. 2017;77(April):70–9. Available from: <http://dx.doi.org/10.1016/j.rser.2017.04.002>
90. Chrissafis K, Bikiaris D. Can nanoparticles really enhance thermal stability of polymers? Part I: An overview on thermal decomposition of addition polymers. *Thermochim Acta* [Internet]. 2011;523(1–2):1–24. Available from: <http://dx.doi.org/10.1016/j.tca.2011.06.010>
91. Chrissafis K, Paraskevopoulos KM, Stavrev SY, Docoslis A, Vassiliou A, Bikiaris DN. Characterization and thermal degradation mechanism of isotactic polypropylene/carbon black nanocomposites. *Thermochim Acta*. 2007;465(1–2):6–17.

92. Wu Q, Liu X, Berglund LA. FT-IR spectroscopic study of hydrogen bonding in PA6/clay nanocomposites. *Polymer (Guildf)*. 2002;43(8):2445–9.
93. Vaia RA, Price G, Ruth PN, Nguyen HT, Lichtenhan J. Polymer/layered silicate nanocomposites as high performance ablative materials. *Appl Clay Sci*. 1999;15(1–2):67–92.
94. Lincoln DM, Vaia RA, Wang ZG, Hsiao BS. Secondary structure and elevated temperature crystallite morphology of nylon-6/layered silicate nanocomposites. *Polymer (Guildf)*. 2001;42(4):1621–31.
95. Shepherd C, Hadzifejzovic E, Shkal F, Jurkschat K, Moghal J, Parker EM, et al. New Routes to Functionalize Carbon Black for Polypropylene Nanocomposites. *Langmuir*. 2016;32(31):7917–28.
96. Pielichowska K, Pielichowski K. Crystallization behaviour of PEO with carbon-based nanonucleants for thermal energy storage. *Thermochim Acta [Internet]*. 2010;510(1–2):173–84. Available from: <http://dx.doi.org/10.1016/j.tca.2010.07.012>
97. Wellen RMR, Canedo EL, Rabello MS. Crystallization of PHB/Carbon black compounds. Effect of heating and cooling cycles. *AIP Conf Proc*. 2016;1779(October 2016).
98. Zhang Q, Khan MU, Lin X, Yi W, Lei H. Green-composites produced from waste residue in pulp and paper industry: A sustainable way to manage industrial wastes. *J Clean Prod [Internet]*. 2020;262:121251. Available from: <https://doi.org/10.1016/j.jclepro.2020.121251>
99. Pan Y, Gao X, Lei J, Li ZM, Shen KZ. Effect of different morphologies on the creep behavior of high-density polyethylene. *RSC Adv*. 2016;6(5):3470–9.
100. Das O, Sarmah AK, Bhattacharyya D. Structure-mechanics property relationship of waste derived biochars. *Sci Total Environ [Internet]*. 2015;538:611–20. Available from: <http://dx.doi.org/10.1016/j.scitotenv.2015.08.073>
101. Hussain M, Choa YH, Niihara K. Fabrication process and electrical behavior of novel pressure-sensitive composites. *Compos - Part A Appl Sci Manuf*. 2001;32(12):1689–96.
102. Hwang J, Jang J, Hong K, Kim KN, Han JH, Shin K, et al. Poly(3-hexylthiophene) wrapped carbon nanotube/poly(dimethylsiloxane) composites for use in finger-sensing piezoresistive pressure sensors. *Carbon N Y [Internet]*. 2011;49(1):106–10. Available from:

<http://dx.doi.org/10.1016/j.carbon.2010.08.048>

103. Knite M, Teteris V, Kiploka A, Kaupuzs J. Polyisoprene-carbon black nanocomposites as tensile strain and pressure sensor materials. *Sensors Actuators, A Phys.* 2004;110(1–3):142–9.
104. Gabhi RS, Kirk DW, Jia CQ. Preliminary investigation of electrical conductivity of monolithic biochar. *Carbon N Y [Internet]*. 2017;116:435–42. Available from: <http://dx.doi.org/10.1016/j.carbon.2017.01.069>
105. Gabhi R, Basile L, Kirk DW, Giorcelli M, Tagliaferro A, Jia CQ. Electrical conductivity of wood biochar monoliths and its dependence on pyrolysis temperature. *Biochar [Internet]*. 2020;(0123456789). Available from: <https://doi.org/10.1007/s42773-020-00056-0>
106. Malas A. Rubber nanocomposites with graphene as the nanofiller [Internet]. *Progress in Rubber Nanocomposites*. Elsevier Ltd; 2017. 179–229 p. Available from: <http://dx.doi.org/10.1016/B978-0-08-100409-8.00006-1>
107. Ren PG, Di YY, Zhang Q, Li L, Pang H, Li ZM. Composites of ultrahigh-molecular-weight polyethylene with graphene sheets and/or MWCNTs with segregated network structure: Preparation and properties. *Macromol Mater Eng.* 2012;297(5):437–43.
108. Zhang C, Ma CA, Wang P, Sumita M. Temperature dependence of electrical resistivity for carbon black filled ultra-high molecular weight polyethylene composites prepared by hot compaction. *Carbon N Y.* 2005;43(12):2544–53.
109. Gao JF, Li ZM, Meng Q jie, Yang Q. CNTs/ UHMWPE composites with a two-dimensional conductive network. *Mater Lett.* 2008;62(20):3530–2.
110. Yan DX, Pang H, Xu L, Bao Y, Ren PG, Lei J, et al. Electromagnetic interference shielding of segregated polymer composite with an ultralow loading of in situ thermally reduced graphene oxide. *Nanotechnology.* 2014;25(14).
111. Giorcelli M, Savi P, Miscuglio M, Yahya MH, Tagliaferro A. Analysis of MWCNT/epoxy composites at microwave frequency: Reproducibility investigation. *Nanoscale Res Lett.* 2014;9(1):1–5.
112. Giorcelli M, Savi P, Yasir M, Miscuglio M, Yahya MH, Tagliaferro A. Investigation of epoxy resin/multiwalled carbon nanotube nanocomposite behavior at low frequency. *J Mater Res.* 2014;30(1):101–7.
113. Savi P, Miscuglio M, Giorcelli M, Tagliaferro A. Analysis of microwave

- absorbing properties of epoxy MWCNT composites. *Prog Electromagn Res Lett.* 2014;44(December 2013):63–9.
114. Giorcelli M, Savi P, Delogu A, Miscuglio M, Yahya YMH, Tagliaferro A. Microwave absorption properties in epoxy resin Multi Walled Carbon Nanotubes composites. *Proc 2013 Int Conf Electromagn Adv Appl ICEAA 2013.* 2013;1139–41.
 115. Miscuglio M, Yahya MH, Savi P, Giorcelli M, Tagliaferro A. RF characterization of polymer multi-walled carbon nanotube composites. *2014 IEEE Conf Antenna Meas Appl CAMA 2014.* 2014;7–10.
 116. Zhu S, Guo Y, Chen Y, Liu S. Low water absorption, high-strength polyamide 6 composites blended with sustainable bamboo-based biochar. *Nanomaterials.* 2020;10(7):1–15.
 117. Kurosaki F, Ishimaru K, Hata T, Bronsveld P, Kobayashi E, Imamura Y. Microstructure of wood charcoal prepared by flash heating. *Carbon N Y.* 2003;41(15):3057–62.
 118. Anstey A, Vivekanandhan S, Rodriguez-Uribe A, Misra M, Mohanty AK. Oxidative acid treatment and characterization of new biocarbon from sustainable *Miscanthus* biomass. *Sci Total Environ* [Internet]. 2016;550:241–7. Available from: <http://dx.doi.org/10.1016/j.scitotenv.2016.01.015>
 119. Keiluweit M, Nico PS, Johnson M, Kleber M. Dynamic molecular structure of plant biomass-derived black carbon (biochar). *Environ Sci Technol.* 2010;44(4):1247–53.
 120. Maurice DR, Courtney TH. The physics of mechanical alloying: A first report. *Metall Trans A.* 1990;21(1):289–303.
 121. Calka A, Radlinski AP. Universal high performance ball-milling device and its application for mechanical alloying. *Mater Sci Eng A.* 1991;134(C):1350–3.
 122. Zhang X, Li YB, Zuo Y, Lv GY, Mu YH, Li H. Morphology, hydrogen-bonding and crystallinity of nano-hydroxyapatite/polyamide 66 biocomposites. *Compos Part A Appl Sci Manuf.* 2007;38(3):843–8.
 123. Pappu A, Pickering KL, Thakur VK. Manufacturing and characterization of sustainable hybrid composites using sisal and hemp fibres as reinforcement of poly (lactic acid) via injection moulding. *Ind Crops Prod* [Internet]. 2019;137(May):260–9. Available from: <https://doi.org/10.1016/j.indcrop.2019.05.040>

124. Huang R, Xu X, Lee S, Zhang Y, Kim B-J, Wu Q. High Density Polyethylene Composites Reinforced with Hybrid Inorganic Fillers: Morphology, Mechanical and Thermal Expansion Performance. *Materials (Basel)*. 2013;6(9):4122–38.
125. Clingerman ML, Weber EH, King JA, Schulz KH. Development of an additive equation for predicting the electrical conductivity of carbon-filled composites. *J Appl Polym Sci*. 2003;88(9):2280–99.
126. Ketabchi MR, Khalid M, Walvekar R. Effect of oil palm EFB-biochar on properties of PP/EVA composites. *J Eng Sci Technol*. 2017;12(3):797–808.
127. Lisuzzo L, Cavallaro G, Milioto S, Lazzara G. Halloysite nanotubes coated by chitosan for the controlled release of khellin. *Polymers (Basel)*. 2020;12(8):1–15.
128. Bertolino V, Cavallaro G, Milioto S, Lazzara G. Polysaccharides/Halloysite nanotubes for smart bionanocomposite materials. *Carbohydr Polym [Internet]*. 2020;245(June):116502. Available from: <https://doi.org/10.1016/j.carbpol.2020.116502>
129. Thomason J, Jenkins P, Yang L. Glass fibre strength-A review with relation to composite recycling. *Fibers*. 2016;4(2):1–24.
130. Handlos AA, Baird DG. Processing and Associated Properties of In Situ Composites Based on Thermotropic Liquid Crystalline Polymers and Thermoplastics. *J Macromol Sci Part C*. 1995;35(2):183–238.
131. Oliveux G, Dandy LO, Leeke GA. Current status of recycling of fibre reinforced polymers: Review of technologies, reuse and resulting properties. *Prog Mater Sci*. 2015;72:61–99.
132. Pereira PHF, De Freitas Rosa M, Cioffi MOH, De Carvalho Benini KCC, Milanese AC, Voorwald HJC, et al. Vegetal fibers in polymeric composites: A review. *Polimeros*. 2015;25(1):9–22.
133. Mohammed L, Ansari MNM, Pua G, Jawaid M, Islam MS. A Review on Natural Fiber Reinforced Polymer Composite and Its Applications. *Int J Polym Sci*. 2015;2015.
134. Das C, Tamrakar S, Kiziltas A, Xie X. Incorporation of biochar to improve mechanical, thermal and electrical properties of polymer composites. *Polymers (Basel)*. 2021;13(16):1–32.
135. Heiser JA, King JA, Konell JP, Sutter LL. Electrical conductivity of carbon filled nylon 6,6. *Adv Polym Technol*. 2004;23(2):135–46.

136. Socher R, Krause B, Hermasch S, Wursche R, Pötschke P. Electrical and thermal properties of polyamide 12 composites with hybrid fillers systems of multiwalled carbon nanotubes and carbon black. *Compos Sci Technol* [Internet]. 2011;71(8):1053–9. Available from: <http://dx.doi.org/10.1016/j.compscitech.2011.03.004>
137. Piñero-Hernanz R, Dodds C, Hyde J, García-Serna J, Poliakov M, Lester E, et al. Chemical recycling of carbon fibre reinforced composites in nearcritical and supercritical water. *Compos Part A Appl Sci Manuf*. 2008;39(3):454–61.
138. Yao SS, Jin FL, Rhee KY, Hui D, Park SJ. Recent advances in carbon-fiber-reinforced thermoplastic composites: A review. *Compos Part B Eng*. 2018;142(July 2017):241–50.
139. Chand S. Carbon fibers for composites. *J Mater Sci*. 2000;35(6):1303–13.
140. Pang H, Xu L, Yan DX, Li ZM. Conductive polymer composites with segregated structures. *Prog Polym Sci* [Internet]. 2014;39(11):1908–33. Available from: <http://dx.doi.org/10.1016/j.progpolymsci.2014.07.007>
141. Vasileva Dencheva N, Braz JFB, Denchev ZZ. Synthesis and properties of neat, hybrid, and copolymeric polyamide 12 microparticles and composites on their basis. *J Appl Polym Sci*. 2022;139(11):1–17.
142. Dul S, Fambri L, Pegoretti A. High-Performance Polyamide/Carbon Fiber Composites for Fused Filament Fabrication: Mechanical and Functional Performances. *J Mater Eng Perform* [Internet]. 2021;30(7):5066–85. Available from: <https://doi.org/10.1007/s11665-021-05635-1>
143. Uchimiya M, Wartelle LH, Klasson KT, Fortier CA, Lima IM. Influence of pyrolysis temperature on biochar property and function as a heavy metal sorbent in soil. *J Agric Food Chem*. 2011;59(6):2501–10.
144. Srinivasan P, Sarmah AK, Smernik R, Das O, Farid M, Gao W. A feasibility study of agricultural and sewage biomass as biochar, bioenergy and biocomposite feedstock: Production, characterization and potential applications. *Sci Total Environ* [Internet]. 2015;512–513:495–505. Available from: <http://dx.doi.org/10.1016/j.scitotenv.2015.01.068>
145. Clingerman ML. Development and Modelling of Electrically Conductive Composite Materials. 2001;1–299.
146. Clingerman ML, King JA, Schulz KH, Meyers JD. Evaluation of electrical conductivity models for conductive polymer composites. *J Appl Polym Sci*. 2002;83(6):1341–56.

147. Mutlay I, Tudoran LB. Percolation behavior of electrically conductive graphene nanoplatelets/polymer nanocomposites: Theory and experiment. *Fullerenes Nanotub Carbon Nanostructures*. 2014;22(5):413–33.
148. Ram R, Rahaman M, Aldalbahi A, Khastgir D. Determination of percolation threshold and electrical conductivity of polyvinylidene fluoride (PVDF)/short carbon fiber (SCF) composites: effect of SCF aspect ratio. *Polym Int*. 2017;66(4):573–82.
149. Bueche F. Electrical resistivity of conducting particles in an insulating matrix. *J Appl Phys*. 1972;43(11).
150. Liu X. Coupled Rheological-Electrical Investigation of Carbon Black Filled Polymer Composites and their Structures. 2016.
151. McLachlan DS, Blaszkiewicz M, Newnham RE. Electrical Resistivity of Composites. *J Am Ceram Soc*. 1990;73(8):2187–203.
152. Mamunya EP, Davidenko V V., Lebedev E V. Effect of polymer-filler interface interactions on percolation conductivity of thermoplastics filled with carbon black. *Compos Interfaces*. 1997;4(4):169–76.
153. Fowkes FM. ATTRACTIVE FORCES AT INTERFACES. *Ind Eng Chem*. 1964;56(12).
154. Owens DK, Wendt RC. Estimation of the surface free energy of polymers. *J Appl Polym Sci*. 1969;13(8):1741–7.
155. Sumita M, Abe H, Kayaki H, Miyasaka K. Effect of Melt Viscosity and Surface Tension of Polymers on the Percolation Threshold of Conductive-Particle-Filled Polymeric Composites. *J Macromol Sci Part B*. 1986;25(1–2).
156. Lux F. Models proposed to explain the electrical conductivity of mixtures made of conductive and insulating materials. Vol. 28, *Journal of Materials Science*. 1993.
157. Słupkowski T. Electrical conductivity of mixtures of conducting and insulating particles. *Phys Status Solidi*. 1984;83(1):329–33.
158. Malliaris A, Turner DT. Influence of particle size on the electrical resistivity of compacted mixtures of polymeric and metallic powders. *J Appl Phys*. 1971;42(2):614–8.
159. Weber M, Kamal MR. Microstructure and volume resistivity of composites of isotactic polypropylene reinforced with electrically

- conductive fibers. *Polym Compos.* 1997;18(6):726–40.
160. Surface Energy Data for Nylon 12, CAS # 24937-16-4 Source. 2009;1989(224):24937.
 161. Yang W, Shang J, Li B, Flury M. Surface and colloid properties of biochar and implications for transport in porous media. *Crit Rev Environ Sci Technol* [Internet]. 2020;50(23):2484–522. Available from: <https://doi.org/10.1080/10643389.2019.1699381>
 162. Ding Y, Liu Y, Liu S, Li Z, Tan X, Huang X, et al. Biochar to improve soil fertility. A review. *Agron Sustain Dev* [Internet]. 2016;36(2). Available from: <http://dx.doi.org/10.1007/s13593-016-0372-z>
 163. Qian K, Kumar A, Zhang H, Bellmer D, Huhnke R. Recent advances in utilization of biochar. *Renew Sustain Energy Rev* [Internet]. 2015;42:1055–64. Available from: <http://dx.doi.org/10.1016/j.rser.2014.10.074>
 164. Lehmann J, Rillig MC, Thies J, Masiello CA, Hockaday WC, Crowley D. Biochar effects on soil biota - A review. *Soil Biol Biochem* [Internet]. 2011;43(9):1812–36. Available from: <http://dx.doi.org/10.1016/j.soilbio.2011.04.022>
 165. Sirico A, Bernardi P, Sciancalepore C, Vecchi F, Malcevschi A, Belletti B, et al. Biochar from wood waste as additive for structural concrete. *Constr Build Mater* [Internet]. 2021;303(June):124500. Available from: <https://doi.org/10.1016/j.conbuildmat.2021.124500>
 166. Abd El-Aziz ME, Shafik ES, Tawfic ML, Morsi SMM. Biochar from waste agriculture as reinforcement filler for styrene/butadiene rubber. *Polym Compos.* 2022;43(3):1295–304.
 167. Das O, Sarmah AK, Bhattacharyya D. A sustainable and resilient approach through biochar addition in wood polymer composites. *Sci Total Environ* [Internet]. 2015;512–513:326–36. Available from: <http://dx.doi.org/10.1016/j.scitotenv.2015.01.063>
 168. Vagholkar P. Nylon (Chemistry , Properties and Uses) Nylon (Chemistry , Properties and Uses) *Chemistry.* 2016;(September):5–8.
 169. Wang L, Kiziltas A, Mielewski DF, Lee EC, Gardner DJ. Closed-loop recycling of polyamide12 powder from selective laser sintering into sustainable composites. *J Clean Prod* [Internet]. 2018;195:765–72. Available from: <https://doi.org/10.1016/j.jclepro.2018.05.235>
 170. Feng L, Wang Y, Wei Q. PA12 powder recycled from SLS for FDM.

- Polymers (Basel). 2019;11(4).
171. Cruz H, Son Y. Effect of Aspect Ratio on Electrical, Rheological and Glass Transition Properties of PC/MWCNT Nanocomposites. *J Nanosci Nanotechnol*. 2017;18(2):943–50.
 172. Fang Q, Lafdi K. Effect of nanofiller morphology on the electrical conductivity of polymer nanocomposites. *Nano Express*. 2021;2(1).
 173. Nasaruddin MM, Sheikh Md Fadzullah SH, Omar G, Mustafa Z, Ramli M, Akop MZ, et al. The effect of aspect ratio on multi-walled carbon nanotubes filled epoxy composite as electrically conductive adhesive. *J Adv Manuf Technol*. 2019;13(1):133–44.
 174. Dorigato A, Brugnara M, Pegoretti A. Novel polyamide 12 based nanocomposites for industrial applications. *J Polym Res*. 2017;24(6):1–13.
 175. Codou A, Misra M, Mohanty AK. Sustainable biocarbon reinforced nylon 6/polypropylene compatibilized blends: Effect of particle size and morphology on performance of the biocomposites. *Compos Part A Appl Sci Manuf* [Internet]. 2018;112(January):1–10. Available from: <https://doi.org/10.1016/j.compositesa.2018.05.018>
 176. Environmental Protection Agency. The 2019 EPA automotive trends report. *Epa* [Internet]. 2020;(March):54. Available from: <https://nepis.epa.gov/Exe/ZyPDF.cgi?Dockkey=P100YVFS.pdf>
 177. Das S. Life cycle assessment of carbon fiber-reinforced polymer composites. *Int J Life Cycle Assess*. 2011;16(3):268–82.
 178. Howarth J, Mareddy SSR, Mativenga PT. Energy intensity and environmental analysis of mechanical recycling of carbon fibre composite. *J Clean Prod* [Internet]. 2014;81:46–50. Available from: <http://dx.doi.org/10.1016/j.jclepro.2014.06.023>
 179. Matovic D. Biochar as a viable carbon sequestration option: Global and Canadian perspective. *Energy* [Internet]. 2011;36(4):2011–6. Available from: <http://dx.doi.org/10.1016/j.energy.2010.09.031>
 180. UNEP. Ministry of housing. spatial planning and the environment directorate-general for environmental protection. 1996; Available from: http://www.sciencenetwork.com/lca/unep_guide_to_lca.pdf
 181. Ilgin MA, Gupta SM. Environmentally conscious manufacturing and product recovery (ECMPRO): A review of the state of the art. *J Environ Manage* [Internet]. 2010;91(3):563–91. Available from:

<http://dx.doi.org/10.1016/j.jenvman.2009.09.037>

182. Rebitzer G, Ekvall T, Frischknecht R, Hunkeler D, Norris G, Rydberg T, et al. Life cycle assessment Part 1: Framework, goal and scope definition, inventory analysis, and applications. *Environ Int.* 2004;30(5):701–20.
183. What Is A Fuel Filter Housing And Why Is It Important? [Internet]. [cited 2022 Dec 7]. Available from: <https://www.gmpartscenter.net/blog/fuel-filter-housing-explained>
184. Tadele D, Roy P, Defersha F, Misra M, Mohanty AK. A comparative life-cycle assessment of talc- and biochar-reinforced composites for lightweight automotive parts. *Clean Technol Environ Policy* [Internet]. 2020;22(3):639–49. Available from: <https://doi.org/10.1007/s10098-019-01807-9>
185. Bare J. TRACI 2.0: The tool for the reduction and assessment of chemical and other environmental impacts 2.0. *Clean Technol Environ Policy.* 2011;13(5):687–96.
186. Di Cesare S., Cartone A. PL. SPRINGER BRIEFS IN ENVIRONMENTAL SCIENCE Perspectives on Social LCA Contributions from the 6th International Conference [Internet]. 2020. Available from: <http://www.springer.com/series/8868>
187. F4TZ9155BB | FORD POWERSTROKE FUEL FILTER HOUSING [Internet]. [cited 2022 Nov 7]. Available from: <https://highwayandheavyparts.com/i-20890755-f4tz9155bb-ford-powerstroke-fuel-filter-housing.html#:~:text=Weight%3A 5.0 lbs.>
188. Tillman AM, Ekvall T, Baumann H, Rydberg T. Choice of system boundaries in life cycle assessment. *J Clean Prod.* 1994;2(1):21–9.
189. Jensen AA, Elkington J, Christiansen K, Hoffmann L, Møller BT, Schmidt A, et al. Life Cycle Assessment (LCA) - A guide to approaches, experiences and information sources. 1997;(6).
190. Wood Pulp Makes Life Better Every Day [Internet]. [cited 2022 Oct 7]. Available from: <https://newsroom.domtar.com/wood-pulp-makes-life-better-every-day/>
191. 1.5 HP Air Direct Drive Sealed Bung Mount Mixer [Internet]. [cited 2022 Nov 7]. Available from: <https://www.mixerdirect.com/collections/drum-mixers/products/1-5-hp-air-direct-drive-bung-mount-1>
192. Quincy lab, Inc. GCE - Digital Gravity Convection Laboratory Ovens

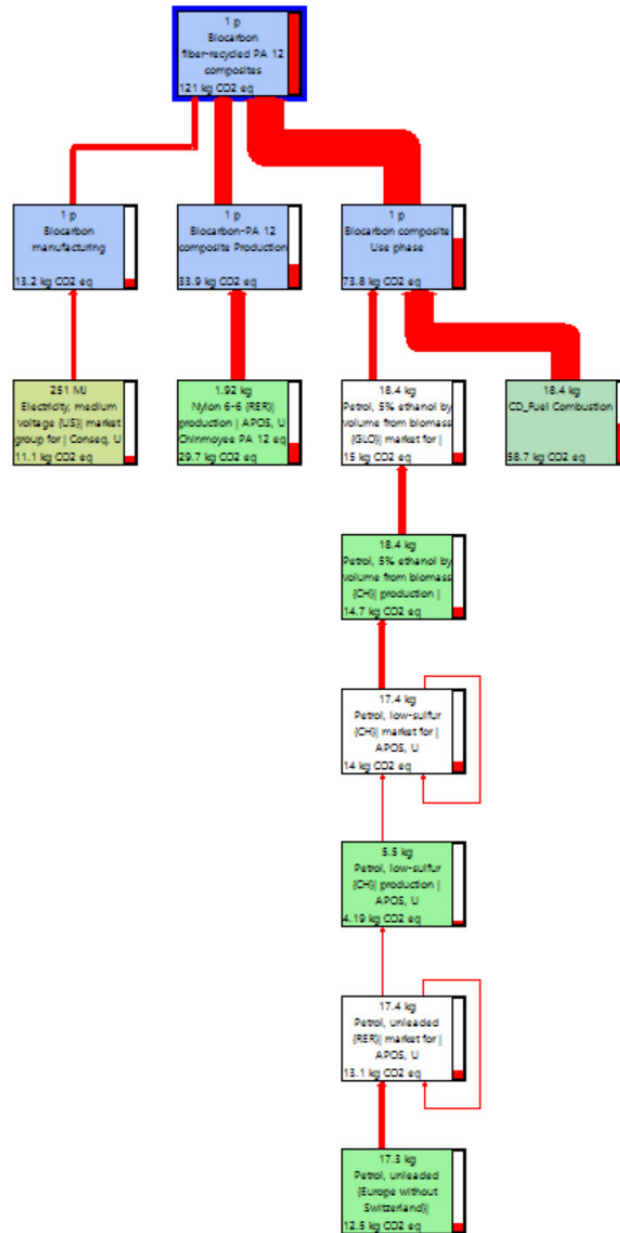
[Internet]. [cited 2022 Oct 7]. Available from:
<https://www.hogentogler.com/quincy-lab/gce-digital-gravity-convection-laboratory-ovens.asp>

193. Shop-Vac® 16 Gallon* 6.5 Peak HP** Stainless Steel Contractor Series Wet/Dry Vacuum with SVX2 Motor Technology [Internet]. [cited 2022 Nov 7]. Available from: <https://www.shopvac.com/products/copy-of-5989500-shop-vac®-12-gallon-5-5-peak-hp-svx2®-stainless-steel-wet-dry-vacuum-3>
194. LARGE INDUSTRIAL CHAMBER FURNACE - LCF [Internet]. [cited 2022 Oct 7]. Available from: <https://www.carbolite-gero.com/products/chamber-furnaces/industrial-furnaces/lcf/models/>
195. He D, Kim HC, De Kleine R, Soo VK, Kiziltas A, Compston P, et al. Life cycle energy and greenhouse gas emissions implications of polyamide 12 recycling from selective laser sintering for an injection-molded automotive component. *J Ind Ecol.* 2022;1–11.
196. London MB, Lewis GM, Keoleian GA. Life Cycle Greenhouse Gas Implications of Multi Jet Fusion Additive Manufacturing. *ACS Sustain Chem Eng.* 2020;8(41):15595–602.
197. Hervy M, Evangelisti S, Lettieri P, Lee KY. Life cycle assessment of nanocellulose-reinforced advanced fibre composites. *Compos Sci Technol* [Internet]. 2015;118:154–62. Available from: <http://dx.doi.org/10.1016/j.compscitech.2015.08.024>
198. Kim HC, Wallington TJ. Life-cycle energy and greenhouse gas emission benefits of lightweighting in automobiles: Review and harmonization. *Environ Sci Technol.* 2013;47(12):6089–97.
199. Kim HC, Wallington TJ. Life Cycle Assessment of Vehicle Lightweighting: A Physics-Based Model to Estimate Use-Phase Fuel Consumption of Electrified Vehicles. *Environ Sci Technol.* 2016;50(20):11226–33.
200. Elgowainy A, Han J, Ward J, Joseck F, Gohlke D, Lindauer A, et al. Cradle-to-Grave Lifecycle Analysis of U.S. Light Duty Vehicle-Fuel Pathways: A Greenhouse Gas Emissions and Economic Assessment of Current (2015) and Future (2025-2030) Technologies [Internet]. Argonne, IL (United States); 2016 Jun. Available from: <http://www.osti.gov/servlets/purl/1254857/>
201. National Overview: Facts and Figures on Materials, Wastes and Recycling [Internet]. 2018 [cited 2022 Oct 7]. Available from: <https://www.epa.gov/facts-and-figures-about-materials-waste-and-recycling/national-overview-facts-and-figures-materials>

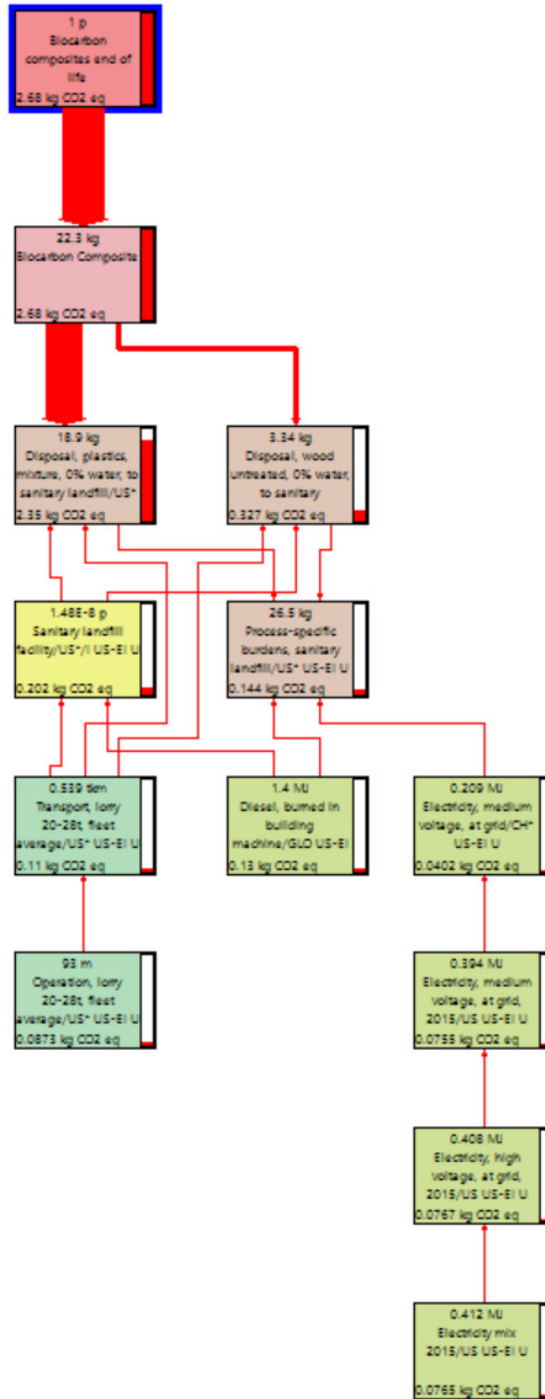
202. Miller L, Soulliere K, Sawyer-Beaulieu S, Tseng S, Tam E. Challenges and alternatives to plastics recycling in the automotive sector. *Materials (Basel)*. 2014;7(8):5883–902.
203. Muñoz E, Curaqueo G, Cea M, Vera L, Navia R. Environmental hotspots in the life cycle of a biochar-soil system. *J Clean Prod*. 2017;158:1–7.
204. Singh AK, Chandra R. Pollutants released from the pulp paper industry: Aquatic toxicity and their health hazards. *Aquat Toxicol* [Internet]. 2019;211(June 2018):202–16. Available from: <https://doi.org/10.1016/j.aquatox.2019.04.007>
205. Bryant PS, Woitkovich CP, Malcolm EW. Pulp and paper mill water use in North America. *Int Environ Conf*. 1996;2(601):451–60.

6.1. Appendix

6.1.1. Supplementary information for Chapter 5



6.1.1.1. GWP of recycled PA 12-biocarbon fiber composites (manufacturing and use phase).



6.1.1.2. GWP of end-of-life scenario of recycled PA 12-biocomposite fiber composites.